# n-Hexadecane, Petroleum Diesel and Biodiesel Fuels for a Direct Hydrocarbon Phosphoric Acid Fuel Cell

**Yuanchen Zhu**

Thesis submitted to the Faculty of Graduate and Postdoctoral in partial fulfillment of the requirements for the M.A.Sc degree

In

Department of Chemical and Biological Engineering

Faculty of Engineering

University of Ottawa

uOttawa

## Abstract

The performance of a phosphoric acid fuel cell reactor, (PAFC), with n-hexadecane, $C_{16}H_{34}$, canola biodiesel, soybean biodiesel and petroleum diesel fuel has been investigated. Fifteen-hour steady-state operation was achieved with each of the diesel fuels. This is the first extensive study reported in the literature in which n-hexadecane is used directly as the fuel. It is also the first study of a fuel cell operated with petroleum diesel fuel. Identification of steady-state conditions (temperature = 190$^{o}$C, molar ratio of fuel to water = 414) is significant because it demonstrates that stable fuel cell operation is technically feasible when operating a PAFC with diesel fuels. Degradation in fuel cell performance was observed prior to reaching steady-state. The degradation was attributed to a carbonaceous material forming on the surface of the anode. After treating the anode with water the fuel cell performance recovered. However, the fuel cell performance degraded again prior to obtaining another steady-state operation. Several consistent observations suggested that the carbonaceous material formed from the diesel fuels might be a reaction intermediate necessary for steady-state operation. Finally, the experiments indicated that water in the phosphoric acid electrolyte could be used as the water required for the anodic reaction. The water formed at the cathode could provide the replacement water for the electrolyte, thereby eliminating the need to provide a water feed system for the fuel cell.

## Résumé

La performance d'un réacteur de pile à combustible à base d'acide phosphorique (PAFC), a été étudiée en utilisant les combustibles suivants: hexadécane normal $C_{16}H_{34}$, biodiesel de Canola, biodiesel de soya et un diesel dérivé du pétrole. Un fonctionnement stable a été réalisé pendant 15 heures avec chacun des carburants. Ce travail est la première étude approfondie rapportée dans la littérature dans laquelle l'hexadécane normal a été utilisé directement comme combustible. C'est également la première étude d'une pile à combustible utilisée avec du pétrodiesel. L'identification d'un état stationnaire (température = 190°C, le rapport molaire de carburant à l'eau = 414) est important car il démontre que le fonctionnement stable de piles à combustible est techniquement faisable lorsqu'un PAFC est utilisé avec les carburants diesel. La dégradation des performances de la pile à combustible a été observée avant l'atteinte de l'état stationnaire. La dégradation a été attribuée à la présence d'une matière carbonisée à la surface de l'anode. Le rendement de la pile à combustible est remonté après avoir traité l'anode avec de la vapeur d'eau. Toutefois, la performance de la pile à combustible s'est dégradée encore une fois avant d'obtenir une autre opération à l'état stationnaire. Plusieurs observations cohérentes ont suggéré que les dépôts carbonisés pourraient être un intermédiaire de réaction nécessaire pour l'obtention d'un état stationnaire. Enfin, les expériences indiquent que l'eau dans l'électrolyte (acide phosphorique) pourrait alimenter la réaction anodique. L'eau formée à la cathode pourrait fournir de l'eau de remplacement pour l'électrolyte, ce qui éliminerait la nécessité de fournir un système d'alimentation d'eau pour la pile à combustible.

## Acknowledgements

To begin with, I would like to thank my supervisors Dr. Marten Ternan and Dr. André Tremblay for their patient guidance and endless support during my work and life. I was lucky to be their students. What I have learned is not only the knowledge of my research project but also the truth of human behavior. I am extremely grateful for their contributions to both my accomplishment of my Master's degree and formation of mature thoughts. Actually, they are my life mentors.

Transport Canada and the Canadian Government's Natural Sciences and Engineering Research Council., are acknowledged for their financial contributions.

I would like to acknowledge the scientific contributions of several researchers in Department of Chemistry of University of Ottawa: Dr. Yun Liu for the SEM images and Dr. Glenn A. Facey for the NMR experiments.

I would also like to thank the Chemical Engineering Technical Officers, Louis Tremblay, Gérard Nina and Franco Ziroldo for their laboratory assistance throughout my graduate studies.

I would like to take this opportunity to express my sincere gratitude and appreciation to all those who touched and contributed to my life in the past several years.

Last and foremost, I would like to thank my family and friends for their endless support. I am very grateful to join this strong internal cohesive group. The individuals of this group make me feel at home. To my father and mother, I would like to thank them for their never ending encouragement during my whole learning career. Thank you all for being in my life. I will never forget the contributions you gave and the moments we shared together throughout my life.

# Contents

## List of Figures

## List of Tables

## Nomenclature

### Abbreviations

| Abbreviations | Definition |
|---|---|
| PAFC | Phosphoric acid fuel cell |
| AFC | Alkaline fuel cell |
| $H_3PO_4$ | Phosphoric acid |
| DPFC | Direct propane fuel cell |
| MCFC | Molten-carbonate fuel cell |
| PEMFC | Polymer electrolyte fuel cell |
| PTFE | Polytetrafluoroethylene |
| SOFC | Solid oxide fuel cell |
| MEA | Membrane electrode assembly |
| DHFC | Direct hydrocarbon fuel cell |
| Ads | Adsorbed |
| AC | Alternating current |
| DC | Direct current |
| GDL | Gas diffusion layers |
| CL | Catalyst layer |
| SR | Stoichiometric ratio |
| TOS | Time-on-stream |
| ASTM | American Society for Testing and Materials |
| EN | European Standards |
| NMR | Nuclear magnetic resonance |
| DEPT | Distortionless enhancement by polarization transfer |

## Symbols

| Symbols | Definition |
|---|---|
| atm | Atmosphere |
| ℃ | Degrees celsius |
| $cm^2$ | Centimeter square |
| H | hour |
| L | Liters |
| mL | Milliliters |
| min | Minute |
| V | Voltage |
| mA | Milliamps |
| Wt | Weight |
| % | Percent |
| J | Current density |
| $E^0_{298}$ | Standard electrochemical potential at 298K |
| ppm | Parts per million |
| $\Delta\Phi$ | Potential difference |

# Chapter 1 - Introduction

*"Where there is a will, there is a way"*

— *An old proverb*

## 1.1 Fossil fuels and their emissions

Ever since the Industrial Revolution in the 18th century, large quantities of fossil fuels have been used to power the economy and thereby make life more enjoyable for people. The economic growth of the most countries is still based on the use of energy stored in fossil fuels - coal, petroleum, and natural gas. At the present time, about 80% of the world energy demand is met by fossil fuels. Fossil fuels in different forms are used everywhere in the world, especially for transportation, because they are storable and portable [1]. While fossil fuels have been the most logical choice for human activities for more than two centuries, there is no question that finding a way to use them more efficiently is needed. As the world's economy develops, demand for fossil fuels is increasing globally. Even though the current production of oil exceeds demand and the price of oil has recently decreased dramatically, the total supply is limited. Thus, energy is still a serious long term issue.

In addition, the burning of the fossil fuels has been connected to a series of serious environmental consequences such as air pollution, climate change and rising sea levels. Air pollution is primarily related to Canada's criteria air contaminants $NO_X$, CO, HC, $SO_X$. Greenhouse gas emissions such as $CO_2$, $CH_4$, and $N_2O$ are also generated during the combustion of fossil fuels. The fossil fuel sources of these emissions are the leading contributors to climate change and rising sea levels [2]. As a result there is a need to decrease both greenhouse gas emissions and emissions of criteria air contaminants.

Reliance on fossil fuels is still important in most countries. Of course, there is no question that a shift to a different source will occur in the future. In the meantime

we are trying to control the emissions of criteria air contaminants and greenhouse gases by developing a more efficient fossil fuel conversion system. Our reliance on limited fossil fuel resources, such as petroleum diesel fuel, for the majority of our transportation energy needs, makes it imperative that we utilize these resources as efficiently as possible. Higher efficiency energy conversion also means less emissions, since less fuel is consumed and less exhaust created for the same energy output.

### 1.2 Fuel cells

Fuel cells are one example of an efficient energy-conversion system. Fuel cells convert chemical energy directly into electrical energy, without the combustion of fuels. Fuel cells offer higher theoretical energy efficiencies compared to gas turbines or internal-combustion engines. Fuel cells are also capable of operating with a wide variety of fuels, either directly or indirectly [3].

In 1839, fuel cells were first described by a physical scientist, William Grove [4]. A schematic diagram of a typical fuel cell is shown in Figure 1.1. The basic physical structure of fuel cells consists of an electrolyte medium between two electrodes. This electrolyte is a barrier between the fuel and oxidant. The anode electrode facilitates electrochemical oxidation of fuel, while the cathode electrode causes the electrochemical reduction of oxidant. Protons and electrons will be generated or used during the oxidation or reduction process. Protons are transported from anode to cathode through an ionically conductive but electronically insulating electrolyte. Electrons generated at the anode during oxidation pass through the external circuit between anode and cathode to produce electrical power [5].

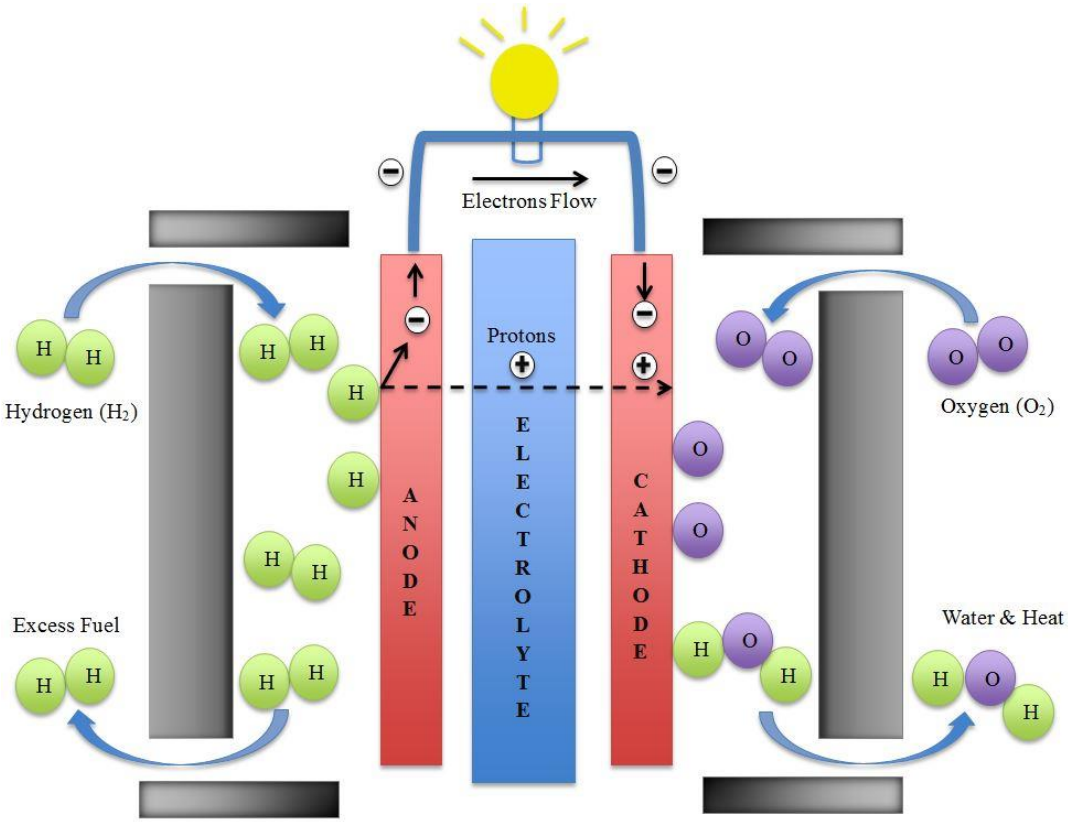


**Figure 1.1** A schematic diagram of a typical hydrogen fuel cell

Among the different types of fuel cells that have been developed in the past, the phosphoric acid fuel cell (PAFC) was the first to be commercialized. The electrolyte used inside PAFCs is a high concentration of phosphoric acid. Due to its mediocre ionic conductivity, it requires operating temperatures between 150 ℃ and 220 ℃ to work [6]. Hydrogen is the most common fuel used in PAFCs. Hydrogen and air are supplied to the anode and cathode respectively. When they contact the catalyst surfaces at the anode and cathode respectively, reactions will happen.

When hydrogen is the fuel, the electrochemical reactions in a phosphoric acid fuel cell are

$$\text{Anodic reaction: } H_2 = 2\,H^+ + 2\,e^- \quad (1.1)$$

$$\text{Cathodic reaction: } \tfrac{1}{2}\,O_2 + 2\,H^+ + 2e^- = H_2O \quad (1.2)$$

The overall reaction is

$$H_2 + \tfrac{1}{2}\,O_2 = H_2O + \text{heat (exothermic reaction, } \Delta H = -286 \text{ kJ mol}^{-1}) \text{ [7]} \quad (1.3)$$

Hydrocarbons are also desirable fuels for PAFCs despite the fact that most PAFCs currently operate using hydrogen. It is clear that hydrocarbons have several advantages: it is easier to store liquid hydrocarbons than hydrogen gas, higher energy storage density, global availability, and ease of transportation [8]. If hydrocarbons were used directly in fuel cells, the theoretical efficiency could reach 97% [9].

Furthermore, the capital cost of a hydrocarbon fuel cell system could be 30% less than that for hydrogen fuel cell system. The fuel processor unit used to convert hydrocarbons to hydrogen is required for hydrogen fuel cells but not for hydrocarbon fuel cells. However, the reaction rate of hydrocarbons in PAFCs is very small so their operation has not been commercialized. It is a widely held view that low-temperature fuel cells cannot directly oxidize hydrocarbons at rates that are of any practical interest [10]. This project attempts to investigate the performance of PAFCs with hydrocarbons and find a set stable operation conditions.

In addition, the performance of bio-diesel fuel and petroleum diesel fuel in PAFCs has also been investigated. n-Hexadecane is a compound used to model diesel fuel. After determining the performance of n-hexadecane in a PAFC, a comparison between bio-diesel fuel and petroleum diesel fuel was made.

Despite such great advantages of using hydrocarbons and diesel fuels directly in PAFCs, there has been little progress in this area. PAFCs that operate on hydrogen are more expensive. The achievements of this thesis can be summarized as: fuel cell performance with different fuels has been determined, a stable operation condition has been found, and a comparison of several typical fuels was made. The overall objective of this project was to replace the diesel combustion engine with a fuel cell system and thereby decrease the emissions of criteria air contaminants and greenhouse gases.

### 1.3 Research objectives

The development of one or more stable operation conditions for different

diesel fuels in PAFCs was required for the success of this research project. Several diesel fuels were considered to be the suitable fuels: n-hexadecane, canola biodiesel fuel, soybean biodiesel fuel and petroleum diesel fuel. With that goal in mind, the following objectives were proposed:

**Objective 1:** Modify a phosphoric acid fuel cell (PAFC) test station system to operate with diesel fuel and calibrate the whole system with hydrogen.

**Objective 2:** Investigate the performance of n-hexadecane, a model compound used to represent diesel fuel, in a phosphoric acid fuel cell (PAFC).

**Objective 3:** Investigate the performance of canola biodiesel fuel, soybean biodiesel fuel and petroleum diesel fuel in the phosphoric acid fuel cell (PAFC).

## 1.4 Thesis Structure

My thesis consists of six chapters. The introduction to the entire thesis is provided in chapter one. Chapter two gives the background of this research project. The following two chapters are independent articles that are to be published in scientific journals. Therefore, these two chapters describe the key problems, ideas and experimental procedures. Chapter 3 describes how we found one set of processing conditions that produced a steady-state when operating with n-hexadecane. Chapter 4 describes experiments with two biodiesel fuels and a petroleum diesel fuel. Chapter five provides a summary and a brief comparison of the preceding chapters. The conclusions and contributions to knowledge are presented in Chapter six. The operation of a phosphoric acid fuel cell test station and the installation of a membrane electrode assembly are shown in the Appendices of this thesis.

## 1.5 References

[1] Veziroğlu, T. N., and F. Barbir. "Initiation of hydrogen energy system in developing countries." International journal of hydrogen energy 17.7 (1992): 527-538.

[2] Kordesch, Karl V., and Guenter R. Simader. "Environmental impact of fuel cell technology." Chemical Reviews 95.1 (1995): 191-207.

[3] Soloveichik, Grigorii L. "Liquid fuel cells." Beilstein journal of nanotechnology 5.1 (2014): 1399-1418.

[4] G. Hoogers, “Fuel cell technology handbook” , CRC press LLC, USA 2003, p. 2-37.

[5] Ramani, Vijay, H. Russell Kunz, and James M. Fenton. "The polymer electrolyte fuel cell." Interface 13.3 (2004): 17-19.

[6] Holland, B. J., J. G. Zhu, and L. Jamet. "Fuel cell technology and application." University of Technology, Sydney (2007).

[7] Haile, Sossina M. "Fuel cell materials and components." Acta Materialia 51.19 (2003): 5981-6000.

[8] Al-Othman, Amani. Composite Zirconium Phosphate/PTFE Polymer Membranes for Application in Direct Hydrocarbon Fuel Cells. Diss. University of Ottawa, 2012.

[9] Ternan, Marten. "The potential of direct hydrocarbon fuel cells for improving energy efficiency." EIC Climate Change Technology, 2006 IEEE. IEEE, 2006.

[10] Perry, Michael Lee, et al. Exploratory fuel-cell research: direct-hydrocarbon polymer- electrolyte fuel cell; mathematical modeling of fuel-cell cathodes. MS thesis. University of California, Berkeley, 1996.

# Chapter 2 - Literature Review

*"Attention to detail; Rapid response; Brutal honesty"*

*— Marten Ternan*

Fuel cells generate electric power from the chemical energy of the fuel used during an oxidation-reduction (redox) reaction. Over the last few decades, the combination of energy issues and environmental issues has caused both government organizations as well as private enterprises to allocate resources for research and development of novel and practical fuel cells [1].

Fuel cells have been classified, according to the electrolyte employed, into the following major types: alkaline fuel cells (AFCs), proton exchange membrane or polymer electrolyte membrane fuel cells (PEMFCs), phosphoric acid fuel cells (PAFCs), molten-carbonate fuel cells (MCFCs), and solid-oxide fuel cells (SOFCs) [2]. The first of these fuel cell technologies to have a significant number of commercial applications was PAFC technology [3-4].

## 2.1 Phosphoric acid fuel cell technology

### 2.1.1 History of PAFCs

The first fuel cells, such as William Grove's first gas battery described in 1842, used acids as the electrolytes. Initially, sulfuric acid was the electrolyte most frequently used. Phosphoric acid was not initially considered to be as attractive as sulfuric acid because its conductivity was comparatively poor [5]. As a result PAFCs were slower to develop than other types of fuel cells.

In 1961 Elmore and Tanner operated a fuel cell using an electrolyte that was 35% phosphoric acid and 65% silica powder pasted on a Teflon gasket [6-7]. Phosphoric acid was not reduced electrochemically under fuel cell operating conditions. Furthermore, their PAFCs ran with air at the cathode rather than pure oxygen. Their phosphoric acid fuel cell was operated for six months at a current

density of 90 mA/cm$^2$ and 0.25V with no apparent deterioration [6, 8].

In the late 1960s and 1970s, with the development of materials science, some major advances in PAFC electrode materials appeared [2]. For example, Kordesch and Scarr developed a thin electrode made of "carbon paper as substrate and a Teflon-bonded carbon support for the catalyst." During the energy crisis in the 1970s researchers begin studying fuel cells at Los Alamos National Laboratory. They designed a golf cart powered by a PAFC.

The early work was followed by the development of large scale PAFC power plants. The TARGET program (Team to Advance Research for Gas Energy Transformation - sponsored by the American Gas Association and the United Technology Corporation, and later included Toshiba) [2, 9-10] contracted Pratt and Whitney to operate 12.5 k W power plants from 1971-73. Development programs organized by the Gas Research Institute – US Department of Energy resulted in the operation of 40 kW power plants from 1976 to 1986. In 1994, a 50 kW Fuji Electric PAFC for transit buses was designed by the U.S. Department of Energy in Georgetown University [11]. Subsequently [12-15], a 200 kW power plant (model PC25) was developed by the ONSI Corporation (United Technologies Corporation, Toshiba, and Ansaldo-Italy were equity investors) [16-17]. Eventually the PC25 technology was held by UTC Power and sold to ClearEdge Power [18] in 2013, and then to the Doosan Group in 2014. Doosan is now offering a 400 kW phosphoric acid fuel cell system. In addition to Doosan, Fuji Electric also has a 100 kW PAFC system. Power systems in the MW range have been built by combining several of the units described above. Nearly 150 units of the model PC25 power plants have been delivered to customers in 13 countries throughout North America, Asia, and Europe, and the fleet has accumulated 1.5 million hours of operations [19-20].

2.1.2 PAFCs Components

A schematic structure of hydrogen PAFC is shown in Figure 2.1. A PAFC consists of liquid electrolyte, two electrodes (anode and cathode), two gaskets, graphite bipolar plates (separator plates) [12,21].

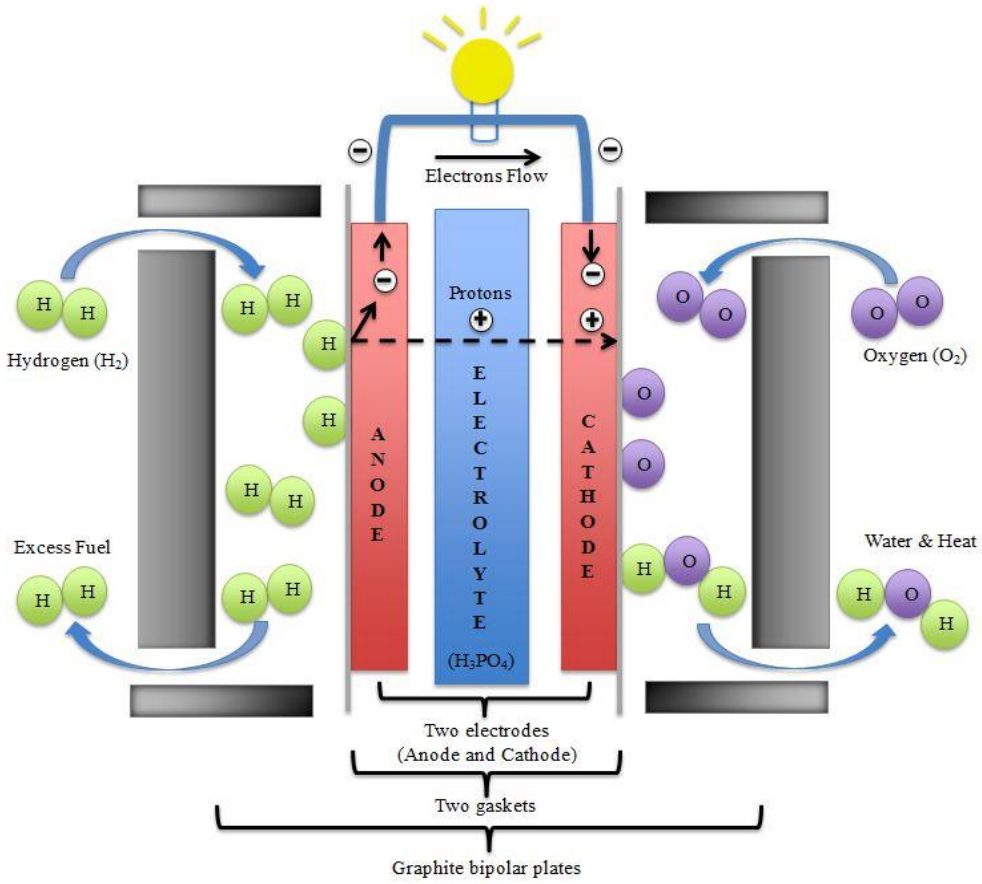


**Figure 2.1** A schematic structure of hydrogen PAFC

The membrane electrode assembly (MEA) is the most important part in the fuel cell. It includes two electrodes (each with a gas diffusion layer and a catalyst layer), and a liquid electrolyte. The concentrated phosphoric acid solution in a PAFC is absorbed into the pores of a porous matrix with fine pores. From the outside, this matrix electrolyte behaves like a solid electrolyte, preventing the reactant gases hydrogen and oxygen from mixing [22-23]. The combination of the gas diffusion layer and the catalyst layer that are in each electrode, are referred to as gas diffusion electrodes. They are made by using platinum catalyst nanoparticles, supported on a high surface area carbon, dispersed in a layer made of carbon bonded with

polytetrafluoro-ethelyne (PTFE). This type of porous material provides a well dispersed highly conductive catalyst. It is also able to collect the electrons efficiently [24]. The electrochemical reactions in the PAFC take place on the electrocatalyst (highly dispersed platinum particles supported on carbon black). Platinum catalyst is commonly used for both anode and cathode. Its loading is typically 0.1-0.2 mg/cm$^2$ [25]. This is a major decrease from 28 mg/cm$^2$ used in the 1960's [26]. Platinum is an expensive precious metal. It has a very low CO tolerance of about 5 –10 ppm that affects the fuel cell power output significantly [27].

Gaskets are used for sealing. They play a crucial role in avoiding gas mixing and leakage. Apart from sealing and gas leakage, they also help to cover the dimensional variations of the components. They also prevent cracking of the bipolar plates and the electrode. Teflon is used as the gasket material because it provides an effective seal that avoids leakage of reactant gases at relatively high temperatures [28-30].

The graphite bipolar plates have various functions. They are separator plates, preventing the mixing of hydrogen at anode of one cell with the oxidant (air) at cathode of the adjacent cell. They should be impermeable to the reactant gases, at least along the "Through plan" direction of the plate. They transmit both electrons and heat generated to the next cell and they are required to be to be both electronically and thermally conducting [30-31]. The flow fields for the reactant gases are machined in the graphite bipolar plates [32].

### 2.1.3 Fuels for PAFCs

PAFCs can operate with different fuels, such as hydrogen, methanol, and hydrocarbons. Hydrogen is the fuel used most frequently [33]. The first hydrogen–oxygen PAFCs were tested in the mid-1960s. 85% phosphoric acid was used and the working temperatures were less than 100°C [34-35]. Approximately 95% percent of all hydrogen is currently produced by "steam-reforming" natural gas. It is the lowest cost, large scale method of production [37-38]. Hydrogen is an attractive fuel because

water is the only species emitted from the fuel cell (nominally zero emissions). Its reaction rate in a fuel cell (the current density) is greater than that of all other fuels. However it has some disadvantages. The infrastructure for its widespread distribution does not yet exist. Storing gases, including hydrogen, is always more difficult than for liquids. As a result there are still some serious challenges for the use of pure hydrogen as the feed for fuel cells in automotive-propulsion [36] and in other applications.

Hydrocarbon fuels also have great potential for use directly as the fuel in PAFCs. This potential is caused by certain advantages that hydrocarbons have in comparison to hydrogen. Hydrocarbons provide higher energy density than hydrogen. There is an established existing infrastructure for distributing hydrocarbons. Liquid hydrocarbons are easy to store. Using hydrocarbons directly in the fuel cell is more energy efficient than hydrogen because the endothermic heat of the steam reforming reaction is not necessary (hence, less $CO_2$ emissions). Because hydrocarbons are fed directly to the fuel cell, the capital cost of fuel processing equipment used to produce hydrogen is eliminated [37, 39-40].

### 2.1.4 PAFCs Performance

The on-going development of phosphoric acid fuel cells since they were first commercialized has resulted in improvements to their durability, performance and cost. The poor ionic conductivity of phosphoric acid ($H_3PO_4$) requires the operating temperature of PAFCs to be between 150$^o$C and 220$^o$C. However, that has the advantage of increasing their catalyst activity. The higher temperatures are also necessary because phosphate anions adsorb on the oxygen (reduction) electrode at temperatures below 100$^o$C, thereby reducing catalytic performance of the PAFC. Other advantages of higher temperatures are that the hydrogen fuel is not required to be pure hydrogen and the reductant at the cathode does not have to be pure oxygen [41-42].

The cell works by dissociating the hydrogen fuel at the anode into protons and electrons. The generation of electrons at the anode and their consumption at the cathode creates an electrical potential gradient that causes an electrical current to flow from the anode to the cathode. Meanwhile, the protons migrate through the phosphoric acid in the matrix layer until they reach the cathode where they recombine with the electrons from the anode and react with oxygen that is fed to the cathode [43-44].

The measured data that indicates the performance of PAFCs is usually plotted as a polarization curve. It is the most frequently used method for reporting a fuel cell's performance [7-8]. In a polarization curve, the potential difference between the cathode and the anode is plotted versus current density. It provides a concise overview of the fuel cell performance. Data for a polarization curve is often measured in the following order. The first datum point is measured at the open circuit potential (zero current density). Then the current density is increased in increments and the potential difference measured at each current density. In the experiments performed in this study, the first measurement was made at a large current density. Then the current density was decreased in increments and the potential difference between the anode and the cathode was measured at each value of the current density. In general the current density was maintained at a constant value for approximately one-half hour before the potential difference was recorded. A typical polarization curve for hydrogen in our PAFCs is shown in Figure 2.2.

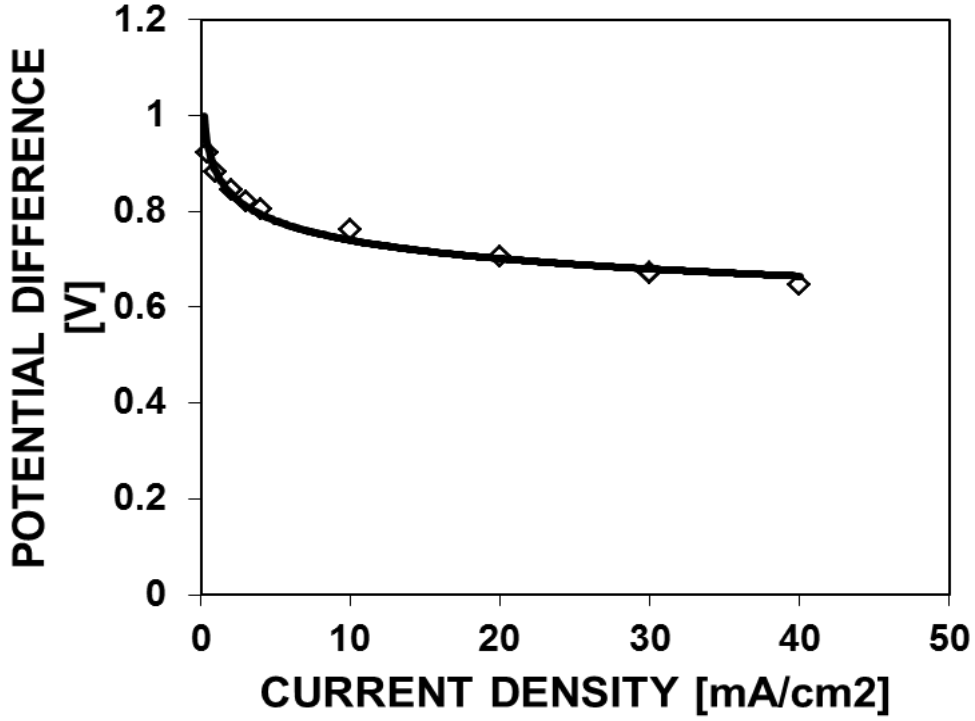


**Figure 2.2** Hydrogen polarization curve in a PAFC

When hydrogen is in a phosphoric acid fuel cell, two electrochemical reactions occur. Both the anodic reaction (Eq. 2.1) and the cathodic reaction (Eq. 2.2) are shown below:

$$H_2 \longrightarrow 2H^+ + 2e^- \quad (2.1)$$

$$\tfrac{1}{2} O_2 + 2H^+ + 2e^- \longrightarrow H_2O \quad (2.2)$$

The overall reaction (Eq. 2.3) is shown as:

$$H_2 + \tfrac{1}{2} O_2 \longrightarrow H_2O + \text{heat (exothermic reaction, } \Delta H = -286 \text{ kJ mol}^{-1}\text{) [45]} \quad (2.3)$$

The theoretical standard electrode potential of hydrogen is 1.23V [7]. The open circuit potential for hydrogen with air at the cathode and acidic is 1.0V (shown in Figure 2.2). These figures can be used to calculate the fuel cell electrical efficiency based on the data obtained in this work.

In all PAFCs, the performance of the cathode (cathode overpotential) is usually the same, regardless of which fuel used at the anode. That is because the

same gas (air or oxygen) is used at the cathode. In contrast the over-potential caused by the electrochemical reactions will be different for each fuel used at the anode, [46].

## 2.2 Direct hydrocarbon fuel cells

The performance of hydrocarbons in fuel cells was investigated extensively in the 1960's. The literature on direct hydrocarbon fuel cells is largely based on experimental research, and there are only a few recent papers on this topic [47-48].

In 1960's, the performance of hydrocarbons such as methane in aqueous electrolyte fuel cells was studied. High performance from direct hydrocarbon fuel cells was demonstrated. It was also shown that the hydrocarbon was oxidized completely to $CO_2$. Grubb and Michalske [49] found that the methane could be oxidized in a PAFC at 150$^o$C, with an electrolyte of 85% phosphoric acid. The methane was found to be quite reactive but the current densities were small. The electro-oxidation at the anode limits the reaction rate [49]. Methane flows along the anode. The anode reaction for complete oxidation (Eq. 2.4) is shown below:

$$CH_4 + 2\ H_2O \longrightarrow CO_2 + 8\ H^+ + 8\ e^{-1} \qquad (2.4)$$

Air enters the cathode and the cathode reaction (Eq.2.5) is shown below:

$$2\ O_2 + 8\ H^+ + 8\ e^{-1} \longrightarrow 4\ H_2O \qquad (2.5)$$

The overall chemical reaction (Eq. 2.6) performed in the fuel cell that is shown as:

$$CH_4 + 2\ O_2 \longrightarrow CO_2 + 2\ H_2O \qquad (2.6)$$

This is exactly the same reaction as occurs in the combustion process [47]. Without combustion, the chemical energy can be converted to electrical energy through electrochemical reactions.

In April 1964, another study, also performed by Grubb [49], showed that propane becomes quite reactive in fuel cells with porous platinum electrodes at 150$^o$C

and when the electrolyte is phosphoric acid at a concentration boiling a few degrees above the operating temperature of the fuel cell.

In 2007, Galea et al. [50] attempted an explanation for the mechanism of methane electro-oxidation at the anode. The reactor in their research was a solid oxide fuel cell, SOFC. SOFCs require a higher working temperature, ranging from 800$^{o}$C to 1000$^{o}$C. Thanks to the high temperatures a wide array of different fuels containing hydrogen (coal gas, bio gas, propane, natural gas, and hydrogen) can be used since fuel reforming takes place directly inside the cell. However, high temperature always brings drawbacks, for example heat control inside this type of fuel cell becomes difficult. The result is that these cells cannot readily be integrated into portable systems for electric generation [51-59].

In a study of methane electro-oxidation, Psofogiannakis et al. investigated the performance of methane in a PEM fuel cell. Psofogiannakis et al. [60] showed that the methane chemisorption step is the rate limiting step. They studied a series of surface reactions that included the chemisorption of methane on Pt, dehydrogenation, and oxygenation of adsorbed intermediates. The fundamental theory and results were based on an investigation of the Bagotzky mechanism (Figure 2.3) [61].

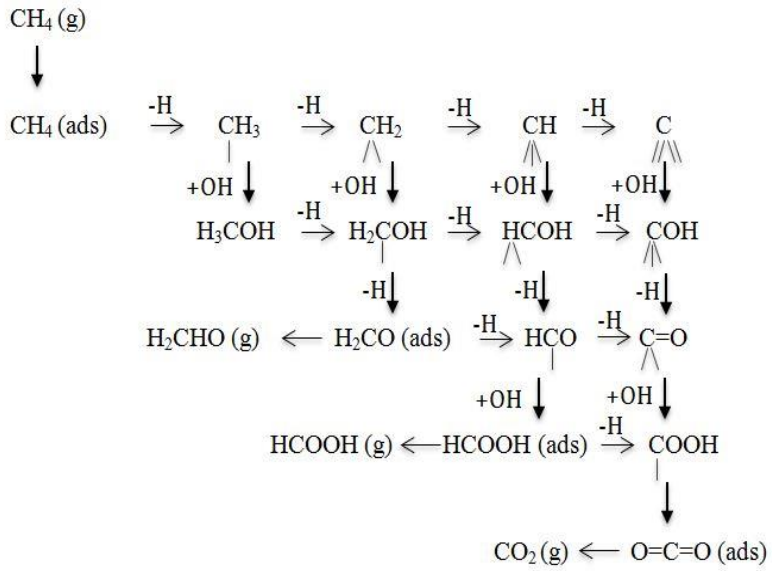


**Figure 2.3** The Bagotzky mechanism [61]: -H = Dehydrogenation， +OH = Hydroxylation.

One of the main intermediates in the anodic reaction in the fuel cell is carbon monoxide. Carbon monoxide is well known to be a contaminant, present in hydrogen reformate fuel. It is strongly adsorbed on the surface of the platinum, especially at the lower temperatures in polymer electrolyte membrane fuel cells, PEMFCs. PEMFCs operate between 70℃ and 90$^{o}$C with a polymer electrolyte membrane. Their low operating temperature causes PEMFC catalysts to be susceptible to CO poisoning even with amounts of only 5-10 ppm CO [62-66].

Janik and Neurock [67] studied the CO oxidation reaction on a Pt anode surface. As a result they proposed a reaction pathway that involves hydroxylation of CO (ads) and dehydrogenation of COOH (ads). The oxidation process is also shown in Figure 2.3.

The mechanism for the electro-oxidation of propane in a direct propane fuel cell, DPFC, used in this work was an extension of the Bagotzky mechanism for methane that is shown in Figure 2.3. The propane electro-oxidation is more difficult than methane due to the C—C. The process is based on methane oxidation on the platinum surface. In previous work in our lab, propane was modeled in a PEM fuel

cell. The electro-oxidation of propane was described below. Propane ($C_3H_8$) reacts at the anode via Equation 2.7 [68]:

$$C_3H_8 + 6\ H_2O \longrightarrow 3\ CO_2 + 20\ H^+ + 20\ e^{-1} \quad (2.7)$$

From the equation, we know six moles of water are consumed per one mole of propane reacted.

Oxygen or air enters the cathode, and the following reaction (Eq. 2.8) takes place:

$$5\ O_2 + 20\ H^+ + 20\ e^{-1} \longrightarrow 10\ H_2O \quad (2.8)$$

The overall reaction (Eq. 2.9) is:

$$C_3H_8 + 5\ O_2 \longrightarrow 3\ CO_2 + 4\ H_2O \quad (2.9)$$

The experimental performance of a direct hydrocarbon fuel cell was addressed in several studies. Savadogo et. el. [69] for example, studied the low temperature performance of a direct propane fuel cell (DPFC) .The study compared the performance an $H_2/O_2$ fuel cell. Savadogo's results showed that DPFC produced small current densities.

The anodic oxidation rate of hydrocarbons is lower than hydrogen. However, it was shown in the 1960's that the complete oxidation of alkanes (methane through hexadecane) at moderate current densities (10 to 500 $mA/cm^2$) and practical overpotential can be achieved in strong-acid electrolytes at temperatures below 200$^oC$, with high loadings of Pt [70]. It was also determined that alkanes yield higher current densities than their corresponding alkenes and methane, and the best alkane oxidation rates were obtained with propane.

During the 1960's and early 1970's, there were some review papers on the direct oxidation of hydrocarbons. Direct hydrocarbon fuel cells with aqueous electrolyte was reviewed by Liebhafksy and Cairns (1968), by Bockris and Srinivasan (1969) and by Cairns (1971) [71].

Liebhafksy and Cairns [71] discussed the experimental studies on the kinetics and mechanism of adsorption and electrochemical oxidation of hydrocarbons on platinum catalysts. The hydrocarbon in the fuel cell is hard to react at the anode. The processes occurring at the anode may include several steps. Firstly, fuel or water will adsorb on the catalyst surface when they enter the anode. Secondly, there would be breaking of bonds, which includes bonds such as C—H and C—C. Thirdly, the electrons will transfer through the external circuit. Then, the oxygenation of intermediates will occur during the reactions on the catalyst surface. Finally, the products such as protons and carbon dioxide will be removed [71-75].

Using the processes described above, the complete oxidation of the normal alkanes appears to be possible because the intermediate products are strongly held by the anode, but the protons are drawn to the cathode and carbon dioxide is readily desorbed.

Although their performance is poor, direct hydrocarbon fuel cells have a theoretically higher efficiency, potentially lower initial cost and lower maintenance cost. These characteristics are motivations for more research.

### 2.2.1 Different systems with different fuels

There are three main different fuels used in the fuel cell. They are hydrogen, methanol and hydrocarbons. Fuel cell systems can be classified using these three different fuels. The three different types of fuels are illustrated in Figure (2.4).

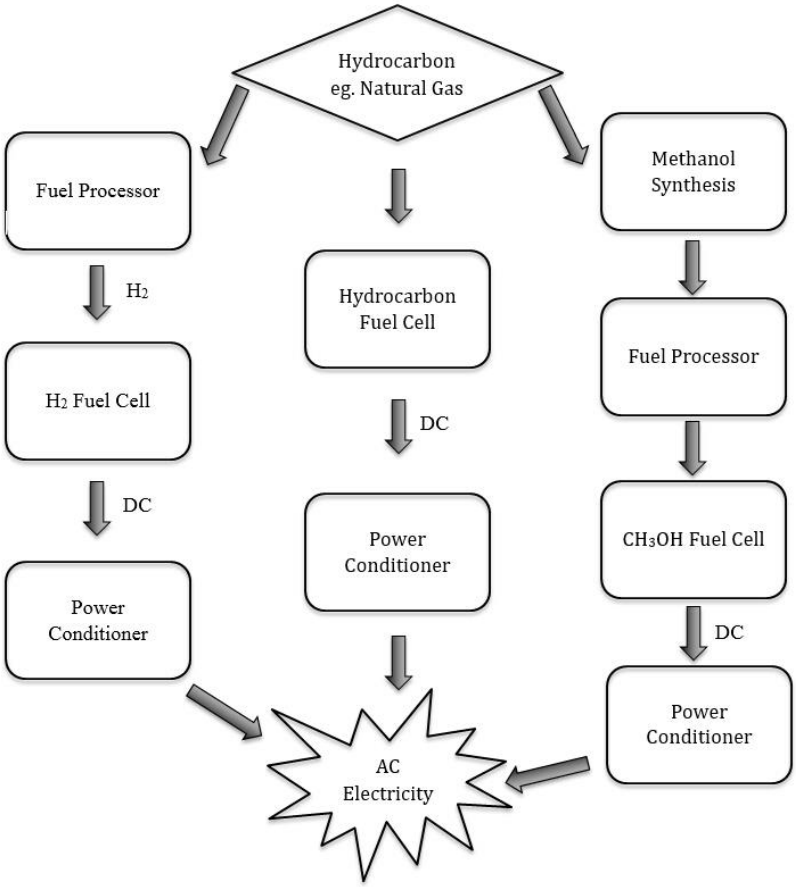


**Figure 2.4** A comparison of hydrogen, methanol and hydrocarbon fuel cell systems [47]. DC= Direct Current, AC= Alternating Current.

Hydrogen is the fuel used in most of the fuel cells currently. The current density obtained using hydrogen fuel is much higher than any other fuels [77-78]. Natural gas is the normal source of hydrogen and methanol. Before entering the hydrogen fuel cell, natural gas needs a fuel processor. The processes inside the fuel processor include methane-steam reforming, high-temperature water gas shift, low-temperature water gas shift, and a hydrogen purification process such as pressure-swing adsorption or preferential oxidation. Then pure hydrogen enters the hydrogen fuel cell, and the generated direct current becomes alternating current through the power conditioner. One of the most attractive advantages is that the emissions for hydrogen fuel in the fuel cell system are only water. Thus, hydrogen could solve part of the environmental problem in the future [79]. However, the hydrogen storage and

transportation are expensive. Currently, there is not enough adequate hydrogen infrastructure [80].

Methanol is a liquid fuel at room temperature. It is quite easy to transport. Direct methanol fuel cell systems require the conversion of natural gas to methanol. Thus, methanol can be used in a direct methanol fuel cell directly or it can be converted to hydrogen and used in a hydrogen fuel cell to produce direct current electricity [81-82].

The hydrocarbon fuel cell system is shown in the center of Figure 2.5. The superiority of this system is obvious comparing with other two systems. There is no need to put a fuel processor in the system. The hydrocarbon is not converted to hydrogen, methanol or any other chemicals before entering the fuel cell system. Unconverted hydrocarbon is the reactant in the electrochemical reaction that occurs inside a direct hydrocarbon fuel cell [83-84].

The fuel processor constitutes one-third of the capital cost of an entire system. Therefore the capital cost of direct hydrocarbon fuel cell systems is much less. Therefore they have great potential for further development in the future.

### 2.3 Diesel fuels for direct hydrocarbon fuel cells

Diesel fuels were the hydrocarbon fuels chosen for this project. Diesel fuel is a complex mixture, which includes many hydrocarbon species such as paraffins, olefins, cycloparaffins, and aromatics [85].

In direct hydrocarbon fuel cells the fuels react on the anode. The performance of several hydrocarbons in fuel cells has been investigated for many years. However, very few of those studies were on fuel cells operating with commercially available diesel fuels. Almost all diesel fuel reports available in the literature have been performed using high temperature (700-1000 $^{o}$C) solid oxide fuel cells [86-90].

Zhou et al. [91] generated electric power using jet fuels and Pennsylvania crude oil in direct oxidation of the fuels in SOFCs. Sasaki et al. performed two

studies using biodiesel [92-93]. Kim et al. [94] reported a power generation system using toluene, n-decane, and a synthetic diesel fuel in SOFCs. Up to the present time, the only study using a lower temperature (150$^{o}$C) phosphoric acid fuel cell was performed with a series of pure n-alkane compounds from methane to n-hexadecane [95]. It only contained three data points with n-hexadecane.

This report is first extensive study to use n-hexadecane, a model compound that represents diesel fuel. After identifying a stable operation condition using n-hexadecane, then canola bio-diesel, soybean bio-diesel and petroleum diesel were tested.

### 2.4 PAFCs and DHFCs related to this work

As discussed above, the PAFCs (Phosphoric Acid Fuel Cells) and DHFCs (Direct Hydrocarbon Fuel Cells) can be combined, using hydrocarbons directly as the fuel for the anode instead of hydrogen. Direct hydrocarbon fuel cells are promising in that they do not require a fuel processor. The hydrogen and methanol fuel cell systems require a fuel processor that accounts for about 30% of the capital cost of the total fuel cell system cost. Hence, the possibility of using hydrocarbon fuels directly without reforming should eliminate a significant portion of the fuel cell system cost.

There is an increasing awareness of energy issues and environmental problems. As a result there is a desire to use fuels more efficiently. The replacement of diesel engines with fuel cell engines offers a possibility of substantially decreasing both greenhouse gas emissions ($CO_2$, $CH_4$, and $N_2O$) and emissions of criteria air contaminants ($NO_X$, CO, HC, $SO_X$).

In this project several diesel fuels will be used. The ones of primary interest will include n-hexadecane (a compound used to model real diesel fuel, cetane number = 100), biodiesel, and petroleum diesel. The maximum theoretical energy efficiency for a hydrocarbon fuel cell operating on n-hexadecane is 96% compared to 65% for locomotive diesel combustion engines [47]. The combination of energy efficiency and

inherent characteristics of hydrocarbon fuel cells make it possible to decrease the emissions of all of the greenhouse gases and all of the criteria air contaminants.

**2.5 References**


[1] Cha, Suk-Won, Whitney Colella, and Fritz B. Prinz. Fuel cell fundamentals. New York: John Wiley & Sons, 2006.

[2] Perry, Mike L., and Tom F. Fuller. "A historical perspective of fuel cell technology in the 20th century." JOURNAL-ELECTROCHEMICAL SOCIETY 149.7 (2002): S59-S67.

[3] Hoogers, Gregor, ed. Fuel cell technology handbook. CRC press, 2014.

[4] Bagotsky, Vladimir S. "Phosphoric Acid Fuel Cells." Fuel Cells: Problems and Solutions, Second Edition: 99-106.

[5] A.J. Appleby, FUEL CELLS – PHOSPHORIC ACID FUEL CELLS | Overview, In Encyclopedia of Electrochemical Power Sources, edited by Jürgen Garche, Elsevier, Amsterdam, 2009, Pages 533-547.

[6] Ortiz-Rivera, Eduardo I., Angel L. Reyes-Hernandez, and Rey A. Febo. "Understanding the history of fuel cells." Electric Power, 2007 IEEE Conference on the History of. IEEE, 2007.

[7] Sharaf, Omar Z., and Mehmet F. Orhan. "An overview of fuel cell technology: Fundamentals and applications." Renewable and sustainable energy reviews 32 (2014): 810-853.

[8] Sandstede, G., et al. "History of low temperature fuel cells." Handbook of Fuel Cells (2003).

[9] Spiegel, Colleen. Designing and building fuel cells. New York, NY, USA: Mcgraw-hill, 2007.

[10] Kinoshita, Kim. Electrochemical oxygen technology. Vol. 30. John Wiley &

Sons, 1992.

[11] Srinivasan, Supramaniam, et al. "Fuel cells: reaching the era of clean and efficient power generation in the twenty-first century." Annual Review of Energy and the Environment 24.1 (1999): 281-328.

[12] Larminie, James, Andrew Dicks, and Maurice S. McDonald. Fuel cell systems explained. Vol. 2. New York: Wiley, 2003.

[13] Steele, Brian CH, and Angelika Heinzel. "Materials for fuel-cell technologies." Nature 414.6861 (2001): 345-352.

[14] Brenscheidt, Th, et al. "Performance of ONSI PC25 PAFC cogeneration plant." International journal of hydrogen energy 23.1 (1998): 53-56.

[15] Czajkowski, Kathleen A., and Stephen R. Rebain. "Variable fuel cell power system for generating electrical power." U.S. Patent No. 6,503,649. 7 Jan. 2003.

[16] Behling, Noriko Hikosaka. Fuel cells: current technology challenges and future research needs. Newnes, 2012.

[17] Hendry, Chris, P. Harbourne, and J. Brown. "Fuel cell strategies for regime change in stationary power." SPRU 40th Anniversary Conference—The Future of Science, Technology and Innovation Policy. 2006.

[18] Zhu, Yuanchen, et al. "n-hexadecane Fuel for a Phosphoric Acid Direct Hydrocarbon Fuel Cell."

[19] Asif, Muhammad, and Tariq Muneer. "Energy supply, its demand and security issues for developed and emerging economies." Renewable and Sustainable Energy Reviews 11.7 (2007): 1388-1413.

[20] Cacciola, G., V. Antonucci, and S. Freni. "Technology up date and new strategies on fuel cells." Journal of power sources 100.1 (2001): 67-79.

[21] Haile, Sossina M. "Fuel cell materials and components." Acta Materialia 51.19

(2003): 5981-6000.

[22] Choudhury, Suman Roy. "Phosphoric acid fuel cell technology." Recent Trends in Fuel Cell Science and Technology. Springer New York, 2007. 188-216.

[23] Gang, Xiao. "Phosphoric acid fuel cell technology." (1991).

[24] Fuller, T. F., and K. G. Gallagher. "Phosphoric acid fuel cells." Mater Fuel Cells (2008): 209-47.

[25] Weidner J., Sethuraman V. A., Van Zee J.W.; Electrochem. Soc. Interface 2003, 12, 40

[26] Ralph T.R., Hogarth M.P.; Platinum Metals Rev. 2002, 46, S14

[27] Haug A.T.,White R., Weidner J.W., Huang W.; J. Electrochem. Soc. 2002, 149, A862

[28] Dillard, David A., et al. "Seals and sealants in PEM fuel cell environments: Material, design, and durability challenges." ASME 2004 2nd International Conference on Fuel Cell Science, Engineering and Technology. American Society of Mechanical Engineers, 2004.

[29] Lebeck, Alan O. Principles and design of mechanical face seals. John Wiley & Sons, 1991.

[30] Mehta, Viral, and Joyce Smith Cooper. "Review and analysis of PEM fuel cell design and manufacturing." Journal of Power Sources 114.1 (2003): 32-53.

[31] Wilson, Mahlon S., and Deanna N. Busick. "Composite bipolar plate for electrochemical cells." U.S. Patent No. 6,248,467. 19 Jun. 2001.

[32] Kumar, Atul, and Ramana G. Reddy. "Materials and design development for bipolar/end plates in fuel cells." Journal of Power Sources 129.1 (2004): 62-67.

[33] Stambouli, A. Boudghene, and E. Traversa. "Solid oxide fuel cells (SOFCs): a

review of an environmentally clean and efficient source of energy." Renewable and Sustainable Energy Reviews 6.5 (2002): 433-455.

[34] Srinivasan, Supramaniam, et al. "Overview of fuel cell technology." Fuel Cell Systems. Springer US, 1993. 37-72.

[35] Huang, Xiaoyu. "Fuel Cells in Energy Production." (2011).

[36] He, C. Z., Kunz, R., Fenton, J. M.; J. Electrochem. Soc. 2001, 148, A1116

[37] Ahmed, S., and M1 Krumpelt. "Hydrogen from hydrocarbon fuels for fuel cells." International journal of hydrogen energy 26.4 (2001): 291-301.

[38] Holladay, Jamie D., et al. "An overview of hydrogen production technologies." Catalysis Today 139.4 (2009): 244-260.

[39] Ellis, Michael W., MICHAEL R. von Spakovsky, and Douglas J. Nelson. "Fuel cell systems: efficient, flexible energy conversion for the 21st century." Proceedings of the IEEE 89.12 (2001): 1808-1818.

[40] Acres, Gary JK. "Recent advances in fuel cell technology and its applications." Journal of Power Sources 100.1 (2001): 60-66.

[41] Behling, Noriko Hikosaka. Fuel cells: current technology challenges and future research needs. Newnes, 2012.

[42] King, J. M., and H. R. Kunz. "Phosphoric acid electrolyte fuel cells." Handbook of Fuel Cells (2010).

[43] Sotouchi, H.; Agiwara, A. Energy Carriers and Conversion Systems; Ohta, T.; Nejat Veziroglu T. Eds.; EOLSS: New York, 2003; vol. 2, pp. 333-339.

[44] Giorgi, Leonardo, and Fabio Leccese. "Fuel Cells: Technologies and Applications." The Open Fuel Cells Journal 6 (2013): 1-20.

[45] Haile, Sossina M. "Fuel cell materials and components." Acta Materialia 51.19

(2003): 5981-6000.

[46] Newman, John, and Karen E. Thomas-Alyea. Electrochemical systems. John Wiley & Sons, 2012.

[47] Ternan, Marten. "The potential of direct hydrocarbon fuel cells for improving energy efficiency." EIC Climate Change Technology, 2006 IEEE. IEEE, 2006.

[48] Song, Chunshan. "Fuel processing for low-temperature and high-temperature fuel cells: Challenges, and opportunities for sustainable development in the 21st century." Catalysis today 77.1 (2002): 17-49.

[49] Grubb, W. T., and Carol J. Michalske. "Electrochemical Oxidation of Methane in Phosphoric Acid Fuel Cells at 150 °C." Nature 201 (1964): 287-288.

[50] Galea, N. M.; Knapp, D.; Ziegler, T.; Journal of Catalysis 2007, 247, 20

[51] McIntosh, Steven, and Raymond J. Gorte. "Direct hydrocarbon solid oxide fuel cells." Chemical reviews 104.10 (2004): 4845-4866.

[52] Singhal, Subhash. High-temperature solid oxide fuel cells: fundamentals, design and applications: fundamentals, design and applications. Elsevier, 2003.

[53] Hammou, Abdelkader, and Jacques Guindet. "Solid oxide fuel cells." The CRC Handbook of Solid State Electrochemistry, CRC Press. Inc (1997): 407.

[54] Shao, Zongping, and Sossina M. Haile. "A high-performance cathode for the next generation of solid-oxide fuel cells." Nature 431.7005 (2004): 170-173.

[55] Singhal, Subhash C. "Solid oxide fuel cells for stationary, mobile, and military applications." Solid State Ionics 152 (2002): 405-410.

[56] Singhal, S. C. "Advances in solid oxide fuel cell technology." Solid state ionics 135.1 (2000): 305-313.

[57] Yamamoto, Osamu. "Solid oxide fuel cells: fundamental aspects and prospects."

Electrochimica Acta 45.15 (2000): 2423-2435.

[58] Stambouli, A. Boudghene, and E. Traversa. "Solid oxide fuel cells (SOFCs): a review of an environmentally clean and efficient source of energy." Renewable and Sustainable Energy Reviews 6.5 (2002): 433-455.

[59] Vafaeyan, Shadi. A DENSITY FUNCTIONAL THEORY STUDY OF A NICKEL-BASED ANODE CATALYST FOR APPLICATION IN A DIRECT PROPANE FUEL CELL. Diss. UNIVERSITY OF OTTAWA, 2012.

[60] Psofogiannakis, G.; St-Amant, A.; Ternan, M.; J. Phys. Chem. B 2006, 110, 24593

[61] Bagotzky, V. S., Yu B. Vassiliev, and O. A. Khazova. "Generalized scheme of chemisorption, electrooxidation and electroreduction of simple organic compounds on platinum group metals." Journal of Electroanalytical Chemistry and Interfacial Electrochemistry 81.2 (1977): 229-238.

[62] Okada, O.; Yokoyama, K. Development of Polymer Electrolyte Fuel Cell Cogeneration Systems for Residential Applications. Fuel Cells, 2001, 1(1), 72-77.

[63] Curtin, Dennis E., et al. "Advanced materials for improved PEMFC performance and life." Journal of power Sources 131.1 (2004): 41-48.

[64] Lee, S. J., et al. "Effects of Nafion impregnation on performances of PEMFC electrodes." Electrochimica Acta 43.24 (1998): 3693-3701.

[65] Yu, Xingwen, and Siyu Ye. "Recent advances in activity and durability enhancement of Pt/C catalytic cathode in PEMFC: part II: degradation mechanism and durability enhancement of carbon supported platinum catalyst." Journal of Power Sources 172.1 (2007): 145-154.

[66] Gamburzev, Sergei, and A. John Appleby. "Recent progress in performance improvement of the proton exchange membrane fuel cell (PEMFC)." Journal of

power sources 107.1 (2002): 5-12.

[67] Neurock, M.; Janik, M. J.; Electrochemica Acta 2007, 52, 5517

[68] H. Khakdaman, Y. Bourgault, M. Ternan, Ind. Eng. Chem. Res.,49, (2010), 49, p. 1079.

[69] O. Savadogo, F.J. Varela , J. New Mat. Electrochem. Sys., 4, (2001), p. 93.

[70] E. J. Cairns, "The Anodic Oxidation of Hydrocarbons and the Hydrocarbon Fuel Cell," in Ahances in Electrochemistry and Electrochemical Engineering Vol. 8, (C. W. Tobias, ed.), p. 337, John Wdey & Sons, Inc., New York, NY (1971)

[71] Liebhafsky, Herman A., and Elton James Cairns. "Fuel cells and fuel batteries. Guide to their research and development." (1968).

[72] Grubb, Willard T., and Herman A. Liebhafsky. "Electrochemical battery." U.S. Patent No. 3,589,943. 29 Jun. 1971.

[73] Grubb, W. T. "Catalysis, electrocatalysis, and hydrocarbon fuel cells." (1963): 883-884.

[74] Grubb, W. T. "High-performance Propane Fuel Cells." (1964): 699-700.

[75] Gasteiger, Hubert A., et al. "Electro-oxidation of small organic molecules on well-characterized Pt Ru alloys." Electrochimica Acta 39.11 (1994): 1825-1832.

[76] S. Bertholet, "Oxydation Electrocatalytique du Methane", Ph.D. Dissertation, Universit éde Poitiers, France, 1998.

[77] Poirier, M. G., and C1 Sapundzhiev. "Catalytic decomposition of natural gas to hydrogen for fuel cell applications." International journal of hydrogen energy 22.4 (1997): 429-433.

[78] Fatsikostas, Athanasios N., Dimitris I. Kondarides, and Xenophon E. Verykios. "Production of hydrogen for fuel cells by reformation of biomass-derived ethanol." Catalysis Today 75.1 (2002): 145-155.

[79] Ball, Michael, and Martin Wietschel. "The future of hydrogen–opportunities and challenges." International Journal of Hydrogen Energy 34.2 (2009): 615-627.

[80] Thomas, G. J., and S. E. Guthrie. "Hydrogen storage development." Proceedings of the 1998 US DOE Hydrogen Program Review, Alexandria, SAD (1998).

[81] McGrath, Kimberly M., GK Surya Prakash, and George A. Olah. "Direct methanol fuel cells." Journal of Industrial and Engineering Chemistry 10.7 (2004): 1063-1080.

[82] Heinzel, A., and V. M. Barragan. "A review of the state-of-the-art of the methanol crossover in direct methanol fuel cells." Journal of Power Sources 84.1 (1999): 70-74.

[83] Lin, Yuanbo, et al. "Direct operation of solid oxide fuel cells with methane fuel." Solid State Ionics 176.23 (2005): 1827-1835.

[84] Park, Seungdoo, et al. "Direct oxidation of hydrocarbons in a solid oxide fuel cell: I. Methane oxidation." Journal of the Electrochemical Society 146.10 (1999): 3603-3605.

[85] Kang, Inyong, Joongmyeon Bae, and Gyujong Bae. "Performance comparison of autothermal reforming for liquid hydrocarbons, gasoline and diesel for fuel cell applications." Journal of Power Sources 163.1 (2006): 538-546.

[86] Ralph, J. M., A. C. Schoeler, and M. Krumpelt. "Materials for lower temperature solid oxide fuel cells." Journal of Materials Science 36.5 (2001): 1161-1172.

[87] Singhal, Subhash. High-temperature solid oxide fuel cells: fundamentals, design and applications: fundamentals, design and applications. Elsevier, 2003.

[88] Singhal, S. C. "Advances in solid oxide fuel cell technology." Solid state ionics 135.1 (2000): 305-313.

[89] Minh, Nguyen Q. "Solid oxide fuel cell technology—features and applications." Solid State Ionics 174.1 (2004): 271-277.

[90] Tao, Shanwen, and John TS Irvine. "A redox-stable efficient anode for solid-oxide fuel cells." Nature materials 2.5 (2003): 320-323.

[91] Z. Zhou, C. Gallo, M. Pague, H. Schobert and S. Lvov, "Direct oxidation of jet fuels and Pennsylvania crude oil in a solid oxide fuel cell," J. Power Sources, vol. 133, pp. 181-187, 2004

[92] Y. Shiratori, T. Q. Tran, Y. Takahashi and K. Sasaki, "Application of biofuels to solid oxide fuel cell," ECS Transactions, vol. 35, pp. 2641-2651, 2011

[93] T. Quang -Tuyen, Y. Shiratori and K. Sasaki, "Feasibility of palm-biodiesel fuel for a direct internal reforming solid oxide fuel cell," Int. J. Energy Res., vol. 37, pp. 609-616, 2013

[94] H. Kim, S. Park, J.M. Vohs, and R.J.Gorte, “Direct oxidation of liquid fuels in a solid oxide fuel cell”, Journal of the Electrochemical Society, vol. 148, no. 7, pp. A-693-A695, 2001.

[95] H. Liebhafsky and W. Grubb, "Normal alkanes at platinum anodes, "American Chemical Society, Division of Fuel Chemistry, Preprints, vol. 11, 1967

# Chapter 3 - n-Hexadecane Fuel for a Phosphoric Acid Direct Hydrocarbon Fuel Cell [(A)]


## Abstract

The objective of this work was to examine fuel cells as a possible alternative to the diesel fuel engines currently used in railway locomotives, thereby decreasing air emissions from the railway transportation sector. We have investigated the performance of a phosphoric acid fuel cell reactor, (PAFC), with n-hexadecane, $C_{16}H_{34}$, (a model compound for diesel fuel, cetane number = 100). This is the first extensive study reported in the literature in which n-hexadecane is used directly as the fuel. Measurements were made to obtain both polarization curves and time-on-stream results. Because deactivation was observed hydrogen polarization curves were measured before and after n-hexadecane experiments, to determine the extent of deactivation of the membrane electrode assembly (MEA). By feeding water only (no fuel) to the fuel cell anode the deactivated MEAs could be regenerated. One set of fuel cell operating conditions that produced a steady-state was identified. Identification of steady-state conditions is significant because it demonstrates that stable fuel cell operation is technically feasible when operating a PAFC with n-hexadecane fuel.



(A) Journal of Fuels, vol. 2015, Article ID 748679, doi.org/10.1155/2015/748679

## 3.1 Introduction

Fuel cells offer many advantages for the conversion of the chemical energy in a fuel to electrical energy. Fuel cell energy efficiencies can be greater than those of conventional combustion engines. For example, because Carnot heat engines are limited to the maximum temperature that their materials can withstand, their theoretical energy efficiency is close to 67%. In contrast, fuel cells do not have materials limitations and can have larger theoretical energy efficiencies. Often emissions from fuel cells are generally less than those from combustion engines. In some applications fuel cells are competing successfully with batteries in part because they can use fuel continuously whereas batteries stop providing electrical power as soon as their charge has been exhausted.

Fossil fuels are usually the lowest cost source of energy and that is not likely to change in the foreseeable future. Unfortunately emissions from fossil fuels have a negative effect on the earth's climate. Direct hydrocarbon fuel cells (DHFCs) can have theoretical energy efficiencies near 95%. Their large energy efficiencies mean that a smaller quantity of fuel is required and therefore they will have lower emissions and have a smaller impact on climate change than heat engines or the more technologically advanced fuel cells that use hydrogen or methanol as their fuels.

The purpose of this work was to decrease both greenhouse gas emissions ($CO_2$, $CH_4$, and $N_2O$) and air contaminants ($NO_X$, CO, HC, $SO_X$) by replacing locomotive diesel engines with fuel cell engines. n-Hexadecane (cetane numer = 100) was used as a model compound to represent commercial diesel fuels. A phosphoric acid fuel cell was used because its temperature is large enough to ensure that the n-hexadecane would be in the vapour phase if an appropriate steam / n-hexadecane ratio is used. Therefore the existence of two liquid phases within the fuel cell could be avoided.

Direct hydrocarbon fuel cells have other advantages. DHFC systems have lower capital costs than other fuel cell systems because the fuel processing systems

(steam reforming etc.) for hydrogen and methanol fuels are not required. In addition, the infrastructure already exists for diesel fuel and other petroleum derived fuels. That is not the case for hydrogen or methanol fuels. Storage of liquid fuels, such as diesel fuel, is much easier than storage of gaseous fuels such as hydrogen.

Unfortunately DHFCs have one major disadvantage. Their current densities are much smaller than those for hydrogen and methanol fuel cells. Work in our laboratory is being performed to understand the characteristics of DHFCs with a long-term objective of improving their performance.

William Grove demonstrated the first fuel cell operation in 1839 using hydrogen as the fuel. He was also credited with suggesting possible commercial opportunities if coal, wood, or other combustibles could replace hydrogen [1] which would be DHFCs. Direct hydrocarbon fuel cells were investigated intensely in the 1960's. Three reviews of the DHFC work up to that time are available [2-4].

Research on DHFCs has continued. Low temperature fuel cell studies (<100°C) were performed on methane by Bertholet [5], on propane by Cheng et al. [6] and by Savadogo and Rodriquez [7,8]. Heo et al. [9] performed intermediate temperature fuel cell studies (100 - 300°C) using propane. A larger number of DHFC studies have been performed on solid oxide fuel cells. Studies using low molecular weight hydrocarbons, methane – butane were performed by Steele [10], Murray et al. [11], Zhu et al. [12], Gross et al. [13], and Lee et al. [14]. Larger molecules were studied by Dong et al. [15] (octane), Kishimoto et al. [16] (n-dodecane), and Zhou et al. [17] (jet fuel). Our own work has focused on modeling the fuel cell reactor [18–20], modeling the fuel cell catalyst [21–23], experimental development of an electrolyte that is appropriate for temperatures above the boiling point of water [24-26], and experimental fuel cell studies [27-28].

Phosphoric acid fuel cell systems have an extensive development history. A 250-400 kW fuel cell system to produce stationary electric power was developed by Pratt and Whitney / ONSI / UTC Power. 300 units were built in 19 different countries.

The company was sold to ClearEdge Power and recently acquired by Doosan Industries. The phosphoric acid fuel cell technology has been documented extensively [29-32].

The fuel in this work was n-hexadecane. There were only three data points reported previously in a fuel cell study that examined a variety of fuels [33]. This is the first fuel cell study devoted exclusively to n-hexadecane. In a direct n-hexadecane phosphoric acid fuel cell, the overall reaction is

$$C_{16}H_{34}\,(g) + 49/2\ O_2\,(g) \longrightarrow 16\ CO_2\,(g) + 17\ H_2O\,(g) \qquad (3.1)$$

The anode half-cell reaction is

$$C_{16}H_{34}\,(g) + 32\ H_2O\,(g) \longrightarrow 16\ CO_2\,(g) + 98\ H^+ + 98\ e^- \qquad (3.2)$$

The cathode half-cell reaction is

$$49/2\ O_2\,(g) + 98\ H^+ + 98\ e^- \longrightarrow 49\ H_2O\,(g) \qquad (3.3)$$

where the (g) represents the gas phase. The anode stoichiometric ratio, SR = $H_2O/C_{16}H_{34}$ is 32. One mole of n-hexadecane reacts with 32 moles of water at the anode and generates 98 moles of protons and electrons, provided the only product is $CO_2$. The protons migrate through the electrolyte to the cathode where the oxygen reduction reaction occurs.

Bagotsky et al. [34] described a reaction mechanism for direct hydrocarbon fuel cells using methane as a feedstock. The Bagotsky mechanism was modified, as shown in Figure 3.1, to describe n-hexadecane. The desired product is $CO_2$. However alcohols, aldehydes, carboxylic acids, and lower molecular weight hydrocarbons are possible by-products. Three reactions are shown in Figure 3.1: dehydrogenation, (from both carbon and oxygen atoms), hydroxylation, and C–C bond cleavage. Two reactions are not shown: water dissociation ($H_2O \rightarrow H + OH$) and hydrogen atom ionization ($H \rightarrow H^+ + e^-$). Hydrogen ionization is an electrochemical reaction and therefore is influenced by potential. The other four

reactions are chemical reactions and are not influenced by potential.

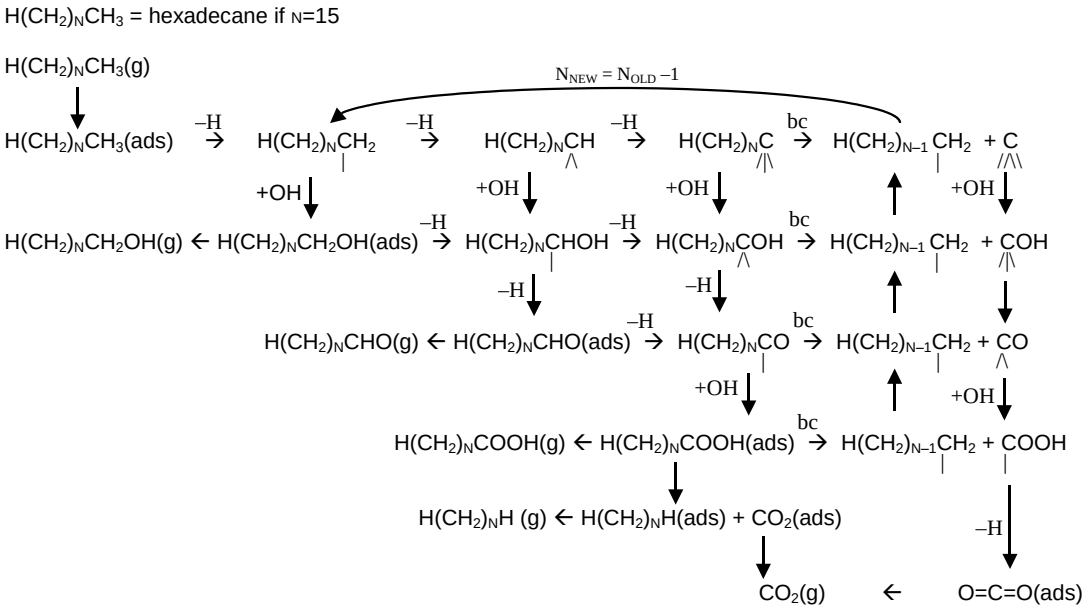


**Figure 3.1** Diagram of a modified Bagotsky anode reaction mechanism: $H(CH_2)_NCH_3$ = hexadecane if N=15, +OH = Hydroxylation, –H = Dehydrogenation, bc = C–C bond cleavage. Two reactions are not shown, water dissociation $H_2O = H + OH$, and the electrochemical reaction $H \rightarrow H^+ + e^-$.

The objective of the work described here was to identify a set of operating conditions that would permit stable continuous operation of a direct hydrocarbon phosphoric acid fuel cell using n-hexadecane as the fuel.

### 3.2 Experimental

A schematic diagram of the direct n-hexadecane fueled phosphoric acid fuel cell system (PAFC) is shown in Figure 3.2. The overall system consists of an air cylinder, a hydrogen cylinder, one galvanostat, two syringe pumps, a vaporizer, a Phosphoric Acid Fuel Cell (PAFC = Electrochem FC-25-02MA), and a fuel cell test station. Both gaseous and liquid fuels can be used in this fuel cell system. Deionized water and n-

hexadecane were introduced into the vaporizer by the syringe pumps. The liquid fuels were expected to vaporize before reaching the anode of the fuel cell. Air was fed to the cathode at a constant flow rate. On those occasions when hydrogen was used as the fuel, the pumps were stopped and the valve in Figure 3.2 was opened.

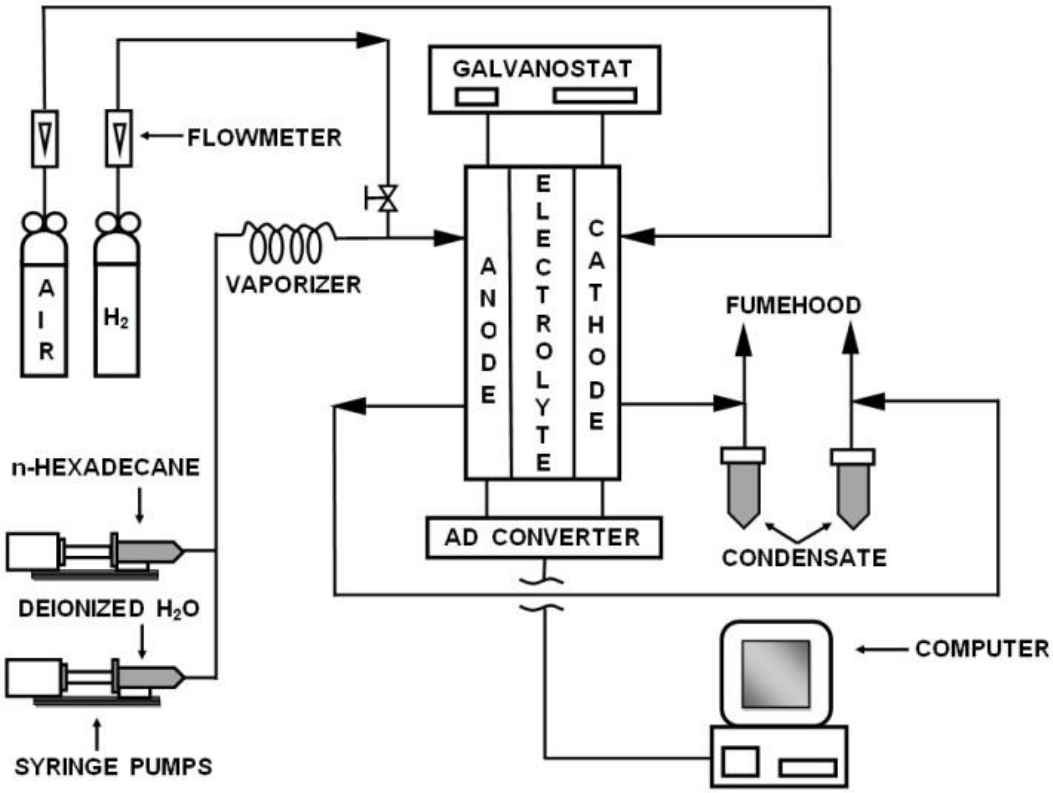


**Figure 3.2** Diagram of A Direct n-Hexadecane Fueled Phosphoric Acid Fuel Cell System.

The membrane electrode assembly (MEA) used in our fuel cell work had five layers: two gas diffusion layers (GDL), two catalyst layers (CL) and a liquid electrolyte layer. The gas diffusion layers were Teflon™ coated Toray paper.

The liquid electrolyte was initially 85% (14.6 M) phosphoric acid, which was held in a SiC matrix between the anode and cathode catalyst layers. Platinum (0.5 mg Pt / $cm^2$) supported on carbon (10% Pt on C) was the catalyst in both anode and cathode catalyst layers. The fuel cells had a face area of 25 $cm^2$. A pin-type flow field was machined in a graphite plate. The current collectors were sheets of copper metal

that had been gold plated on both sides. Silicone rubber flexible heaters were attached to each current collector.

Several types of experiments were performed. Hydrogen polarization curves were measured to determine the state of the MEA in the fuel cell. A polarization curve shows the potential difference as a function of current density. n-Hexadecane polarization curves were measured. Two types of time-on-stream experiments were performed ($H_2O$ with n-$C_{16}H_{34}$ and $H_2O$ only). The time-on-stream experiments were performed at (a) different molar ratios of water to n-hexadecane, (b) different current densities, and (c) different temperatures.

The following operating conditions were used. Separate syringe pumps were used to feed both water and n-hexadecane. The water flow rate was expressed as a function of the stoichiometric ratio (SR) of $H_2O$ / $C_{16}H_{34}$ in Equation 3.2 for the anode half reaction. A constant flow rate of n-hexadecane (0.2 mL/h) was used in all experiments. The two water flow rates and their stoichiometric ratios were 1 mL/h (2.5*SR, $H_2O$ / $C_{16}H_{34}$ = 80) and 5.1 mL/h (12.9*SR, $H_2O$ / $C_{16}H_{34}$ = 414). Some experiments were performed with only water being fed to the fuel cell. The experiments were performed at two temperatures, 160 ℃ and 190 ℃.

A Hokuto Denko HA-301 Galvanostat was used to adjust the potential difference between the anode and cathode of the phosphoric acid fuel cell to maintain the chosen current at a constant value. The potential difference was recorded every second using a Lab View data logger.

### 3.3 Results and Discussion

Two hydrogen / air polarization curves obtained with a PAFC are shown in Figure 3.3. The upper curve was the first experiment performed with a new MEA. The lower curve was measured after some conditioning experiments had been performed with low molecular weight hydrocarbons (ethylene, propane). It is an indication of the condition of the MEA at the beginning of this investigation, and will

be referred to as the Reference polarization curve. The open-circuit potential in Figure 3 is about 0.93 V. It is comparable to the 0.9 V value reported by Fuller et al. [35] with an air cathode half-cell having a hydrogen reference electrode.

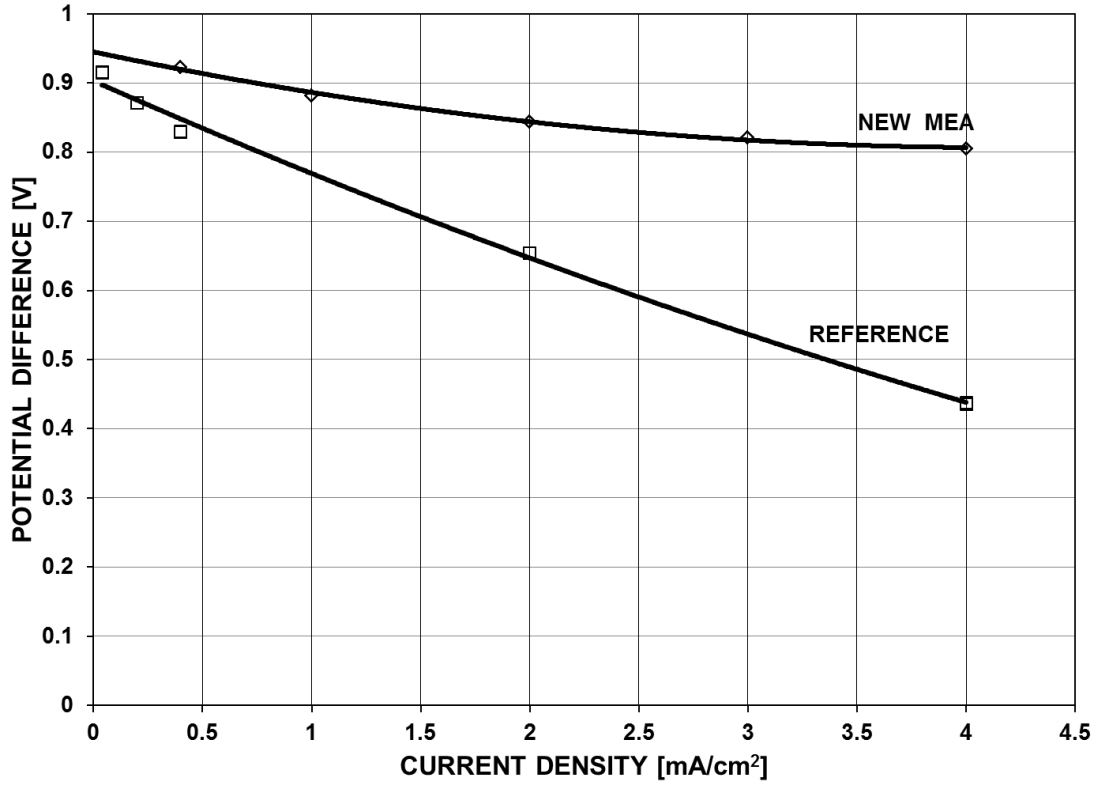


**Figure 3.3** Polarization curve for a hydrogen fueled PAFC: Potential difference between the electrodes [Volts] versus current density [mA/cm$^2$]. Open diamonds are data obtained on a new MEA. Open squares are data obtained on an MEA that had been conditioned in previous experiments with low molecular weight hydrocarbons (ethylene, propane). Anode: Hydrogen flow rate = 9.6 mL/h. Cathode: Air flow rate = 245 mL/min. Temperature = 160°C. Pressure = 1 atm.

The results of two time-on-stream experiments at 160°C are shown in Figure 3.4. Both curves show deactivation, indicated by a decrease in potential difference with time. The data show that deactivation continued for at least 20 h. The two sets of data were obtained at different current densities and different $H_2O$ / n-$C_{16}H_{34}$ molar ratios. The deactivation reported here with n-hexadecane is consistent with deactivation reported earlier by Okrent and Heath [36] during direct hydrocarbon fuel

cell experiments with decane.

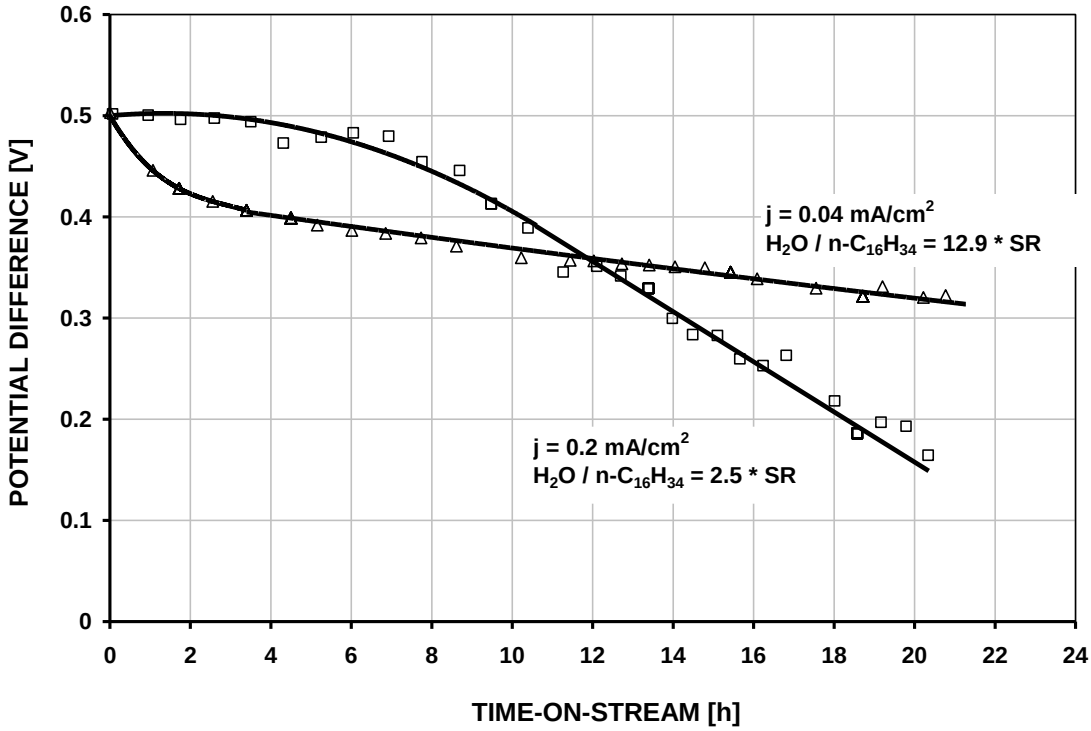


**Figure 3.4** Potential difference between the electrodes [V] versus time-on-stream [h] for an n-hexadecane fueled PAFC. Anode: n-Hexadecane flow rate = 0.2 mL/h. Cathode: Air flow rate = 245 mL/min. Temperature= 160 ℃. Pressure = 1 atm. Open triangles are data obtained with Current density j = 0.04 mA/cm$^2$, Water flow rate = 5.1 mL/h, and $H_2O$ / n-$C_{16}H_{34}$ = 12.9 * SR. Open squares are data obtained with Current density j = 0.2 mA/cm$^2$, Water flow rate = 1 mL/h, and $H_2O$ / n-$C_{16}H_{34}$ = 2.5 * SR.

Two hypotheses can be suggested to explain deactivation. Carbon monoxide, a reaction intermediate formed during the overall reaction to produce the $CO_2$, shown in Figure 3.1, could poison the platinum catalyst at the anode. Carbon monoxide is a well-known poison on fuel cell platinum catalysts [27]. The other possibility is the formation of carbonaceous deposits. Liebhafsky and Cairns [37] indicated the formation of dehydrogenated residues or carbonaceous materials during the operation of fuel cells with hydrocarbon fuels.

The current densities in Figure 3.4 were integrated with respect to time to

obtain the cumulative amount of charge transferred. The potential difference in Figure 3.4 was plotted as a function of cumulative charge transferred in Figure 3.5.

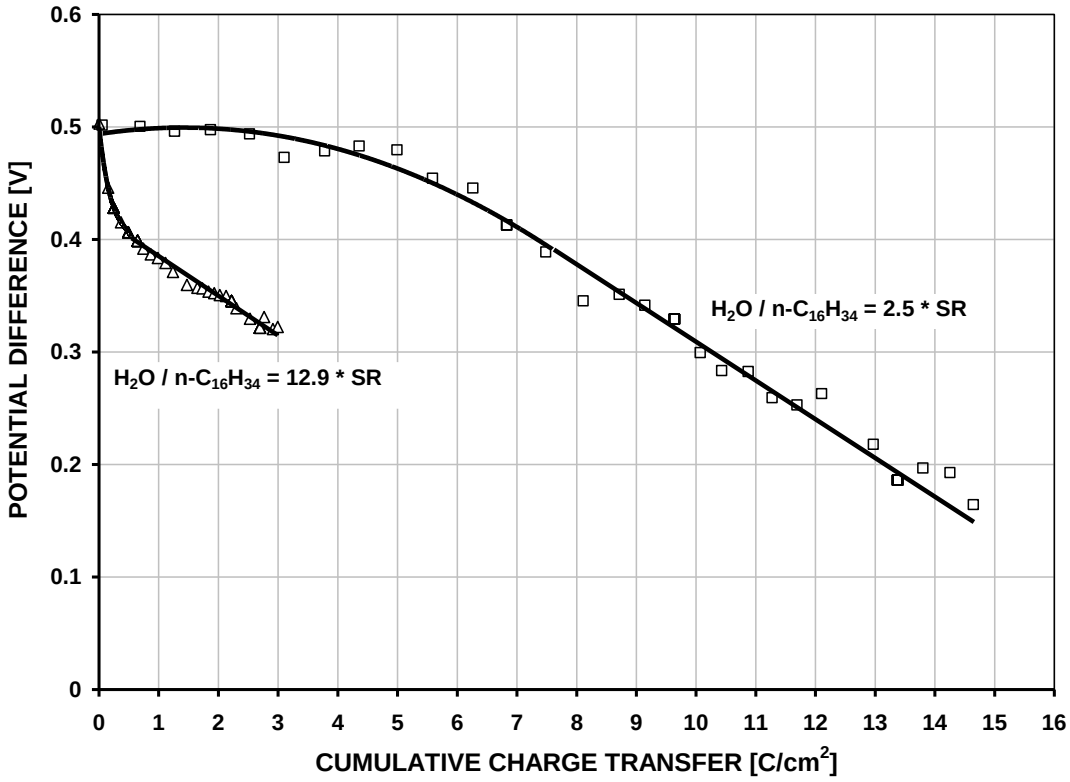


**Figure 3.5** Potential difference between the electrodes [V] versus Cumulative charge transfer [C/cm$^2$] for an n-hexadecane PAFC. Anode: n-hexadecane flow rate =0.2mL/h. Cathode: Air flow rate = 245 mL/min. Pressure = 1 atm. Temperature = 160 ℃. Open triangles are data obtained with Water flow rate = 5.1 mL/h, Current density = 0.04 mA/cm$^2$, and $H_2O$ / n-$C_{16}H_{34}$ = 12.9 * SR. Open squares are data obtained with water flow rate = 1 mL/h, Current density = 0.2 mA/cm$^2$, and $H_2O$ / n-$C_{16}H_{34}$ = 2.5 * SR.

The data indicate that at potential differences less than 0.4 V, the slopes of the two lines are the same. In other words, deactivation is a linear function of charge transferred. That observation suggests that deactivation, as represented by a decrease in potential difference, is related to some phenomenon that correlates with the amount of charge transferred, regardless of the $H_2O$ / n-$C_{16}H_{34}$ molar ratio.

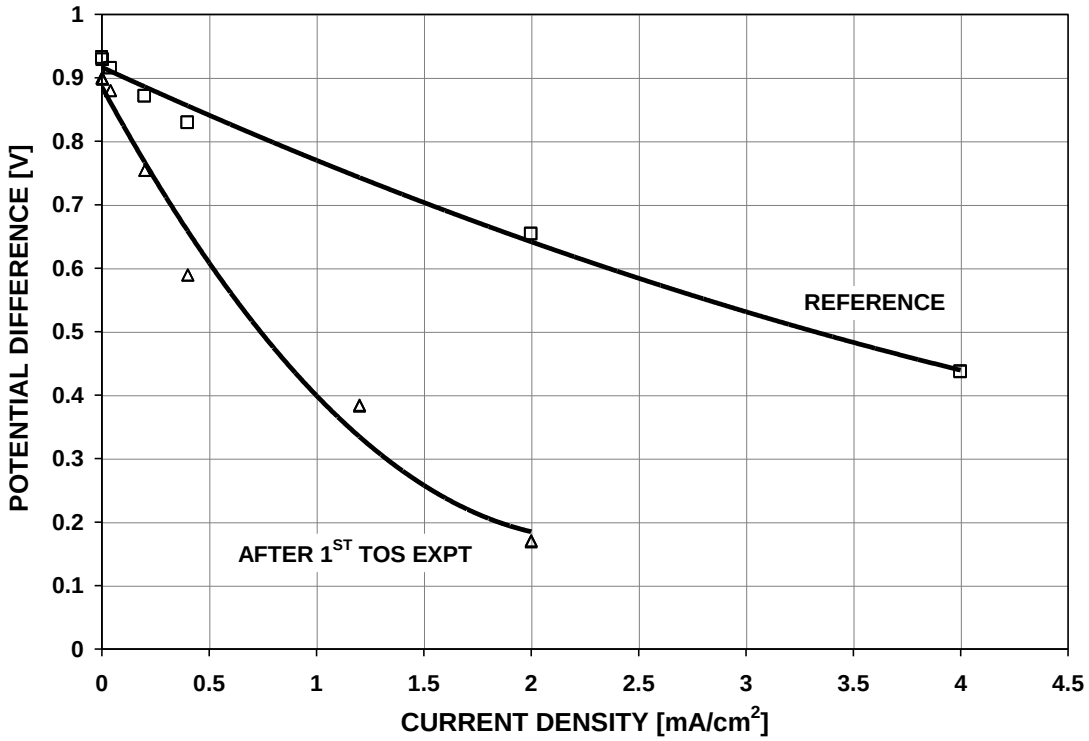


**Figure 3.6** Polarization curve for a hydrogen fueled PAFC: Potential difference between the electrodes versus current density [mA/cm$^2$]. Anode: Hydrogen flow rate = 9.6 mL/min. Cathode: Air flow rate = 245 mL/min. Temperature = 160 ℃. Pressure = 1 atm. Open squares are the Reference polarization curve. Open triangles are the polarization curve obtained after the first time-on-stream experiment.

A hydrogen / air polarization curve was measured using the PAFC after the first TOS experiment at 160°C (2.5*SR, $H_2O$ / n-$C_{16}H_{34}$ = 81). In Figure 3.6, it is compared to the "Reference" hydrogen / air polarization curve, from Figure 3.3. The change between the Reference polarization curve and the one after the first time-on-stream experiment indicates that there had been a definite deterioration in the fuel cell performance. The data in Figure 3.6 are consistent with the deactivation observed during the TOS experiments in Figure 3.4. If the two polarization curves are compared at a constant value of potential difference, the current density is much smaller after the TOS measurements than before. Either the turnover frequency on a reaction site is much smaller, or there are fewer reaction sites at which the reaction

occurs. The only explanation is that something has prevented small hydrogen molecules from reacting to form electrons.

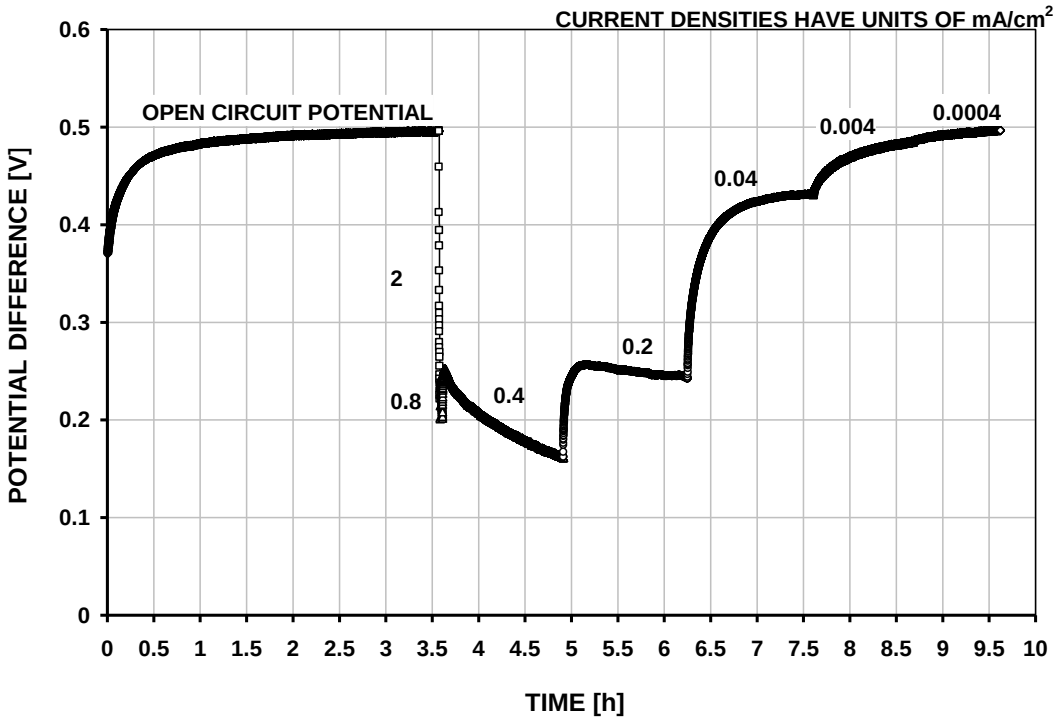


**Figure 3.7** Potential difference between electrodes [V] as a function of time [h] obtained with a PAFC. Anode: Water flow rate = 5.1 mL/h, n-hexadecane flow rate = 0.2 mL/h. Cathode: Air flow rate = 245 mL/min. Temperature = 190°C, Pressure = 1 atm. with an $H_2O/C_{16}H_{34}$ ratio =12.9 * SR. The numbers on the top of each line represent different current densities.

Since deactivation during the TOS experiments was observed using both sets of operating conditions at 160°C, further experiments were performed at a temperature of 190°C. The MEA was treated by operating sequentially with hydrogen (6 h), water (6 h), and hydrogen (6 h). Then a polarization curve was measured. The technique for measuring the polarization curve is indicated in Figure 3.7. The current density was set to a constant value. Then the potential difference was recorded until a steady-state value for the potential was obtained. For one datum point, corresponding to 0.4 mA/cm$^2$, the steady-state value of the potential difference

was extrapolated from the data in Figure 3.7. Generally at least one hour was required to obtain a steady-state value for the potential difference. Finally, the steady-state values of the potential differences obtained in Figure 3.7 were used in Figure 3.8 to construct a polarization curve for the n-hexadecane / water – air fuel cell.

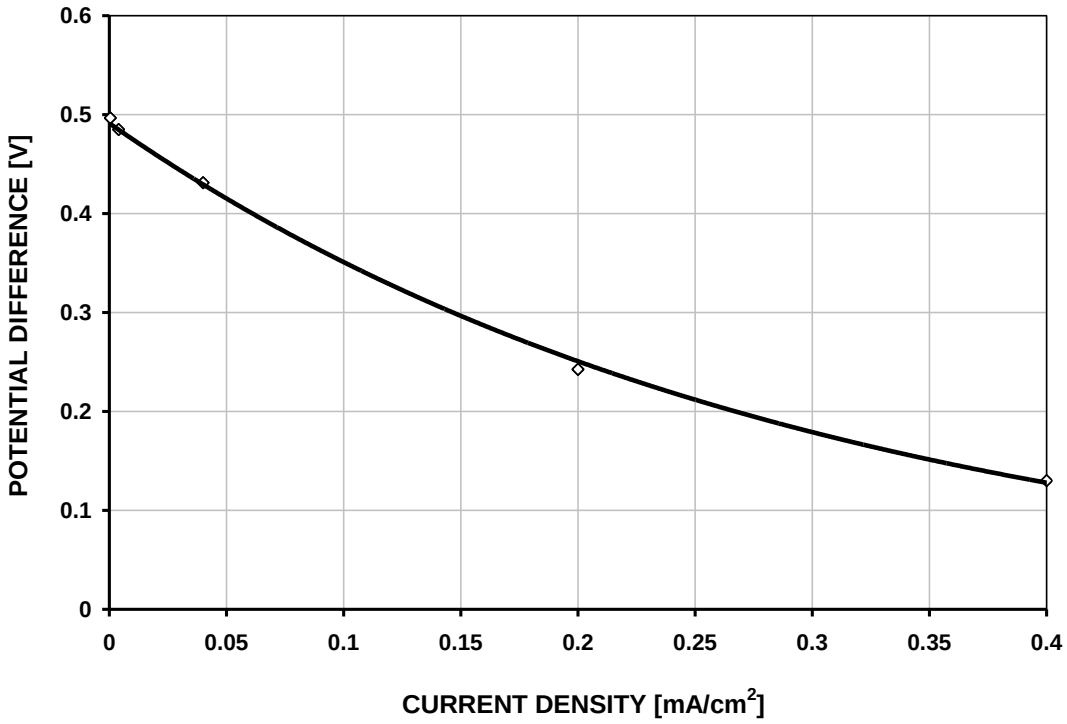


**Figure 3.8** Polarization curve for an n-hexadecane fueled PAFC: Potential difference between the electrodes [V] versus current density [$mA/cm^2$]. Anode: Water flow rate = 5.1 mL/h, n-hexadecane flow rate = 0.2 mL/h. Cathode: Air flow rate = 245 mL/min. Temperature = 190°C. Pressure = 1 atm.

Some of the characteristics of the 190°C n-hexadecane / air polarization curve in Figure 3.8 are noteworthy. The open circuit potential of 0.5 V is much smaller than that of 0.93 V obtained for the hydrogen / air fuel cell in Figure 3.3. It suggests that the results in Figure 3.8 might represent the partial oxidation of carbon,

$$C + \tfrac{1}{2}\, O_2 \longrightarrow CO \qquad E^0_{298} = 0.711 \text{ V} \tag{3.4}$$

as the rate limiting step in the overall reaction rather than the oxidation of n-hexadecane in Equation 3.2. Equation 3.4 is composed of two half-cell reactions:

$$C + H_2O \longrightarrow CO + 2\,H^+ + 2\,e^- \quad \text{anode} \qquad (3.5)$$

$$2\,H^+ + 2\,e^- + \tfrac{1}{2}\,O_2 \longrightarrow H_2O \quad \text{cathode} \qquad (3.6)$$

The difference between 0.711 V and 0.5 V might be caused by a combination of factors: a temperature of 190°C rather than 25°C, a cathode oxygen mole fraction of 0.21, and an anode water vapour mole fraction representing equilibrium water vapour over phosphoric acid. The open circuit potential, 0.5 V, in Figure 3.8 is more consistent with the standard electrochemical potential of the partial oxidation of carbon to carbon monoxide reaction, 0.711 V than with the standard electrochemical potential of the oxidation of carbon monoxide to carbon dioxide ( $CO + \tfrac{1}{2}\,O_2 = CO_2$ $E^0_{298} = 1.33$ V). Initially two possible hypotheses were suggested to explain deactivation: either carbon monoxide poisoning or deposition of carbonaceous material. Equation 3.4 is consistent with the carbonaceous material hypothesis and not consistent with carbon monoxide hypothesis. On that basis the hypothesis of deposition of carbonaceous material seems to be the most likely explanation for the deactivation observed during the time-on-stream experiments.

Time-on-stream measurements were also made at 190°C. The TOS results at 190°C are compared with those at 160°C in Figure 3.9. A steady-state operation was achieved for the last six hours of the experiment at 190°C. A steady-state operation is a highly desirable result that is not always achieved with a comparatively large hydrocarbon molecule, such as hexadecane. For example, Liebhafsky and Cairns [36] reported unsteady cycling during which both the potential and the current oscillated over time periods of approximately 15 minutes, when octane was the hydrocarbon fuel. Although we also observed cycling in some of our experiments, that phenomenon was not the object of our investigation. The fact that a steady-state has been demonstrated here for one set of operating conditions means that in principle fuel cells can operate continuously using n-hexadecane (and presumably other diesel type fuels).

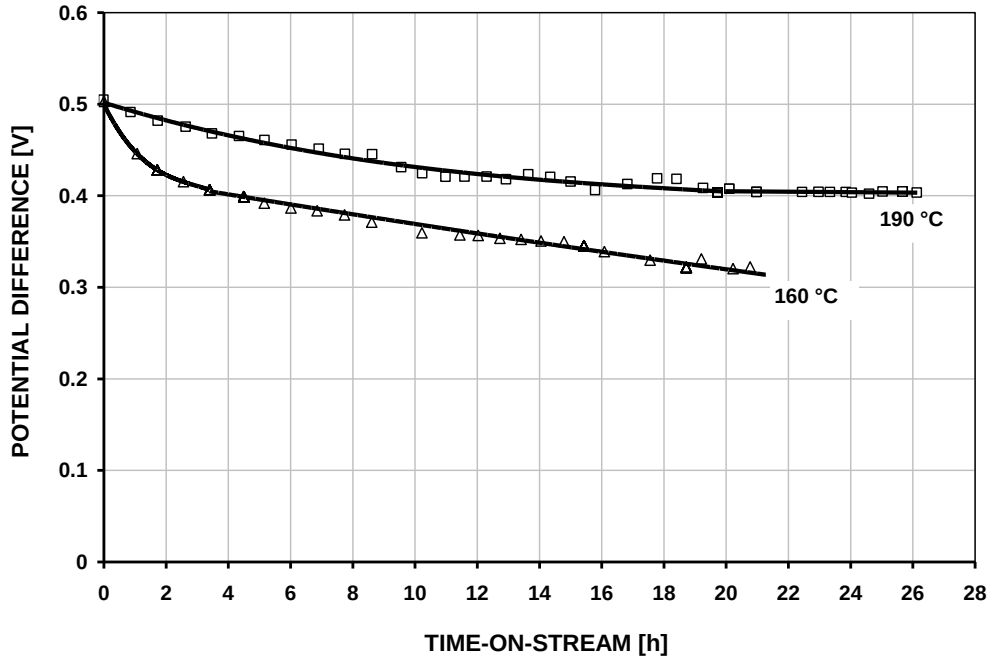


**Figure 3.9** Potential differences between the electrodes [V] versus time-on-stream [h] for an n-hexadecane PAFC. Current density j = 0.04 mA/cm$^2$. Anode: Water flow rate = 5.1 mL/h, n-hexadecane flow rate = 0.2 mL/h. Cathode: Air flow rate = 245 mL/min. Pressure = 1 atm.

Cleaning the MEA with water was mentioned in the discussion pertaining to Figure 3.7. An example of water being the only reactant entering the fuel cell is shown in Figure 3.10. The data in Figure 3.10 were obtained from an MEA that had been used previously for 10 weeks in TOS experiments. When the current density was maintained constant at a value of 0.2 mA/cm$^2$ the potential difference decreased continuously for a period of 6 h. That indicated that a progressively larger over-potential was necessary (a larger driving force was necessary) to maintain the current density at a constant value. When the current density was decreased to 0.1 mA/cm$^2$, there was an initial increase in the potential difference (smaller over-potential). The potential difference gradually decreased over the next 7 h and then remained constant at 0.35 V for the last 6 hours.

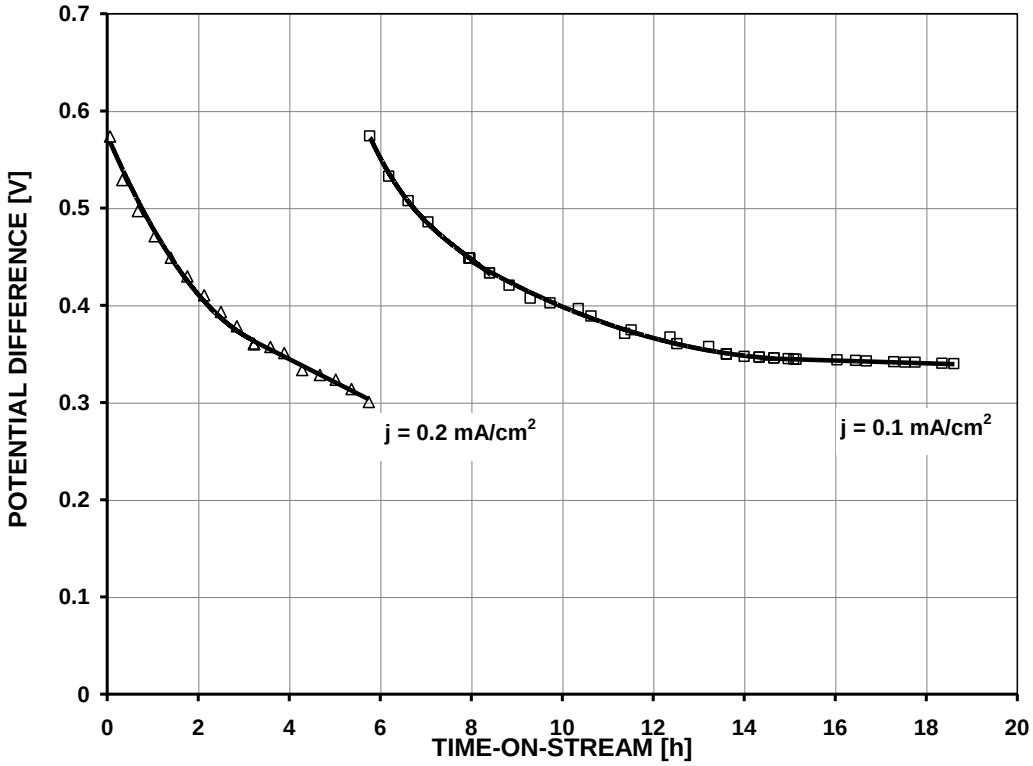


**Figure 3.10** Potential differences between the electrodes [V] as a function of time-on-stream [h] when $H_2O$ was the only feed stock for the anode of a PAFC with a fouled MEA. Anode: Water flow rate = 5.1mL/h. Cathode: Air flow rate = 245 mL/min. Temperature = 190°C. Pressure = 1 atm.

The existence of a current density when only water was fed to the fuel cell would require that some reaction must have been occurring. Since no fuel (eg. no n-hexadecane) was fed to the fuel cell, it is plausible that the reaction may have occurred between water and the carbonaceous material that had been previously deposited on the MEA. The existence of a current density would also require proton migration across the electrolyte. The occurrence of the anode reaction shown in Equation 5 would be consistent with both of these requirements. The measurement of current density when only water was fed to the fuel cell is consistent with the hypothesis that carbonaceous material was formed during deactivation, and was available for reaction during the water only experiment.

After the water-only experiments in Figure 3.10 were completed, a hydrogen

polarization curve was measured. It is compared with the Reference hydrogen polarization curve in Figure 3.11. A comparison of the results in Figure 3.11 (after the water-only experiment) with the results in Figure 3.6 (after the first TOS experiment) indicates that a substantial improvement was caused by the water-only treatment. That suggests the water-only experiment cleaned the MEA. Cleaning of the MEA would be consistent with removal of a carbonaceous deposit from the catalyst surface.

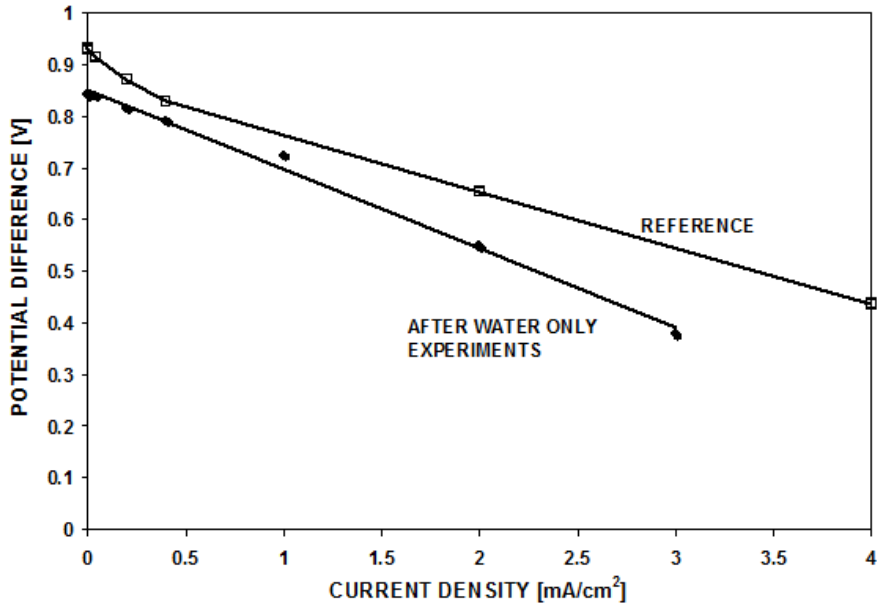


**Figure 3.11** Polarization curve for a hydrogen fueled PAFC: Potential difference between the electrodes versus current density [mA/cm$^2$]. Anode: Hydrogen flow rate = 9.6 mL/min. Cathode: Air flow rate = 245 mL/min. Temperature = 160 ℃. Pressure = 1 atm. Solid circles are data obtained after a one-week experiment with water only (on an MEA that had been used in TOS experiments for ten weeks), Open squares are data for the Reference polarization curve.

The results reported here can be compared with other fuel cell systems. Two of the important criteria are capital cost and energy efficiency. The capital cost is strongly influenced by the size of the fuel cell stack that in turn is a function of current density. The theoretical energy efficiency is related to the thermodynamic

efficiency of the reactions that occur. The reaction networks that occur vary with the particular type of fuel cell system. The operating cost of a fuel cell system is strongly influenced by the energy efficiency.

Small current densities were obtained for the low temperature (190°C) direct hydrocarbon (n-hexadecane) PAFC results without a reforming unit reported here. There are extensive reviews describing results obtained by PAFCs operating on hydrocarbons without a reforming unit [2-4]. In general the current densities are quite small. Therefore large reactors having a large capital cost would be required. In contrast Kim et al. [38] reported much larger current densities using a higher temperature (700°C) solid oxide fuel cell, SOFC, without a reforming unit when it was operating on synthetic diesel fuel. Interest in these systems, specifically the development of anodes continues to be an active area of research [39, 40]. There have been several reviews of direct hydrocarbon SOFCs without reforming units [13, 41, 42]. Although no reforming unit was used, they indicate that internal reforming occurs [13]. Unfortunately the reforming reaction (internal or external) has a negative effect on energy efficiency. Approximately 25 % percent of the hydrocarbon fuel must be used to provide the endothermic heat of reaction for the reforming reaction. At the low temperatures used in this study the reforming reaction is thermodynamically unfavourable and does not occur. Therefore the high temperature SOFC systems will have a capital cost advantage over the lower temperature PAFC system used here. However, the lower temperature PAFC system used here will have a theoretical energy efficiency advantage over the SOFC system.

The use of an external reformer in combination with a PAFC system is a well-established technology that converts the hydrocarbon to hydrogen in a fuel processing system and then uses the hydrogen as the fuel in a fuel cell system. By the year 2006 more than 200 commercial plants had been sold [43]. Nevertheless research on improving the reforming process continues [44]. The reforming reaction in an external reformer has the same negative effect on energy efficiency that was mentioned above for internal reforming. The fuel processing system includes four

processes: steam reforming, high-temperature water shift, low-temperature shift, and hydrogen purification. Equipment for those four processes has a substantial capital cost. In contrast there is no capital cost for a reformer / fuel processor with the low-temperature direct hydrocarbon PAFC system described here.

### 3.4 Conclusions

This study reported the first polarization curve ever measured for which n-hexadecane was the fuel at the anode of a fuel cell. The current densities were found to be very small.

Deactivation was observed in time-on-stream experiments. Deactivation, as measured by the change in potential difference, was found to be a linear function of the cumulative charge transferred across the electrolyte of the fuel cell. Deactivation during fuel cell experiments with n-hexadecane was confirmed by comparing hydrogen polarization curves before and after the time-on-stream measurements. For a given potential difference the current densities were much smaller for the hydrogen polarization curves measured after the time-on-stream experiments.

Experiments were performed in which water was the only reactant entering the fuel cell that had been used previously for 10 weeks in time-on-stream experiments. Current densities were measured during those experiments, indicating that the water must have reacted with some type of species that remained on the fuel cell catalyst at the end of the time-on-stream experiments. When a hydrogen polarization curve was measured at the end of the water-only experiments, it was close to that measured before the time-on-stream experiments. That indicates that the deactivating species on the surface of the platinum particles had been removed, and that it was possible to regenerate deactivated MEAs.

A hypothesis, that carbonaceous material was deposited on the platinum anode catalyst particles, was suggested to explain the deactivation. Four types of

observations were consistent with that hypothesis: (a) The change in potential difference during time-on-stream measurements, (b) When hydrogen polarization curves measured before and after the time-on-stream experiments were compared, the current densities measured after TOS were much smaller than those measured before TOS, (c) Current densities were measured when water was the only reactant entering the fuel cell. In order to produce a current density, water must have reacted with some type of species that had been deposited on the surface of the platinum particles, and (d) The open circuit potential of a n-hexadecane fuel cell, 0.5 V, was much closer to the standard electrochemical potential for the carbon – water reaction, 0.711 V than to that for the carbon monoxide – water reaction, 1.33 V. Observation (d) makes a hypothesis of deactivation by carbonaceous materials more likely than deactivation by carbon monoxide poisoning.

Steady-state operation of the n-hexadecane fuel cell, without additional deactivation, was observed at one set of fuel cell operating conditions. That observation demonstrates that stable fuel cell operation is technically feasible when n-hexadecane is the fuel at the anode of a fuel cell. It suggests there is merit in investigating fuel cell operation with commercial fuels such as petroleum diesel or bio-diesel.

### 3.5 Conflict of Interests

The authors declare that there is no conflict of interest regarding the publication of this paper.

### 3.6 Acknowledgment

The authors gratefully acknowledge that this research and development project was supported by a grant from Transport Canada's Clean Rail Academic Grant Program, and by a Discovery Grant from the Canadian Government's Natural Sciences and Engineering Research Council.

## 3.7 References


[1] J.A.A. Ketelaar, “History”, in Fuel Cell Systems (eds. L.J.M.J. Blomen and M.N. Mugerwa, Plenum Press, New York, p. 20, 1993.

[2] E.J.Cairns, “Anodic oxidation of hydrocarbons and the hydrocarbon fuel cell,” *Advances in Electrochemistry Science and Electrochemical Engineering*”, vol. 8, pp. 337-392, 1971.

[3] J.O.M. Bockris and S. Srinivasan, “Electrochemical combustion of organic substances”, in Fuel Cells Their Electrochemistry, pp. 357-411, McGraw-Hill, New York, 1969.

[4] H.A. Liebhafsky and E.J. Cairns, “The direct hydrocarbon fuel cell with aqueous electrolytes”, in Fuel Cells and Fuel Batteries, pp. 458-523, Wiley, New York, 1968.

[5] S. Bertholet, “Oxydation Electrocatalytique du Methane”, Ph.D. Dissertation, Universit éde Poitiers, France, 1998.

[6] C.K. Cheng, J.L. Luo, K.T. Chuang, and A. Sanger, ‘’Propane fuel cells using phosphoric-acid-doped polybenzimidazole membranes’’, *Journal of Physical Chemistry B*, vol. 109, pp. 13036-13042, 2005.

[7] O. Savadogo, F.J. Rodriguez Varela, ‘’Low-temperature direct propane polymer electrolyte membrane fuel cells’’, *Journal of New Materials for Electrochemical Systems*, vol. 4, pp. 93-97, 2001.

[8] F.J. Rodriguez Varela, “Real-time mass spectrometric analyses of the anode exhaust gases of a direct propane fuel cell”, *Journal of the Electrochemical Society*, vol. 152, pp. A1755-A1762, 2005.

[9] Heo, P., Ito, K., Tomita, A., Hibino, T., “A proton-conducting fuel cell operating with hydrocarbon fuels”, *Angewandte Chemie International Edition*, vol. 47, pp. 7841-7844, 2008.

[10] Steele, B.C.H., Kelly, H., Middleton, H., Rudkin, R., "Oxidation of methane in solid state electrochemical reactors", **Solid State Ionics**, vol. 28-30, pp. 1547-1552, 1988.

[11] Murray, E.P., Tsai, T., Barnett, S.A., "A direct-methane fuel cell with a ceria based anode", *Nature*, vol. 400, pp. 649-651, 1999.

[12] Zhu, W, Xia, C., Fan, J., Peng, R., et Meng, G., "Ceria coated Ni as anodes for direct utilization of methane in low-temperature solid oxide fuel cells", *Journal of Power Sources*, vol. 160, pp. 897-902, 2006.

[13] Gross, M.D., Vohs, J.M., Gorte, R.J., "Recent progress in SOFC anodes for direct utilization of hydrocarbons", *Journal of Materials Chemistry*, vol. 17, pp. 3071-3077, 2007.

[14] Lee, J.G., Lee, C.M., Park, M, Shul, Y.G., "Direct methane fuel cell with $La_2Sn_2O_7$ – $Gd_{0.1}Ce_{0.9}O_{1.95}$ anode and electrospun $La_{0.6}Sr_{0.4}Co_{0.2}Fe_{0.8}O_{3-\delta}$ a –a $Gd_{0.1}Ce_{0.9}O_{1.95}$ cathode", *Royal Society of Chemistry Advances*, vol. 3, pp. 11816-11822, 2013.

[15] Dong, D., Liu, Z., Li, L., Xia, C., "An octane-fueled low temperature solid oxide fuel cell with Ru-free anodes*", Electrochemistry Communications*, vol. 10, pp. 1295-1298, 2008.

[16] Kishimoto, H., Yamaji, K., Horita, T., Xiong, Y., Sakai, N., Brito, M., Yokokawa, H., "Feasibility of liquid hydrocarbon fuels for SOFC with Ni-ScSZ anode", *Journal of Power Sources*, vol. 172, pp. 67-71, 2007.

[17] Zhou, Z.F., Callo, C. Pague, M.B., Schobert, H., Lvov, S.N., ''Direct oxidation of jet fuels and Pennsylvania crude oil in a solid oxide fuel cell'', *Journal of Power Sources*, vol. 133, pp. 181-187, 2004.

[18] G. Psofogiannakis, Y. Bourgault, B.E. Conway, and M. Ternan: "Mathematical model for a direct propane phosphoric acid fuel cell", *Journal of Applied*

*Electrochemistry*, vol 36, pp. 115-130, 2006.

[19] H.R. Khakdaman, Y. Bourgault, M. Ternan, "Computational modeling of a direct propane fuel cell", *Journal of Power Sources*, vol. 196, pp. 3186-3194, 2011.

[20] H.R. Khakdaman, Y. Bourgault, M. Ternan, "A direct propane fuel cell anode with interdigitated flow-fields: 2D model", *Industrial Engineering Chemistry Research*, vol. 49, pp. 1079-1085, 2010.

[21] G. Psofogiannakis, A. St-Amant, and M. Ternan, "Ab-initio DFT study of methane electro-oxidation mechanism on platinum", *Journal of Physical Chemistry B*, vol. 110, pp. 24593-24605, 2006.

[22] S. Vafaeyan, A. St-Amant, and M. Ternan, "Nickel alloy catalysts for the anode of a high temperature PEM direct propane fuel cell", *Journal of Chemistry*, doi.org/10.1155/2014 /151638, 8 pages, 2014a.

[23] S.Vafaeyan, A. St-Amant, M. Ternan, "Propane fuel cells: Selectivity for partial or complete reaction", *Journal of Fuels*, doi.org/10.1155/2014/485045, 9 pages, 2014b.

[24] A. Al-Othman, A.Y. Tremblay, W. Pell, S. Letaief, B.A. Peppley, M. Ternan, "A modified silicic acid (Si) and sulphuric acid (S) – ZrP/PTFE/glycerol composite membrane for high temperature direct hydrocarbon fuel cells", *Journal of Power Sources*, vol. 224, pp. 158-167, 2013.

[25] A. Al-Othman, A.Y. Tremblay, W. Pell, Y. Liu, B.A. Peppley, M. Ternan, "The effect of glycerol on the conductivity of Nafion-free ZrP/PTFE composite membrane electrolytes for direct hydrocarbon fuel cells", *Journal of Power Sources*, vol. 199, 14-21, 2012.

[26] A. Al-Othman, A.Y. Tremblay, W. Pell, S. Letaief, T.J. Burchell, B.A. Peppley, M. Ternan, "Zirconium phosphate as the proton conducting material in direct

hydrocarbon PEM fuel cells operating above the boiling point of water", *Journal of Power Sources*, vol. 195, pp. 2520-2525, 2010.

[27] C.G. Farrell, C.L. Gardner, and M. Ternan, "Experimental and modeling studies of CO poisoning in PEM fuel cells", *Journal of Power Sources*, vol. 171, pp. 282-293, 2007.

[28] R. Fonocho, C. Gardner, M. Ternan, "A study of the electrochemical hydrogenation of o-xylene in a PEM hydrogenation reactor", *Electrochimica Acta*, vol. 75, pp. 171-178 2012.

[29] N. Sammes, R. Bove and K. Stahl, "Phosphoric acid fuel cells: Fundamentals and applications," *Current Opinion in Solid State and Materials Science*, vol. 8, pp. 372-378, 2004.

[30] J.M. King and H.R. Kunz, "Phosphoric acid electrolyte fuel cells," in *Handbook of Fuel Cells*, eds. W. Vielstich, A. Lamm, H.A. Gasteiger, and H.Yokokawa, Wiley, New York, vol. 1, pp. 287-300, 2010.

[31] S. R. Choudhury, "Phosphoric acid fuel cell technology," in *Recent Trends in Fuel Cell Science and Technology*, ed. S. Basu Springer, pp. 188-216, 2007.

[32] W.T. Grubb and C.J. Michalske, "A high performance propane fuel cell operating in the temperature range of 150°-200°C", *Journal of the Electrochemistry Society*, vol. 111, no. 9, pp.1015-1019, 1964.

[33] H.A. Liebhafsky, and W.T. Grubb, "Normal Alkanes at platinum anodes", American Chemical Society, *Fuel Preprints*, vol. 11, no. 2, p.134, 1967

[34] V.S. Bagotzky, Yu. Vassiliev, and O.A. Khazova, "Generalized Scheme of Chemisorpiton, Electrooxidation, and Electroreduction, of simple organic compounds on platinum group metals", *Journal of Electroanalytical Chemistry*, vol. 81, pp. 229-238, 1977.

[35] T.F. Fuller, F.J. Luczak, and D.J. Wheeler, "Electrocatalyst utilization in

phosphoric acid fuel cells", *Journal of the Electrochemical Society*, vol. 142, no. 8, pp. 1752-1755, 1995.

[36] E.H. Okrent and C.E. Heath, "A liquid hydrocarbon fuel cell battery", in Fuel Cell Systems (ed. B. Baker). *Advances in Chemistry*, American Chemical Society, Washington, D.C., pp. 328-340, 1969.

[37] H.A. Liebhafsky, and E.J. Cairns, "The direct hydrocarbon fuel cell with aqueous electrolytes", in *Fuel Cells and Fuel Batteries*, Wiley, New York, 1968, p.485, p. 510.

[38] H. Kim, S. Park, J.M. Vohs, R.J. Gorte, "Direct oxidation of liquid fuels in a solid oxide fuel cell", *Journal of the Electrochemical Society*, vol. 148, no. 7, pp. A693-A695, 2001

[39] S. Islam, J.M. Hill, "Barium oxide promoted Ni/YSZ solid-oxide fuel cells for direct utilization of methane", *Journal of Materials Chemistry A*, vol. 2, no. 6, pp.1922-1929, 2014.

[40] C. Yang, J. Li, Y. Lin, J. Liu, F.Chen, M. Liu, "In-situ fabrication of CoFe allot nanoparticles structure $(Pr_{0.4}Sr_{0.6})_3$ $(Fe_{0.85}Nb_{0.15})O_7$ ceramic anode for direct hydrocarbon solid oxde fuel cells", *Nano Energy*, 11, pp.704-711, 2015.

[41] S. McIntosh, R.J. Gorte, "Direct hydrocarbon solid oxide fuel cells", *Chemical Reviews*, Vol. 104, pp. 4845-4865, 2004.

[42] Y. Zhao, C. Xia, L. Jia, Z. Wang, H. Li, J. Yu, Y. Li, "Recent progress on solid oxide fue cells: Lowering temperature and utilizing non-hydrogen fuels", *International Journal of Hydrogen Energy*", vol. 38, pp. 16498-16517, 2013.

[43] S. Srinivasan, "*Fuel cells: from fundamentals to applications*", Springer, New York, 2006, pp. 505-514.

[44] M.R. Walluk, J. Lin, M.G. Waller, D.F. Smith, T.A. Trabold, "Diesel auto-thermal reforming for solid oxide fuel cell systems: Anode off-gas recycle

simulation", Applied Energy, vol. 130, pp. 94-102, 2014.

# Chapter 4 - Petroleum diesel and biodiesel fuels used in a direct hydrocarbon phosphoric acid fuel cell


## Abstract

The performance of a direct hydrocarbon phosphoric acid fuel cell, PAFC, was investigated using petroleum diesel, biodiesel, and n-hexadecane as the fuels. We believe this is the first study of a fuel cell being operated with petroleum diesel as the fuel at the anode. Degradation in fuel cell performance was observed prior to reaching steady-state. The degradation was attributed to a carbonaceous material forming on the surface of the anode. Regardless of the initial degradation, a steady-state operation was achieved with each of the diesel fuels. After treating the anode with water the fuel cell performance recovered. However, the fuel cell performance degraded again prior to obtaining another steady-state operation. There were several observations that were consistent with the suggestion that the carbonaceous material formed from the diesel fuels might be a reaction intermediate necessary for steady-state operation. Finally, the experiments indicated that water in the phosphoric acid electrolyte could be used as the water required for the anodic reaction. The water formed at the cathode could provide the replacement water for the electrolyte, thereby eliminating the need to provide a water feed system for the fuel cell.

## 4.1 Introduction

The long-term objective of this research is to replace the diesel fuel combustion engines currently used in rail locomotives with fuel cell stacks operating on low sulphur (15 ppm) diesel fuel. Fuel cells have at least three advantages.

Greater energy efficiency is one advantage. The maximum operating temperature of the steel in combustion engines limits the engine's theoretical Carnot energy efficiency to about 67%. Many types of fuel cells operate at much lower temperatures and are not limited by the temperature characteristics of materials. Theoretically some fuel cells can have much greater energy efficiencies than combustion engines.

Diminished emissions of both greenhouse gas emissions ($CO_2$, $CH_4$, and $N_2O$) and other air contaminants ($NO_X$, CO, HC, $SO_X$, particulate matter) are another advantage. Because fuel cells are expected to have greater energy efficiency they will use less fuel and therefore emit less $CO_2$ and less $SO_X$. The formation of $N_2O$ and $NO_X$ by reaction between $O_2$ and $N_2$ in air are thermodynamically unfavorable at low fuel cell operating temperatures ( < 200°C). $CH_4$ is not produced because H radicals from diesel fuel become protons and are not available to form $CH_4$. Oligomerized hydrocarbon molecules that might become particulate matter (PM) are adsorbed by the fuel cell catalyst. Because CO is strongly adsorbed by platinum fuel cell catalysts, it is unlikely to be emitted.

Diminished locomotive idling is another advantage. Low temperature (< 200°C) fuel cells can start and stop quickly. The rapid start-up ability would also permit locomotives to shut down on some of the occasions during which they now idle. That would use less fuel and increase both energy efficiency and diminish emissions.

There is another advantage. Fuel cells have almost no moving parts. As a result maintenance costs for fuel cells may be a fraction of those for combustion engines.

In this work the performance of real diesel fuels (petroleum diesel and biodiesel) and n-hexadecane, a pure compound used as a model for diesel fuel (Cetane Number = 100), were investigated in a low temperature (T< 200°C) phosphoric acid fuel cell. Currently fuel cells using hydrogen fuel are being used in locomotives for underground mining where constraints on air quality exist. However, technology for fuel cells using real diesel fuel in locomotives operating above ground is essentially non-existent.

Real diesel fuels are composed of many different compounds. As a result many different reactions will occur in fuel cells that use them as fuels. The reactions with the n-hexadecane model compound provide a basis for an extrapolation to real diesel fuels that may indicate the complexity of their reactions.

In a direct n-hexadecane phosphoric acid fuel cell, the overall reaction is

$$C_{16}H_{34}\,(g) + 49/2\ O_2\,(g) \longrightarrow 16\ CO_2\,(g) + 17\ H_2O\,(g) \qquad (4.1)$$

The anode half-cell reaction is

$$C_{16}H_{34}\,(g) + 32\ H_2O\,(g) \longrightarrow 16\ CO_2\,(g) + 98\ H^+ + 98\ e^- \qquad (4.2)$$

The cathode half-cell reaction is

$$49/2\ O_2\,(g) + 98\ H^+ + 98\ e^- \longrightarrow 49\ H_2O\,(g) \qquad (4.3)$$

where the (g) represents the gas phase. The anode stoichiometric ratio, SR = $H_2O/C_{16}H_{34}$ is 32. One mole of n-hexadecane reacts with 32 moles of water at the anode and generates 98 moles of protons and electrons. The protons migrate through the electrolyte to the cathode where the oxygen reduction reaction occurs.

Very few studies of fuel cells operating with commercially available diesel

fuels have been reported. Almost all of the reports available in the literature have been performed using high temperature (700-1000°C) solid oxide fuel cells. Zhou et al. [1] used jet fuel. Sasaki et al. [2] performed two studies using biodiesel [2,3]. Kim et al. [4] used a synthetic diesel fuel. The other studies were performed using pure compounds, n-hexadecane [5], dodecane [6], and iso-octane [7]. The only study using a lower temperature (150°C) phosphoric acid fuel cell was performed with a series of pure n-alkane compounds from methane to n-hexadecane [8].

Direct hydrocarbon fuel cells, DHFCs, operating at low temperature were investigated in the past. Three reviews of the DHFC work up to the 1960's [9-11] are available. Since then research on DHFCs has continued. Low temperature fuel cell studies (<100°C) were performed on methane by Bertholet [12], on propane by Cheng et al. [13] and by Savadogo and Rodriquez [14,15]. Heo et al. [16] performed intermediate temperature fuel cell studies (100 - 300°C) using propane.

Phosphoric acid fuel cell technology using hydrogen as a fuel is used in commercial practice. By the year 2006 more than 200 commercial plants had been sold [17]. Appleby [18] has described the current state of PAFC technology using hydrogen as a fuel.

### 4.2 Experimental

A schematic diagram of the direct diesel fueled phosphoric acid fuel cell system (PAFC) is shown in Figure 4.1. The overall system consists of an air cylinder, a hydrogen cylinder, one galvanostat, two syringe pumps, a vaporizer, a Phosphoric Acid Fuel Cell (PAFC = Electrochem FC-25-02MA), and a fuel cell test station. Both gaseous and liquid fuels can be used in this fuel cell system. Deionized water and a diesel fuel were introduced into the vaporizer by separate syringe pumps. The liquid fuels were expected to vaporize before reaching the anode of the fuel cell. Air was fed to the cathode at a constant flow rate. On those occasions when hydrogen was used as the fuel, the pumps were stopped and the valve in Figure 4.1 was opened.

Three diesel fuels were compared with n-hexadecane. The petroleum diesel fuel was purchased from an Imperial Oil service station. It meets the specifications in the American Standards for Testing Materials standard ASTM D-975. Its minimum cetane number is 40 and its sulphur content was less than 15 ppm. The soybean biodiesel used in this study was produced from degummed soybean oil. The following reagents were used in its production: sodium methoxide (25 wt% in methanol solution, Sigma Aldrich), methanol (Assay: 99.3-99.9 %, Optima® grade, Fisher scientific), and hydrochloric acid (36.5–38%, reagent grade, Fisher Scientific). The soya-biodiesel was produced by transesterifying degummed soybean oil in a two-stage process using a solution of sodium methoxide in methanol. The first transesterification was performed in a membrane reactor [19] using a mole ratio of 5/1 methanol to oil. The methanol used in this reaction contained 0.5 wt% sodium methoxide on an oil basis. The mixture having passed through the membrane was further reacted in a batch process using a mole ratio of 2/1 methanol to oil. The methanol in the second reaction contained 0.2 wt% sodium methoxide catalyst on an oil basis. The fatty acid methyl ester, FAME, from the second reaction was neutralized and washed with water and then dried under vacuum. It was tested and met ASTM 6751 and EN14105 standards for glycerol, mono, di and triglycerides. The biodiesel produced from canola oil was purchased from Milligan Biofuels Inc. (Foam Lake, SK, Canada). It was used as received from the manufacturer and labeled "canola-biodiesel". It was specified to have a cetane number of 50.34 and a sulphur content of 2.8 ppm.

The membrane electrode assembly (MEA) used in our fuel cell work had five layers: two gas diffusion layers (GDL), two catalyst layers (CL) and a liquid electrolyte layer. The gas diffusion layers were Teflon™ coated Toray paper. The liquid electrolyte was initially 85% (14.6 M) phosphoric acid, which was held in a SiC matrix between the anode and cathode catalyst layers. Platinum (0.5 mg Pt / $cm^2$) supported on carbon (10% Pt on C) was the catalyst in both anode and cathode catalyst layers. The fuel cells had a face area of 25 $cm^2$. A pin-type flow field was

machined in a graphite plate. The current collectors were sheets of copper metal that had been gold plated on both sides. Silicone rubber flexible heaters were attached to each current collector.

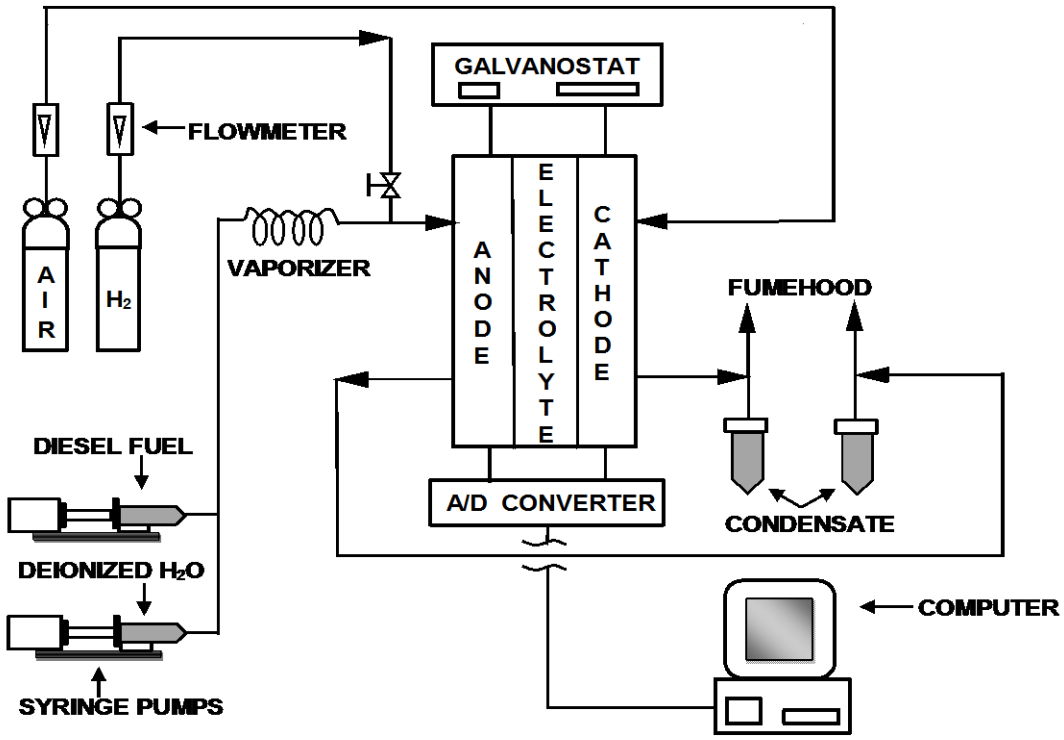


**Figure 4.1** Diagram of A Direct Hydrocarbon Phosphoric Acid Fuel Cell System.

Several types of experiments were performed. A polarization curve shows the potential difference as a function of current density. Diesel fuel polarization curves were measured. Three types of time-on-stream experiments were performed ($H_2O$ with diesel fuel, n-$C_{16}H_{34}$ only, and $H_2O$ only). The time-on-stream experiments were performed at (a) an anode diesel fuel flow rate of 0.2 mL/h, anode water flow rate of 5.1 mL/h, cathode air flow rate of 245 mL/min, (b) current densities of 0.4 mA/cm$^2$, and (c) a temperature of 190°C and a pressure of 1 atm. Hydrogen polarization curves were measured to determine the state of the MEA in the fuel cell, using an anode hydrogen flow rate of 9.6 mL/min, cathode air flow rate of 245 mL/min., a temperature of 160°C, and a pressure of 1 atm.

A Hokuto Denko HA-301 Galvanostat was used to adjust the potential difference between the anode and cathode of the phosphoric acid fuel cell to maintain the chosen current at a constant value. The potential difference was recorded every second using a Lab View data logger.

Concentrated petroleum diesel or biodiesel samples were prepared in $CDCl_3$ and placed in 5 mm NMR tubes. The volume ratio of sample to $CDCl_3$ was approximately 80:20. All $^{1}H$ and $^{13}C$ NMR data were collected on a Bruker AVANCE 500 NMR spectrometer operating at 500.13 MHz and 125.77 MHz for $^{1}H$ and $^{13}C$, respectively. The $^{1}H$ NMR spectra were collected using a 30 ° pulse, 16 scans and a 3.9 s inter-pulse spacing. The time domain data were processed without apodization. The $^{13}C$ NMR spectra with inverse gated $^{1}H$ decoupling were collected using a 30 ° pulse, a 60 s recycle delay and at least 1024 scans. Under these conditions the $^{13}C$ NMR spectra were deemed to be semi-quantitative. $^{13}C$ DEPT-135 spectra were collected with a 2 s recycle delay and at least 32 scans. All $^{13}C$ time domain data were processed with 3 Hz of exponential line broadening.

**4.3 Results and Discussion**

Polarization curves for a phosphoric acid fuel cell operating on n-hexadecane are shown in Figure 4.2. As with all polarization curves, the potential difference decreases as the current density increases. The decrease is greater for the polarization curve obtained with the used MEA than with the cleaned MEA. As will be explained later, carbonaceous deposits may have accumulated on the used MEA during previous experiments. The larger decrease in potential difference observed with the used MEA might have been caused by a greater quantity of carbonaceous material on the anode surface and therefore by the availability of a smaller number of catalyst sites. It should be noted that the potential difference at open circuit potential (at current density = zero) is somewhat greater for the used MEA than for the cleaned MEA. This phenomenon is also apparent in some of the other data in subsequent figures. One explanation is that the accumulated carbonaceous deposits on the used MEA

provide more reactant than is available on the cleaned MEA.

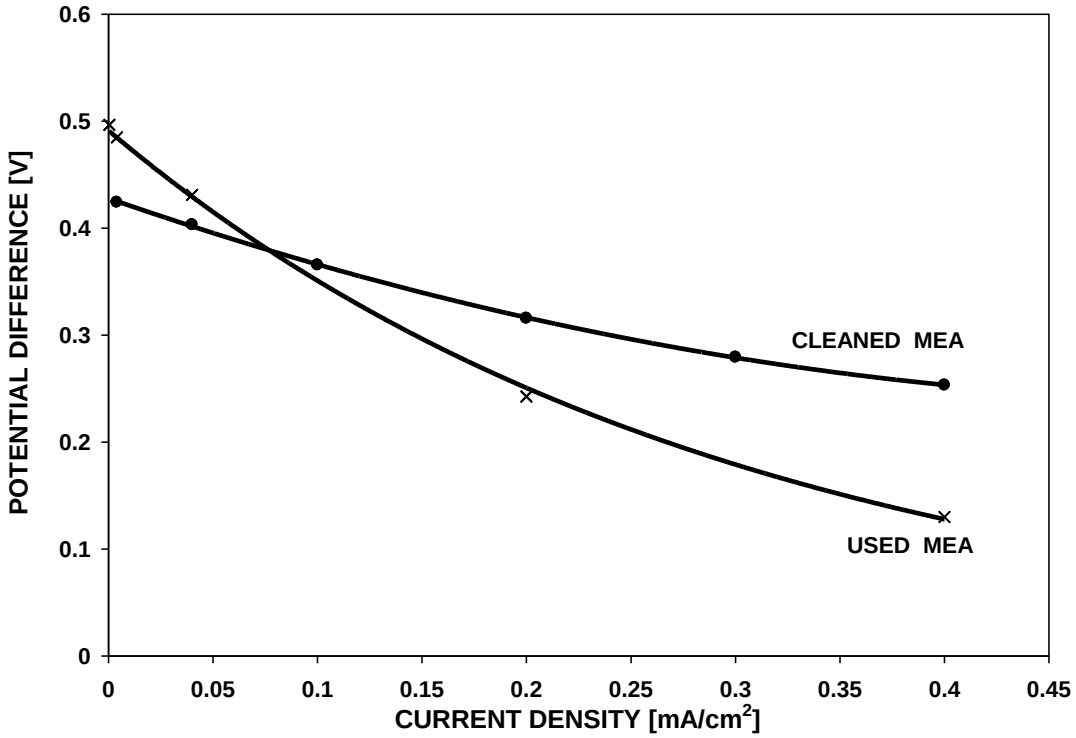


**Figure 4.2** Polarization curve for an n-hexadecane fueled PAFC: Potential difference between the electrodes [V] versus current density [mA/cm$^2$]. Anode: Water flow rate = 5.1 mL/h, n-hexadecane flow rate = 0.2 mL/h. Cathode: Air flow rate = 245 mL/min. Temperature = 190 ℃. Pressure = 1 atm.

Polarization curves for several diesel fuels, petroleum diesel, canola biodiesel, and soybean biodiesel, are compared with n-hexadecane in Figure 4.3. Each of the data sets was obtained immediately prior to the beginning of a time-on-stream, TOS, experiment with the same diesel fuel. The data for the Canola biodiesel were obtained using a recently cleaned MEA. The data for the other diesel fuels were obtained with an MEA that had been used for many experiments prior to the measurements in Figure 4.3. The data obtained with the used MEA are substantially worse than those obtained with the recently cleaned MEA. The diminished performance with the used MEA in Figure 4.3 is consistent with an accumulation of carbonaceous deposits during the prior TOS experiments. CO poisoning of the

platinum catalyst would have been an alternative explanation for the degradation in fuel cell performance. That explanation was discounted since the rapid oscillations in potential difference [20] observed with CO poisoning were not observed here.

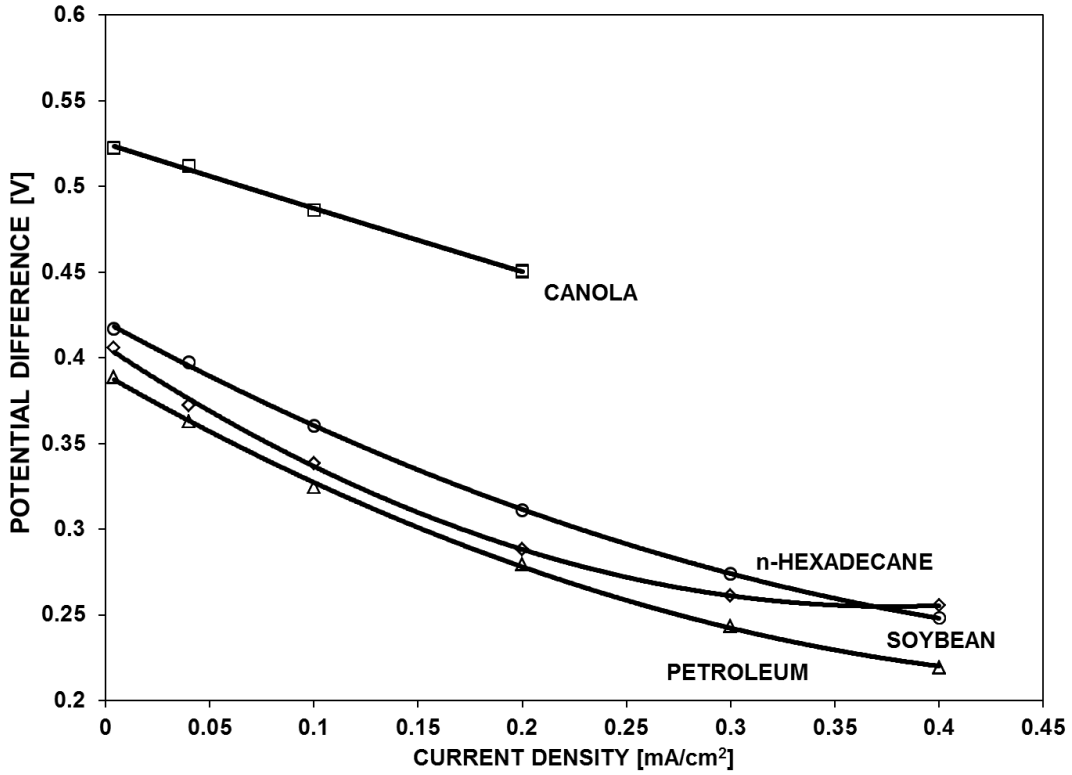


**Figure 4.3** Potential difference between the electrodes [V] versus current density [mA/cm$^2$] for a diesel fuel / water PAFC. Current density j = 0.04 mA/cm$^2$. Anode: Water flow rate = 5.1 mL/h, Fuel flow rate = 0.2 mL/h. Cathode: Air flow rate = 245 mL/min. Temperature=190 ℃. Pressure = 1 atm.

Polarization curves for the same four fuels, measured with a used MEA following each of their respective 15 h TOS experiments, are shown in Figure 4.4. They are generally similar to one another. The open circuit potential after the TOS experiments, in Figure 4.4, is slightly greater for each fuel than that at the beginning of the TOS experiments in Figure 4.3. That observation is consistent with the data in Figure 4.2.

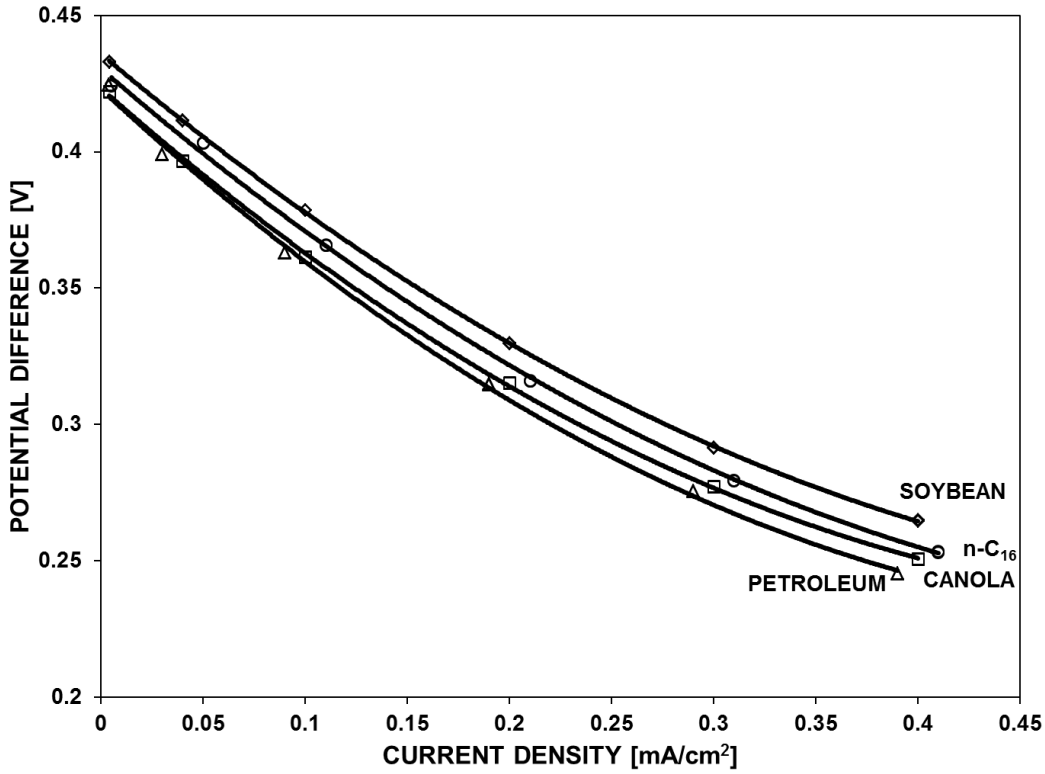


**Figure 4.4** Potential difference between the electrodes [V] versus current density [mA/cm$^2$] for a diesel fuel / water PAFC. Current density j = 0.04 mA/cm2. Anode: Water flow rate = 5.1 mL/h, Fuel flow rate = 0.2 mL/h. Cathode: Air flow rate = 245 mL/min. Temperature=190 ℃. Pressure = 1 atm.

Measurements of potential difference across the fuel cell using four different feedstocks, petroleum diesel, canola biodiesel, soybean biodiesel, and n-hexadecane are compared as a function of TOS in Figure 4.5. The numbers on the figures represent the sequence in which the experiments were performed. Initially a degradation in fuel cell performance occurred. However, for all feedstocks a steady-state operation was obtained during the last 6 h of operation. For petroleum diesel a steady-state operation was observed throughout the 15 h period. The steady state operation was an indication that there was no additional degradation in fuel cell performance. That was interpreted as there being no additional net accumulation of carbonaceous material. However the carbonaceous material hypothesized previously would have been present on the anode surface during the steady-state operating periods. That suggests that the carbonaceous material might have been a reaction

intermediate. The rate of its reaction to form products would have been equal to its rate of formation if there were no net accumulation. The formation of carbonaceous material in direct hydrocarbon fuel cells has been reported previously [11].

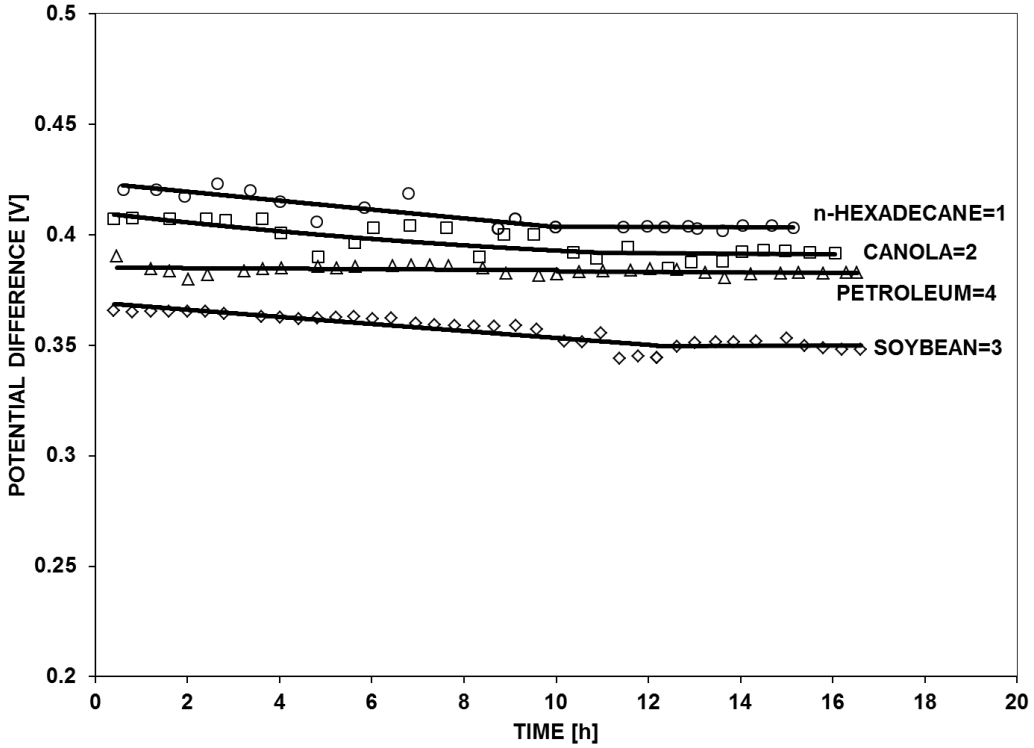


**Figure 4.5** Potential difference between the electrodes [V] versus time-on-stream [h] for a diesel fuel / water PAFC. Current density j = 0.04 mA/cm$^2$. Anode: Water flow rate = 5.1 mL/h, fuel flow rate = 0.2 mL/h. Cathode: Air flow rate = 245 mL/min. Temperature = 190 ℃. Pressure = 1 atm.

The diesel fuels in Figure 4.5 have different compositions which are conveniently analyzed via NMR spectroscopy. The $^1$H NMR spectra of petroleum diesel, canola biodiesel and soybean biodiesel are shown in Figure 4.6 (a), (b) and (c), respectively.

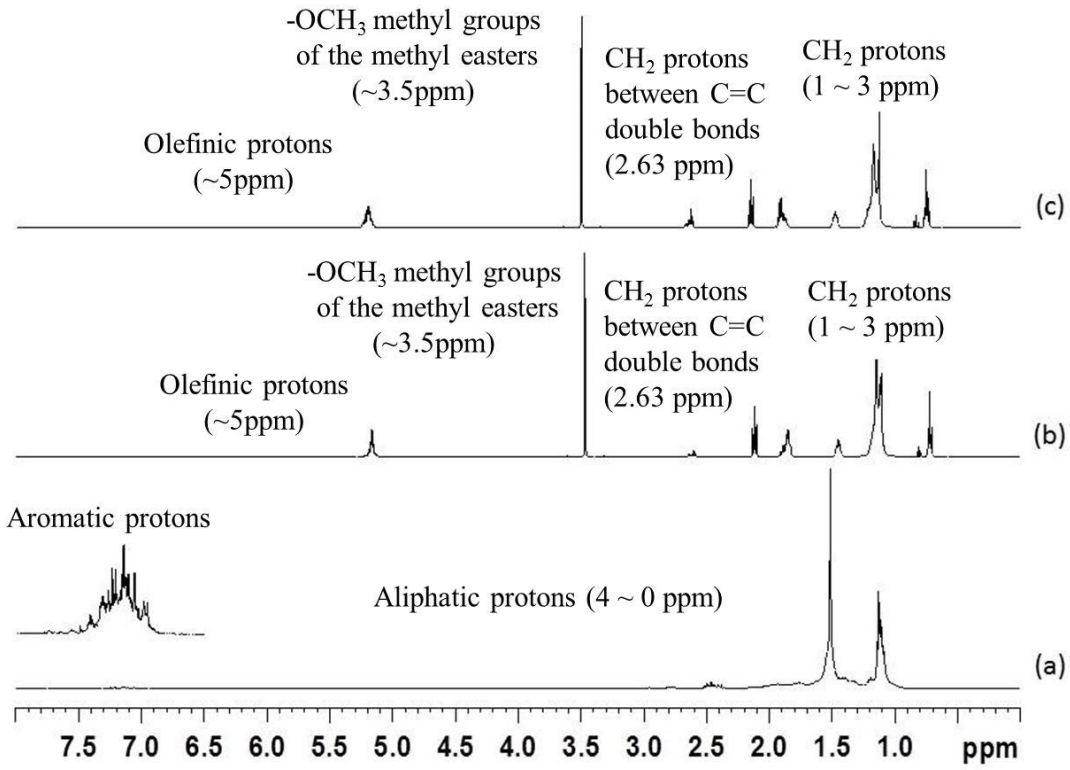


**Figure 4.6**: $^{1}$H NMR spectra for (a) petroleum diesel (with vertically expanded inset showing the aromatic protons); (b) canola biodiesel and (c) soybean biodiesel.

Petroleum diesel is a complex mixture of primarily aliphatic hydrocarbons. However, there is a small aromatic component shown in the vertically expanded inset of Figure 4.6(a). The aromatic protons are in the 6.5 ppm – 8 ppm range. The aliphatic CH, $CH_2$ and $CH_3$ protons are in the 4 ppm – 0 ppm range. The ratio of aromatic / aliphatic protons is 1 / 35.7. Canola and soybean biodiesel consist of the methyl esters of the fatty acids derived from the corresponding triglyceride oils. The $^{1}$H NMR spectra of the two biodiesel samples are similar in general appearance. Unlike petroleum diesel, there are no aromatic protons in the canola or soybean biodiesels. There are however, olefinic CH protons at ~ 5 ppm. The $CH_2$ protons are between 1 ppm and 3 ppm. The $CH_3$ protons terminating the aliphatic chains are between 0.5 ppm and 1 ppm. The large peak at ~ 3.5 ppm represents the $–OCH_3$ methyl groups of the methyl esters. The major difference between the $^{1}$H NMR spectra of the biodiesels is in the group of resonances at 2.63 ppm which represents

$CH_2$ protons between C=C double bonds (-C=C-$CH_2$-C=C-). The soybean biodiesel has more intensity in this region compared to canola biodiesel, consistent with the fact that soybean oil contains more polyunsaturated fatty acids than canola oil [21].

The quantitative $^{13}C$ NMR spectra of petroleum diesel, canola biodiesel and soybean biodiesel are shown in Figure 4.7 (a), (b) and (c), respectively.

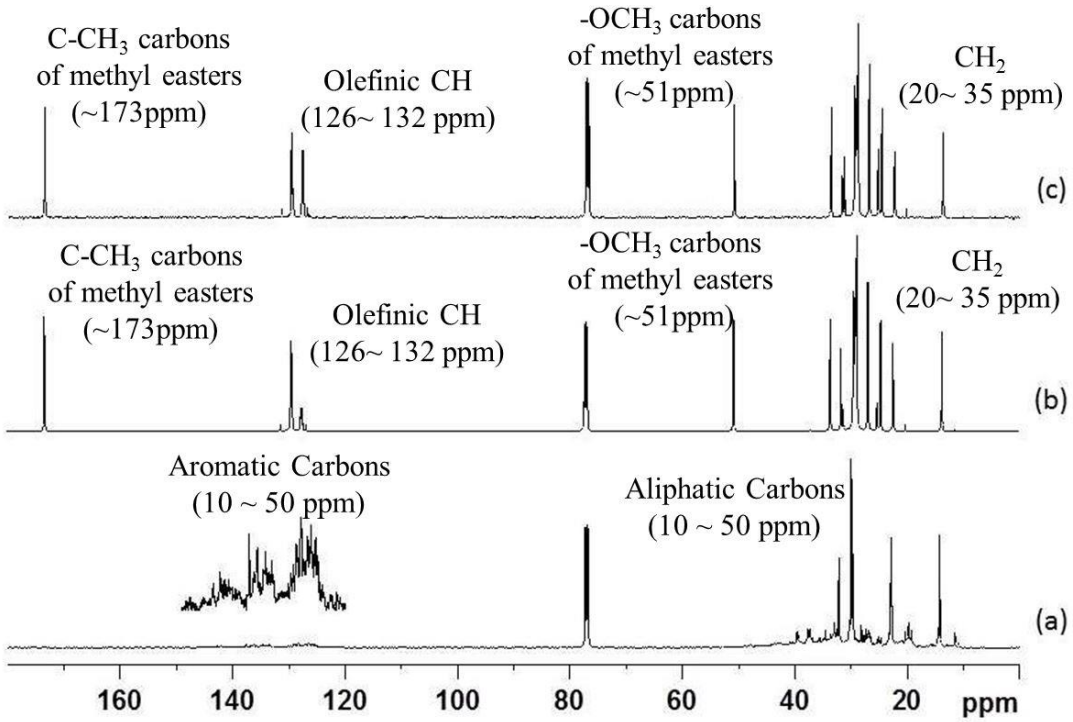


**Figure 4.7**: Quantitative $^{13}C$ NMR spectra for (a) petroleum diesel (with vertically expanded inset showing the aromatic carbons); (b) canola biodiesel and (c) soybean biodiesel.

The spectrum of petroleum diesel in Figure 4.7(a) reflects the predominantly aliphatic nature of the petroleum diesel. The aliphatic CH, $CH_2$ and $CH_3$ $^{13}C$ resonances are between 10 ppm and 50 ppm. The vertically expanded inset shows more clearly the aromatic carbons in the petroleum diesel in the range 120 ppm – 150 ppm. A $^{13}C$ DEPT-135 spectrum of the petroleum diesel showed that the $^{13}C$ resonances between 132 ppm and 150 ppm are due only to quaternary aromatic carbon atoms whereas the resonances between 120 ppm and 132 ppm are due to aromatic CH carbon atoms. The DEPT 135 data also revealed that there were no

detectable quaternary aliphatic carbon atoms. The $^{13}C$ NMR spectra of the biodiesels are similar in general appearance. In these spectra the olefinic CH resonances are between 126 ppm and 132 ppm. The $CH_2$ resonances are between 20 ppm and 35 ppm. The $CH_3$ groups terminating the fatty acid chains are at ~ 14 ppm. The $OCH_3$ and carbonyl carbons of the methyl esters are at ~51 ppm and ~173 ppm, respectively. The composition data obtained from the $^{1}H$ and $^{13}C$ NMR spectra are summarized in Table 4.1 compared to the composition data for n-hexadecane obtained by its structural formula.

**Table 4.1 – Carbon Types in Diesel Fuels From NMR**

| | n-hexadecane | Petroleum Diesel | Canola Biodiesel | Soybean Biodiesel |
|---|---|---|---|---|
| CH (olefinic) | 0% | - | 6.8% | 8.5% |
| CH (aromatic) | 0% | 2.7% | 0% | 0% |
| $CH_2$ (total) | 82.4% | >70% | 76.3% | 74.1% |
| CH-**$CH_2$**-CH | 0% | - | 1.7% | 3.8% |
| -(CO)-**$CH_2$** | 0% | - | 5.7% | 5.8% |
| -(CO)-$CH_2$-**$CH_2$**- | 0% | - | 5.9% | 5.9% |
| -$CH_2$-**$CH_2$**-CH=CH | 0% | - | 10.4% | 9.5% |
| -$(CH_2)_n$- | 82.4% | - | 52.6% | 49.1% |
| C-**$CH_3$** | 17.6% | - | 8.7% | 8.8% |
| O-**$CH_3$** | 0% | - | 8.2% | 8.6% |
| H : C ratio | 2.125 | 1.84 | 1.85 | 1.83 |
| ***Boiling Points** [22]: | 286.8 ℃ | 188 ~ 343 ℃ | 182 ~338 ℃ | 182 ~338 ℃ |

The resistance to current, $E^0 - \Delta\Phi$, can be related to the sum of the overpotentials at the anode and cathode plus the ohmic polarization. $E^0$ is the standard electrochemical potential (eg. $E^0 = 1.09$ V for hexadecane / oxygen). $\Delta\Phi$ is the measured potential difference between the anode and the cathode. For the various feedstocks, the fuel cell potential differences were ordered from largest to smallest as follows: n-hexadecane, canola biodiesel, petroleum diesel, and soybean biodiesel. This trend correlates with both the H / C ratio and the total % $CH_2$ of the feedstock. It

implies that the resistance to current in the fuel cell may be related to the number of available aliphatic hydrogen atoms per carbon atom in the feedstock. The feedstock with the largest H/C ratio had the smallest resistance to current. There does not appear to be an obvious relationship between the potential difference across the fuel cell and the percentage of olefinic or aromatic CH protons in the feedstock.

Additional experiments with n-hexadecane are seen in Figure 4.8 as potential difference versus time-on-stream. The first experiment in the sequence, n-hexadecane from Figure 4.5, is compared with the fifth experiment, also with n-hexadecane. For the fifth experiment, a steady-state operation was observed throughout the 15 h period. Therefore, based on these data in Figures 4.5 and 4.8, it can be stated with some confidence that it is possible to operate a direct hydrocarbon fuel cell with a variety of diesel fuels at steady-state for at least several hours.

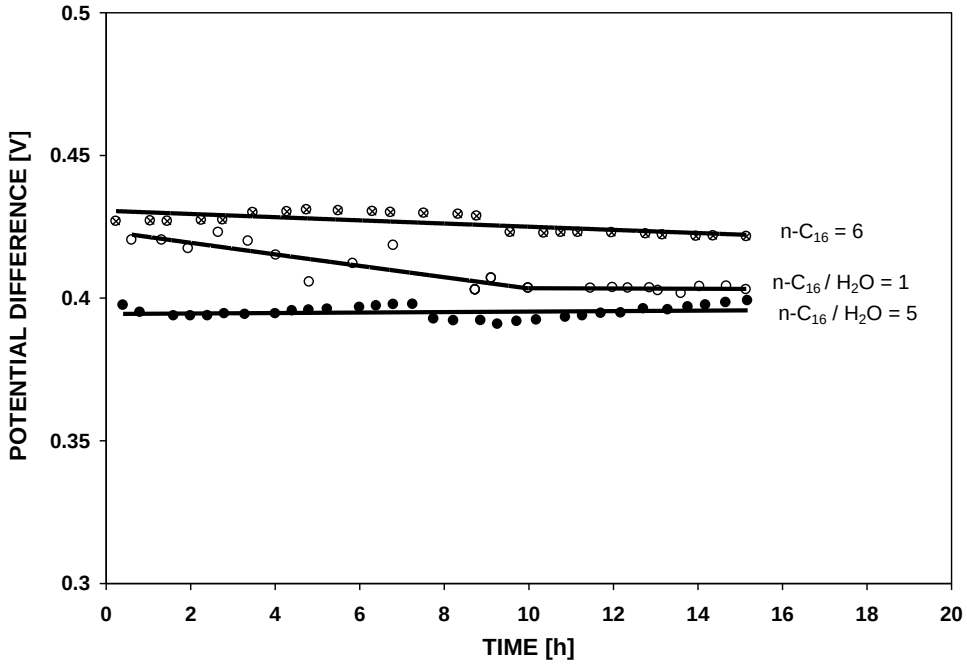


**Figure 4.8** Potential difference between the electrodes [V] versus time-on-stream [h] for an n-hexadecane PAFC. Current density j = 0.04 mA/cm$^2$. For first run and fifth run with Anode: Water flow rate = 5.1 mL/h, n-hexadecane flow rate = 0.2 mL/h. Cathode: Air flow rate = 245 mL/min. Temperature=190 ℃. Pressure = 1 atm. For the sixth run, there was no water flow.

The sixth experiment in the sequence is also shown in Figure 4.8. It was also performed with n-hexadecane. However, in this experiment no water was included with the n-hexadecane that was fed to the anode of the fuel cell. As shown in Equation 4.2, water reacts with the n-hexadecane in the anode half-cell reaction. The only water available for the sixth experiment would be the water in the phosphoric acid electrolyte. In principle the water removed from the phosphoric acid electrolyte at the anode could be replenished by water produced at the cathode, via its half-cell reaction. Equation 4.3 indicates that more water is produced by the cathode half-cell reaction than is consumed by the anode half-cell reaction, Equation 4.2.

The data in Figure 4.8 show that the fuel cell performance with n-hexadecane was slightly better when no water was fed to the anode. This suggests that n-hexadecane may compete with water for reaction sites in the anode catalyst layer. In any case the data in Figure 4.8 demonstrate that it is not necessary to feed water to the anode with the diesel fuel feedstock. In some respects fuel cell operation could be simpler if an anode water feeding system is not required. It also means that less water will have to be removed from the cathode.

Steady-state values for n-hexadecane were 0.42 V in Figure 4.5 and 0.39 V in Figure 4.8. It can be compared with the steady-state values in Figure 4.5 for canola biodiesel (0.40 V), soybean biodiesel (0.35 V) and petroleum diesel (0.38 V). There is not much difference among them, which is consistent with the results for the H/C ratios obtained by $^{1}$H NMR and $^{13}$C NMR in Table 4.1.

Degradation was indicated by a decrease in potential during the initial portion of some of the time-on-stream experiments in Figures 4.5 and 4.8. The decrease of potential was caused by degradation of the MEA. The condition of the MEA, was documented by measuring hydrogen polarization curves at different times in the sequence of experiments.

The hydrogen polarization curves shown in Figure 4.9 were measured when the MEA was in three different conditions. The middle curve (open circles) was

measured after the first TOS experiment with n-hexadecane shown in Figure 4.5. Air at the cathode and the hydrogen fuel at anode of a phosphoric acid fuel cell normally produce an open circuit potential in the 0.8 – 0.9 volt range [23].

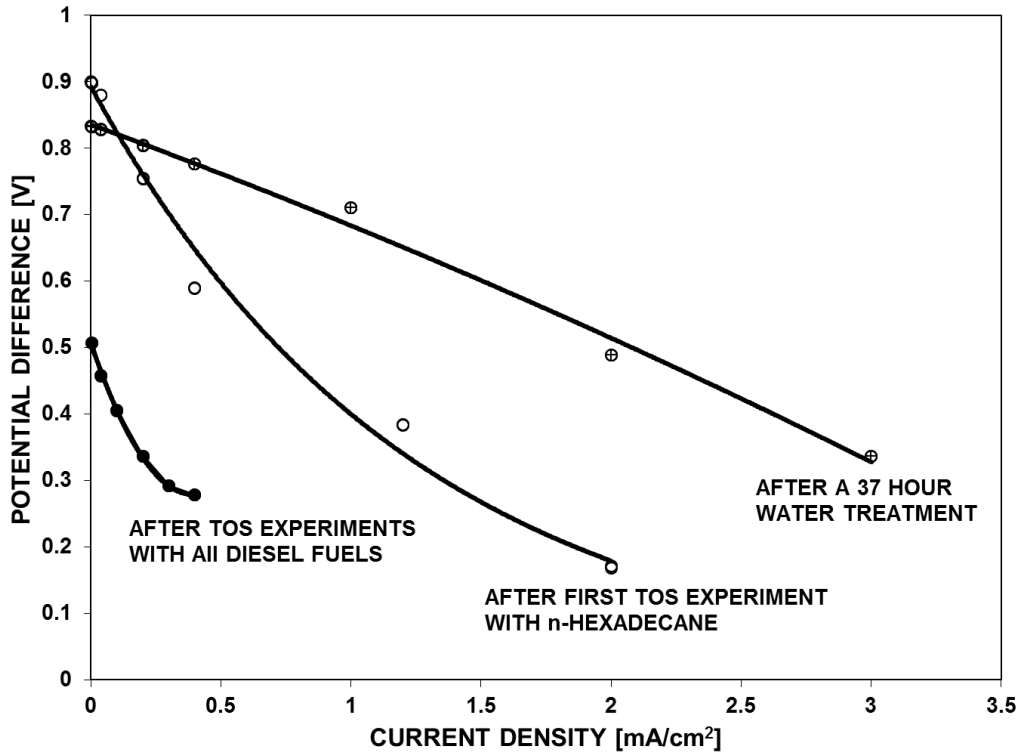


**Figure 4.9** Polarization curve for a hydrogen fueled PAFC: Potential difference [V] between the electrodes versus current density [mA/cm$^2$]. Anode: Hydrogen flow rate = 9.6 mL/min. Cathode: Air flow rate = 245 mL/min. Temperature = 160 ℃. Pressure = 1 atm.

The hydrogen polarization curve (solid circles in Figure 4.9) measured at the conclusion of all of the experiments in Figure 4.5 and 4.8 is worse than the polarization curve obtained after one n-hexadecane TOS experiment (the middle curve in Figure 4.9). The hydrogen polarization curve at the end of all the TOS experiments (solid circles in Figure 4.9) and the diesel fuel polarization curve at the end of the TOS experiments (Figure 4.4) were similar. That similarity supports the suggestion that the hydrogen flowing through the MEA was not contacting the catalyst surface and that the carbonaceous material that had accumulated on the MEA (not the hydrogen) was the material that was reacting at the anode. This observation

is also consistent with the suggestion that the carbonaceous material is a reaction intermediate.

The upper polarization curve shown in Figure 4.9 (cross inside circles) was obtained after cleaning the MEA by flowing water through the anode after the MEA had been used in all the TOS experiments. The water at the anode could react with the accumulated carbonaceous deposits to form carbon dioxide, via an electrochemically assisted carbon-steam reaction. The improved polarization curve is consistent with water removing the carbonaceous deposits thereby making additional reaction sites available for the hydrogen reaction at the anode. The open circuit potential for the cleaned MEA in Figure 4.9 is less than that for the MEA that had been used in only one TOS experiment. The same phenomenon had been observed in Figure 4.2 and in the comparison between Figures 4.3 and 4.4. This observation is also consistent with the suggestion that the carbonaceous material is a reaction intermediate.

Experiments in Figure 4.10 were performed at a current density of 0.2 $mA/cm^2$ using water as the only reactant fed to the anode. The fuel for the reaction that created the current was attributed to a carbonaceous deposit on the MEA. The carbonaceous deposit would have been gradually consumed when the water reacted with the carbon, as the reaction continued. Two different situations are shown in Figure 4.10. The data shown as solid squares were obtained using the MEA immediately after the diesel fuel TOS experiments. Later that MEA was treated with water for 37 h. Then a hydrogen polarization curve was measured. The data shown as open squares represent an additional 5 h of water treatment after the hydrogen polarization curve measurements. At Time = 0, in Figure 4.10, the potential difference for both curves was near 0.5 V. The value of 0.5 V is also the value of the open circuit potential of one of the polarization curves in Figure 4.9. That curve was measured in the presence of a hydrogen atmosphere reaction but the measurements were attributed to the reaction between carbonaceous material and water. On that basis the results in Figure 4.10 can also be attributed to the reaction of water with carbonaceous material even though water was the only reactant being fed to the fuel cell.

The experiment in Figure 4.10 performed after the 37 h water treatment had a much greater rate of decrease in potential difference than the one performed immediately after the diesel fuel TOS experiments. However the rates of reacting the carbonaceous material (current density = 0.2 $mA/cm^2$) were identical. That difference in rate of change of potential difference might be explained by the MEAs containing different amounts of carbonaceous material. When the change in amount of carbonaceous material on the anode surface is small compared to the total amount of carbonaceous material (MEA after TOS experiments), the fraction of the anode surface covered by carbonaceous material should be almost constant. In that case the potential difference, in Figure 4.10, is almost constant. In contrast, when the change in amount of carbonaceous material on the anode surface compared to the total amount of carbonaceous material is substantial (MEA after 37 h of water treatment), then the fraction of the anode surface covered by carbonaceous material should decrease. The change in fraction of anode surface covered by carbonaceous material may be responsible for the greater rate of decrease in potential difference observed for the MEA that had 37 h of water treatment.

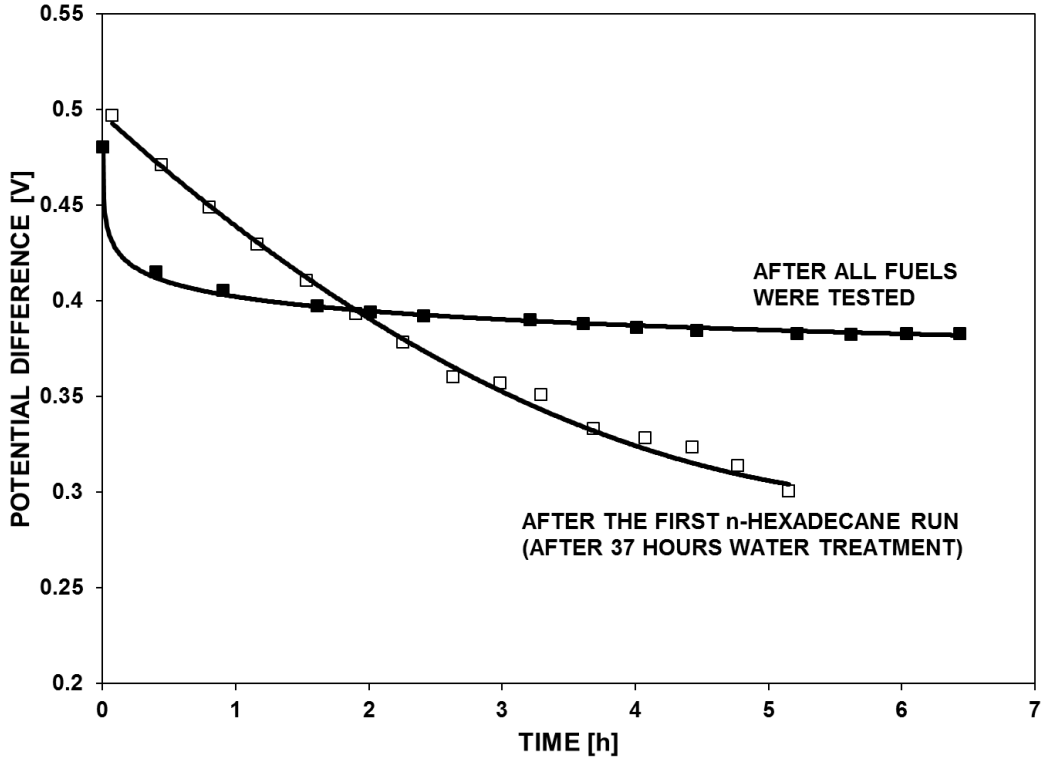


**Figure 4.10** Polarization curves obtained with water as the only reactant flowing to the anode of a PAFC with different condition of MEA, one was after all fuels were tested and the other one is that had been used for several TOS experiments with various diesel fuels. Potential difference between the electrodes [V] versus time of water treatment [h]. Anode: Water flow rate = 5.1mL/h. Cathode: Air flow rate = 245 mL/min. Temperature = 190 ℃. Pressure = 1 atm

### 4.4 Summary

A 15 hour period of steady state operation was demonstrated using petroleum diesel in a direct hydrocarbon phosphoric acid fuel cell. A relationship was found between the potential difference between the fuel cell electrodes at steady state and the H / C atomic ratio as determined by NMR measurements. A greater the H / C ratio in the diesel fuel feedstock correlates with a greater potential difference between the fuel cell electrodes.

The degradation in fuel cell performance was attributed to the deposition of carbonaceous material on the anode catalyst of the MEA. Degradation was indicated

by the difference in performance between cleaned and used MEAs, in Figures 4.2 and 4.3. There were several observations consistent with the suggestion that the carbonaceous material was a reaction intermediate. (a) The results in Figure 4.5 indicate that no net accumulation of carbonaceous material occurred at steady state. That might have occurred if at steady state the rate of deposition of carbonaceous material had been equal to its rate of removal (by reaction). (b) At open circuit potential the used MEA (containing a greater amount of carbonaceous material) had a smaller potential difference than the clean MEA (containing a lesser amount of carbonaceous material). (See Figure 4.2 and a comparison of the data in Figure 4.4). (c) The hydrogen polarization curve obtained using the MEA that had been used in all the TOS experiments in Figure 4.9, was similar to the diesel fuel polarization curves in Figures 4.3 and 4.4. (d) The polarization curves in Figure 4.10 obtained with water as the only feedstock showed that the rate of decrease in potential difference was much smaller when there was an abundance of carbonaceous material on the MEA. The presence of carbonaceous deposits on the MEA was indicated by the fact that electrical current and power were produced when water was the only reactant fed to the anode. After water treatment, the cleaned MEA would typically require more than 10 hours to re-deposit a sufficient quantity of carbonaceous material to develop a steady-state reaction condition.

The electrochemical driving force for the fuel cells was correlated with the number of available aliphatic hydrogen atoms per carbon atom of feedstock molecule. It was found that water for the reaction at the anode could be provided by water in the phosphoric acid electrolyte. In principle, water in the electrolyte could be made-up by water produced at the cathode. That could simplify the fuel cell system by eliminating the need for a water feed system.

### 4.5 Conflict of Interest

The authors declare that there is no conflict of interest regarding the publication of this paper.

## 4.6 Acknowledgment

The authors gratefully acknowledge that this research and development project was supported by a grant from Transport Canada's Clean Rail Academic Grant Program, and by a Discovery Grant from the Canadian Government's Natural Sciences and Engineering Research Council.

## 4.7 References

[1] Z. Zhou, C. Gallo, M. Pague, H. Schobert and S. Lvov, "Direct oxidation of jet fuels and Pennsylvania crude oil in a solid oxide fuel cell," *J. Power Sources,* vol. 133, pp. 181-187, 2004

[2] Y. Shiratori, T. Q. Tran, Y. Takahashi and K. Sasaki, "Application of biofuels to solid oxide fuel cell," *ECS Transactions,* vol. 35, pp. 2641-2651, 2011

[3] T. Quang -Tuyen, Y. Shiratori and K. Sasaki, "Feasibility of palm-biodiesel fuel for a direct internal reforming solid oxide fuel cell," *Int. J. Energy Res.*, vol. 37, pp. 609-616, 2013

[4] H. Kim, S. Park, J.M. Vohs, and R.J.Gorte, "Direct oxidation of liquid fuels in a solid oxide fuel cell", *Journal of the Electrochemical Society,* vol. 148, no. 7, pp. A-693-A695, 2001.

[5] Y. Zhu, A.Y. Tremblay, T. Robinson, A. Al-Othman, M. Ternan, "n-hexadecane fuel for a phosphoric acid direct hydrocarbon fuel cell, "*Journal of Fuels*," Volume 2015, Article ID 748679, doi.org/10.1155/2015/748679.

[6] Kishimoto, H., Yamaji, K., Horita, T., Xiong, Y., Sakai, N., Brito, M., Yokokawa, H., "Feasibility of liquid hydrocarbon fuels for SOFC with Ni-ScSZ anode", *Journal of Power Sources,* vol. 172, pp. 67-71, 2007.

[7] Dong, D., Liu, Z., Li, L., Xia, C., "An octane-fueled low temperature solid oxide fuel cell with Ru-free anodes*", Electrochemistry Communications*, vol. 10, pp. 1295-1298, 2008.

[8] H. Liebhafsky and W. Grubb, "Normal alkanes at platinum anodes, "*American Chemical Society, Division of Fuel Chemistry, Preprints,* vol. 11, 1967

[9] E.J.Cairns, "Anodic oxidation of hydrocarbons and the hydrocarbon fuel cell," *Advances in Electrochemistry Science and Electrochemical Engineering*", vol. 8, pp. 337-392, 1971.

[10] J.O.M. Bockris and S. Srinivasan, "Electrochemical combustion of organic substances", *in Fuel Cells Their Electrochemistry*, pp. 357-411, McGraw-Hill, New York, 1969.

[11] H.A. Liebhafsky and E.J. Cairns, "The direct hydrocarbon fuel cell with aqueous electrolytes", *in Fuel Cells and Fuel Batteries,* pp. 458-523, Wiley, New York, 1968.

[12] S. Bertholet, "Oxydation Electrocatalytique du Methane", Ph.D. Dissertation, Universit éde Poitiers, France, 1998.

[13] C.K. Cheng, J.L. Luo, K.T. Chuang, and A. Sanger, ''Propane fuel cells using phosphoric-acid-doped polybenzimidazole membranes'', *Journal of Physical Chemistry B,* vol. 109, pp. 13036-13042, 2005.

[14] O. Savadogo, F.J. Rodriguez Varela, ''Low-temperature direct propane polymer electrolyte membrane fuel cells'', *Journal of New Materials for Electrochemical Systems,* vol. 4, pp. 93-97, 2001.

[15] F.J. Rodriguez Varela, "Real-time mass spectrometric analyses of the anode exhaust gases of a direct propane fuel cell", *Journal of the Electrochemical Society,* vol. 152, pp. A1755-A1762, 2005.

[16] Heo, P., Ito, K., Tomita, A., Hibino, T., "A proton-conducting fuel cell operating with hydrocarbon fuels", *Angewandte Chemie International Edition,* vol. 47, pp. 7841-7844, 2008.

[17] S. Srinivasan, "*Fuel cells: from fundamentals to applications*", Springer, New

York, 2006, pp. 505-514.

[18] A. J. Appleby, "Fuel cells – Phosphoric Acid Fuel Cells: An Overview," in *Encyclopedia of Electrochemical Power Sources*, J. Garche, Ed. Amsterdam: Elsevier, 2009, pp. 533-547.

[19] A.Y. Tremblay and M.A. Dubé, Fuel additive from plant oils, animal fats; for diesel engines US patent # 8366794 B2, 5 Feb 2013.

[20] C.G. Farrell, C.L. Gardner, M. Ternan, "Experimental and modeling studies of CO poisoning in PEM fuel cells", Journal of Power Sources, vol. 117, pp. 282-293, 2007.

[21] R.C. Zambiazi, R. Przymbylski, M.W. Zambiazi, C.B. Menonca, "Fatty acid composition of vegetable oils and fats", *Brazilian Centro de Pesquisa e Procesamento de Alimentos*, vol. 25, no. 1, pp.111-120, 2007.

[22] Strong, Christopher, Charlie Erickson, and Deepak Shukla. Evaluation of Biodiesel Fuel: Literature Review. No. FHWA/MT-04-001/8117-20,. Montana Department of Transportation Research Section, 2004.

[23] R.H. Song, C.S. Kim, D.R. Shin, "Effects of flow rate and starvation of reactant gases on the performance of phosphoric acid fuel cells", *Journal of Power Sources*, vol. 86, pp. 289-293, 2000.

# Chapter 5 - General Discussion

## 5.1 Results and Discussion

The materials in Chapter 3 and Chapter 4 are results. Chapter 3 presents results obtained with n-hexadecane. Chapter 4 presents results with petroleum diesel, canola biodiesel and soybean biodiesel.

At the beginning of this project, the first step was modifying and calibrating the entire phosphoric acid fuel cell system. The phosphoric acid fuel cell system was calibrated by using hydrogen fuel. Water is a necessary reactant at the anode as can be observed from the stoichiometric equation for the fuel cell reaction. For each mole of n-hexadecane oxidized, thirty-two moles of water are consumed.

The results concluded in Chapter 3 and 4 have been explained in terms of a reaction mechanism. Initially, Bagotsky et al. [1] described a reaction mechanism for direct hydrocarbon fuel cells using methane as a feedstock. The Bagotsky mechanism was modified, as shown in Figure 3.1, to describe n-hexadecane. However alcohols, aldehydes, carboxylic acids, and lower molecular weight hydrocarbons are possible by-products. Three reactions are shown in Figure 3.1: dehydrogenation, (from both carbon and oxygen atoms), hydroxylation, and C–C bond cleavage. Two reactions are not shown: water dissociation ($H_2O \longrightarrow H + OH$) and hydrogen atom ionization ($H \longrightarrow H^+ + e^-$). Hydrogen ionization is an electrochemical reaction and therefore is influenced by potential. The other four reactions are chemical reactions and are not influenced by potential.

The results obtained in Chapter 3 identified a temperature and a molar ratio of water at which a stable operation with n-hexadecane could be obtained. The TOS results at 190$^o$C are compared with those at 160$^o$C in Figure 3.9. A steady-state operation was achieved for the last six hours of the experiment at 190$^o$C. A steady-state operation is a highly desirable result that is not always achieved with a comparatively large hydrocarbon molecule.

The other three diesel fuels, canola bio-diesel, soybean bio-diesel and petroleum diesel were investigated in Chapter 4 at the same operating conditions. Steady state results were obtained for all of the real diesel fuels. The results with real diesel fuels, obtained in Chapter 3, were generally similar to those for n-hexadecane in Chapter 4. However there were small differences in the results with real diesel fuels. Those differences appeared to be related to the different compositions of the diesel fuels. The results obtained in Chapter 4 are compared in Figure 4.5. The numbers on the figures represent the sequence in which the experiments were performed. Initially there was a degradation in performance. However, for all feedstocks a steady-state operation was obtained during the last 6 h of operation. For petroleum diesel a steady-state operation was observed throughout the 15 h period.

In both Chapter 3 and 4, the results were obtained using same Pt catalyst and the same operating conditions. Steady state was obtained with all four diesel fuels. Figure 4.5 is also a good comparison for these different fuels. Furthermore, it was hypothesized that a carbonaceous material accumulated at the anode surface and that the carbonaceous material would have been present on the anode surface during the steady-state operating periods. That suggests that the carbonaceous material may have been a reaction intermediate.

Since the membrane electrode assembly has been operated for a considerable period of time, replacing the membrane electrode assembly with a new one would likely enhance the fuel cell performance [2-3]. Also, increasing the operating temperature may help to improve performance [4].

## 5.2 Conclusion

Exploratory work in this project involved an investigation of the operating conditions when n-hexadecane was the feedstock for the anode of a phosphoric acid fuel cell. In addition four different real diesel fuels, n-hexadecane, canola bio-diesel, soybean bio-diesel, and petroleum diesel were used in the phosphoric acid fuel cell. The performance of different diesel fuels in PAFCs was reported in Chapter 3 and 4.

It can be concluded from the combined results of Chapter 3 and Chapter 4 that these four diesel fuels can be operated at a steady state in our PAFCs. A diagram illustrating a possible reaction mechanism for the oxidization process was also presented.

This work has provided an indication of the performance of diesel fuels in PAFCs. Suggestions for future research include changing or modifying the Pt catalyst and developing in-house membrane electrode assemblies. Eventually, this type of research may lead to fuel cells that have higher efficiencies and produce less pollution and therefore replace locomotive diesel engines used throughout the world.

### 5.3 References


[1] V.S. Bagotzky, Yu. Vassiliev, and O.A. Khazova, “Generalized Scheme of Chemisorpiton, Electrooxidation, and Electroreduction, of simple organic compounds on platinum group metals”, Journal of Electroanalytical Chemistry, vol. 81, pp. 229-238, 1977.

[2] Frey, Th, and M. Linardi. "Effects of membrane electrode assembly preparation on the polymer electrolyte membrane fuel cell performance." Electrochimica Acta 50.1 (2004): 99-105.

[3] Barton, Russell H., et al. "Membrane electrode assembly for an electrochemical fuel cell and a method of making an improved membrane electrode assembly." U.S. Patent No. 6,057,054. 2 May 2000.

[4] Baker, Bernard S., and Hossein G. Ghezel-Ayagh. "Fuel cell system." U.S. Patent No. 4,532,192. 30 Jul. 1985.

# Chapter 6 - Conclusions

## 6.1 Summary of Results

Deactivation was observed in time-on-stream experiments. Deactivation, as measured by the change in potential difference, was found to be a linear function of the cumulative charge transferred across the electrolyte of the fuel cell. Deactivation during fuel cell experiments with n-hexadecane was confirmed by comparing hydrogen polarization curves before and after the time-on-stream measurements. For a given potential difference the current densities were much smaller for the hydrogen polarization curves measured after the time-on-stream experiments.

Experiments were performed in which water was the only reactant entering the fuel cell that had been used previously for 10 weeks in time-on-stream experiments. Current densities were measured during those experiments, indicating that the water must have reacted with some type of species that remained on the fuel cell catalyst at the end of the time-on-stream experiments. When a hydrogen polarization curve was measured at the end of the water-only experiments, it was close to that measured before the time-on-stream experiments. That indicates that the species on the surface of the platinum particles had been removed, and that it is possible to regenerate deactivated MEAs.

A hypothesis, that carbonaceous material was deposited on the platinum anode catalyst particles, was suggested to explain the deactivation. Four types of observations were consistent with that hypothesis: (a) the change in potential difference during time-on-stream measurements, (b) when hydrogen polarization curves measured before and after the time-on-stream experiments were compared, the current densities measured after the TOS experiments were much smaller than those measured before the TOS experiments, (c) current densities were measured when water was the only reactant entering the fuel cell. In order to produce a current density, water must have reacted with some type of species that had been deposited on

the surface of the platinum particles, and (d) the open circuit potential of a n-hexadecane fuel cell, 0.5 V, was much closer to the standard electrochemical potential for the carbon – water reaction, 0.711 V than to that for the carbon monoxide – water reaction, 1.33 V. Observation (d) makes a hypothesis of deactivation by carbonaceous materials more likely than deactivation by carbon monoxide poisoning.

Steady-state operation of the n-hexadecane fuel cell, without deactivation, was observed at one set of fuel cell operating conditions. That observation demonstrates that stable fuel cell operation is technically feasible when n-hexadecane is the fuel at the anode of a fuel cell. It suggested there would be merit in investigating fuel cell operation with commercial fuels such as petroleum diesel or bio-diesel.

Following the results obtained in the n-hexadecane study, an extended study on diesel fuel was reported in the next section. Steady state operation of a direct hydrocarbon phosphoric acid fuel cell was demonstrated when operating on petroleum diesel, Canola biodiesel, and Soybean biodiesel. The results are shown in Figure 4.5. It was found that water for the reaction at the anode could be provided by water in the phosphoric acid electrolyte. In principle, water in the electrolyte could be made-up by water produced at the cathode. The presence of carbonaceous deposits on the MEA was indicated by the fact that electrical current and power were produced when water was the only reactant fed to the anode. After water treatment, the cleaned MEA would typically require more than 10 hours to re-deposit a sufficient quantity of carbonaceous material to develop a steady-state reaction condition.

### 6.2 Contributions to Knowledge

Direct hydrocarbon fuel cells have been studied over a long period of time. Direct hydrocarbon fuel cells have shown some advantages such as theoretically higher efficiency and lower capital cost. However, the development of hydrocarbon fuel cells was slow. No breakthroughs have been made and few studies of diesel fuels in a phosphoric acid fuel cell have been reported. n-Hexadecane is representative of the paraffinic compounds in low-sulfur diesel fuel [1]. It was used to model the diesel

fuels in this project. After finding the optimal operating conditions, experiments were performed using different diesel fuels, canola bio-diesel, soybean bio-diesel and petroleum diesel fuel in our phosphoric acid fuel cell.

1. This study reported the first polarization curve ever measured for which n-hexadecane was the fuel at the anode of a fuel cell.

2. Steady state operation of a direct hydrocarbon phosphoric acid fuel cell was demonstrated when operating on petroleum diesel, Canola biodiesel, and Soybean biodiesel. For each diesel fuel, it took approximately 15 hours to reach a steady state. The conditions used were: a temperature of 190$^{o}$C and a molar ratio of water to n-hexadecane of 414.

3. Several observations listed in the conclusions to Chapter 4 suggest that deactivation may have been caused by the deposition of a carbonaceous material on the anode catalyst and that the carbonaceous material may have been a reaction intermediate.

4. The improvement in the fuel cell performance obtained after treating the anode with water indicated that water can at least partially clean the MEA (membrane electrode assembly).

5. Water for the reaction at the anode could be provided by water in the phosphoric acid electrolyte. Make-up water for the electrolyte can be provided by water formed at the cathode. As a result a water feed system for the anode may not be required, thereby simplifying the overall fuel cell process flow sheet.

6. The open circuit potential of a n-hexadecane fuel cell was measured to be 0.5V, which is relatively close to the standard electrochemical potential for the oxidation for carbon atoms. That is consistent with the presence of a carbonaceous material on the anode catalyst surface.

## 6.3 Recommendations

Some changes can be made that may increase the current density thus enhancing the performance of the fuel cell.

In general, there are three major things we can do to improve the performance of fuel cells. The first is the electrocatalytic reaction in the cathode of the fuel cell. The oxygen reduction reaction is slow on all the electrocatalysts that have ever been tested. Moreover, the overpotential caused by the oxygen reduction reaction causes most of the power loss in hydrogen fuel cells. Research on the electrocatalytic reaction at the cathode merits continuation since the same cathodic reaction occurs in both hydrogen fuel cells and direct hydrocarbon fuel cells [2].

The second thing is the electrocatalysis reaction in the anode of the fuel cell. In direct hydrocarbon fuel cells the overpotential at the anode is slightly larger than for the oxygen reduction reaction at the cathode. The oxidation reaction occurs at the anode. Cairns reported some work on the reactions occurring on platinum in 1971[3]. However, little work has been done since then. Currently, the most common catalyst is still platinum and platinum alloys [4-5]. They can be used on both cathode and anode. In the experiments reported here, platinum was used. However, platinum is extremely expensive. Finding a substitute for platinum and optimizing the amount of catalyst are objectives for future research.

The third thing is the optimization of the operating conditions (temperature, pressure and flowrate of the reactant gases) in the fuel cell. In addition, the electrode structure, design parameters such as effective surface area and thickness of the electrode, and concentration of the liquid electrolyte merit further study [2].

In conclusion, finding an efficient catalyst for both cathode and anode is important. The optimization of the operating conditions is also necessary and is relatively easy compared to catalyst improvement. Increasing temperature and adjusting the composition of the reactant gases are examples of processing parameters

that would improve the performance.

In addition, very few studies have focused on diesel fuels operated in phosphoric acid fuel cells. Perhaps, this is an opportunity to extend research on this topic. For example, more diesel fuels could be tested.

### 6.4 References


[1] Kang, Inyong, Joongmyeon Bae, and Gyujong Bae. "Performance comparison of autothermal reforming for liquid hydrocarbons, gasoline and diesel for fuel cell applications." Journal of Power Sources 163.1 (2006): 538-546.

[2] Psofogiannakis, George, et al. "Mathematical model for a direct propane phosphoric acid fuel cell." Journal of applied electrochemistry 36.1 (2006): 115-130.

[3] Cairns, E.J., Adv. Electrochem. Electrochem. Eng. 8: 337-392, 1971.

[4] Mukerjee, Sanjeev, and Supramaniam Srinivasan. "Enhanced electrocatalysis of oxygen reduction on platinum alloys in proton exchange membrane fuel cells." Journal of Electroanalytical Chemistry 357.1 (1993): 201-224.

[5] Colón-Mercado, Héctor R., and Branko N. Popov. "Stability of platinum based alloy cathode catalysts in PEM fuel cells." Journal of Power Sources 155.2 (2006): 253-263.

# Appendices

This section includes content that was not contained in either Chapter 3 or 4. Both the equipment used and the experimental procedure were same through all the experiments in the Thesis.

## A.1 Fuel cell test station

**Figure A.1** Fuel cell test station in D219

The fuel cell test station in our lab is shown in Figure A.1. The overall system consists of an air cylinder, a hydrogen cylinder, one galvanostat, two syringe pumps, a vaporizer, a Phosphoric Acid Fuel Cell (PAFC = Electrochem FC-25-02MA), and a fuel cell test station.

A Hokuto Denko HA-301 Galvanostat (shown in Figure A.2) was used to adjust the potential difference between the anode and cathode of the phosphoric acid fuel cell to maintain the chosen current at a constant value. Syringe pumps provided the suitable flow rate of reactants (shown in Figure A.3).The concentration of phosphoric acid is 85 wt% (shown in A.4).

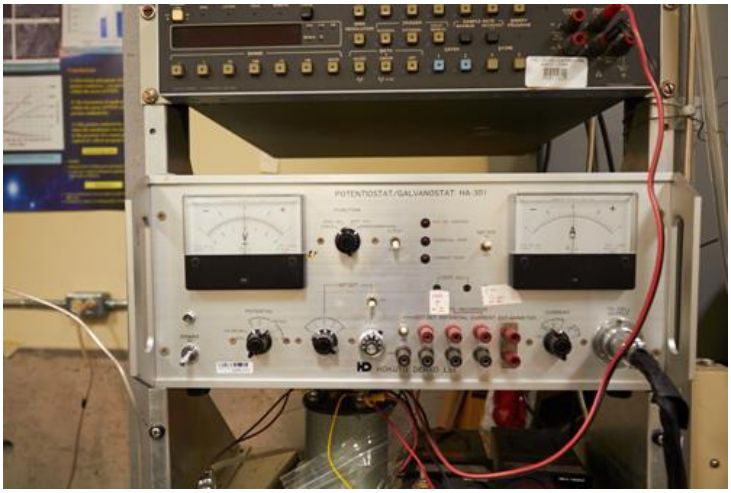

**Figure A.2** A Hokuto Denko HA-301 Galvanostat


**Figure A.3** Syringe pump

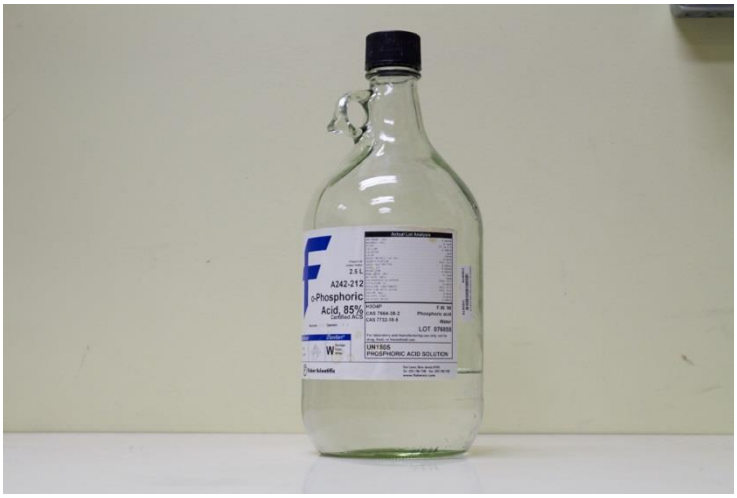


**Figure A.4** Phosphoric Acid (85 wt%)

## A.2 Fuel cell experimental procedure

All the experiments followed the experimental procedure below:

1. Self Calibration: Click on Measure and Automation icon on the desktop, then Configure, devices and interface. Right click on: NI-PCI-6010 and choose: Self-test then self-calibrate [1].

2. Open Lab view, plug in the fuel cell heater and heat the fuel cell to the target temperature (160 $^{o}$C or 190 $^{o}$C).

3. Turn on the main power source to start the galvanostat.

4. Turn on the computer and open the (software) to calibrate and self-test fuel cell. This done by right clicking the software and selecting NCIS which allows you to first calibrate and self-test afterwards.

5. Turn on the Galvanostat and turn the node to Open circuit potential

6. Open the hydrogen and air tanks; check the ball in the flow meter goes up. Open the hydrogen node to allow hydrogen to enter into the anode.

7. Go to lab view and click on Rec. change the recording time to 1sec to record data at every minute, click on record to record upcoming data.

8. Adjust the axis of the graph if you desire to see the initial voltage.

9. Click on “Run”, and then “Save” to start recording the open circuit potentials. When steady state is reached start changing the current using the node on the galvanostat.

10. Before changing the current, click on the lab view as the following order: “Save”, “Stop”, “Run”, “Save”, Current change.

11. Increase the current starting from high to low by using the current changer on the Galvan stat.

12. For each interval wait 30 min for the process to stabilize (steady state).

13. When all experiments were done, click “Save” first and then “Stop”.

14. Access the data from the computer and organized to their various current densities.

15. Shut down the process, close the hydrogen and air tanks and unplug all plugs and turn off computer. Switch back the galvanostat.

16. Open the nitrogen cylinder for a while to cool down the whole system.

**A.3 Membrane Electrode Assembly (MEA) Installation Procedure**

The membrane electrode assembly is the most important part in the fuel cell. The phosphoric acid is required to be "Immobilized" in between the two electrodes. For this, an acid holder matrix is created on one or both the electrodes [2-3], which is shown in Figure A.2.

This different structure make the whole installation procedure difficult than proton exchange membrane fuel cell. The following procedure was proposed before I installed the new MEA:

1. Open the fuel cell on a table top.

2. Separate the fuel cell and keep the plate (flow fields) facing up.

3. Keep all bolts in one set of plates. The bolts will be served as alignment pins.

4. Place first gasket.

5. Place the MEA and line up the electrode to the first gasket.

6. Place the second gasket and line up the gasket with the electrode on the MEA.

7. Place the graphite and copper plates.

8. Install the insulation washers, flat washers, and nuts.

9. Stand the fuel cell up and align the plates and MEA on a flat table.

10. First, tighten the nuts with fingers.

11. Tighten the bolts and nuts symmetrically using an adjustable wrench at 5 and then15 in-lb.

**Hints:**

Before operating, the phosphoric acid fuel cell needs to be taken apart. Lay the anode plate down, with reservoir face up. Lay the anode gasket on top. Place the smallest electrode on top the anode gasket and coat with a thin layer of phosphoric acid. Place face gasket on top the anode electrode. Drop 1 to 2 large drops of phosphoric acid the anode electrode. Coat the cathode electrode with a thin coat of phosphoric acid place on top of the face gasket. Cover with cathode gasket and cathode graphite plate; Re-assemble the fuel cell. The lower Teflon fitting on the left side of the anode plate the reservoir fill. Fill the reservoir with acid while the fuel cell is upside-down. After filled, place fuel cell right side up. The fuel cell is ready for operation.

To ensure the phosphoric acid is distributed properly inside the face gasket, external tubing should be attached and fill with acid to a level equal to the top of the PAFC fuel cell test cell.

**A.4 GC Analysis**

During the exploration stage, we did GC analysis for liquid waste to find how much n-hexadecane coming out from the cell. The results were summarized and shown in Table A.1. Six-day experiments were performed at different temperature. In the first three days, the cell temperature is 160℃. And for last three days, the temperature is 190℃. From the GC results, we knew that how much n-hexadecane coming out, thus, we calculated how much n-hexadecane accumulated in cell. Based on the results, the fraction of n-hexadecane leaving the cell was calculated.

It is obvious that the fraction of n-hexadecane leaving the cell decreases over the 3 day run at 160 ℃, which indicated that hexadecane is accumulating in the cell over this period. For the results at 190 ℃ the inverse occurs, the fraction of hexadecane leaving the cell increases over time. This means it is not accumulating in the cell.

**Table A.1 Summary of GC results**

| Conditions | Run Time (Day) | Cumulative amount in cell (mL) | Cumulative input (mL) | Fraction of hexadecane leaving the cell (mL) |
|---|---|---|---|---|
| T=160°C, j=1mA | 1 | 0.646 | 1.596 | 0.594 |
| | 2 | 2.154 | 3.350 | 0.14 |
| | 3 | 3.766 | 4.966 | 0.002 |
| T=190°C, j=1mA | 4 | 5.133 | 6.535 | 0.128 |
| | 5 | 5.800 | 8.149 | 0.586 |
| | 6 | 6.210 | 9.802 | 0.751 |

The following plot of cumulative n-hexadecane in cell versus run time was shown in Figure A.5. It shows it decreasing and possibly leveling off once the temperature changes from 160 ℃ to 190 ℃ on day 4. The results show that operating at 190 ℃ reduced the accumulation of n-hexadecane in the cell. This indicates that a temperature above 190 ℃ is required for steady state operation.

This fits extremely well with Figure 3.9 where you see that a true steady state is only reached at 190 ℃ whereas the potential for the run at 160 ℃ decreases over time. The potential levels off in the middle of the 190 ℃ run which corresponds to the bend in the cumulative plot below after day 4 and the jump in the fraction of hexadecane leaving the cell from day 4 to 5.

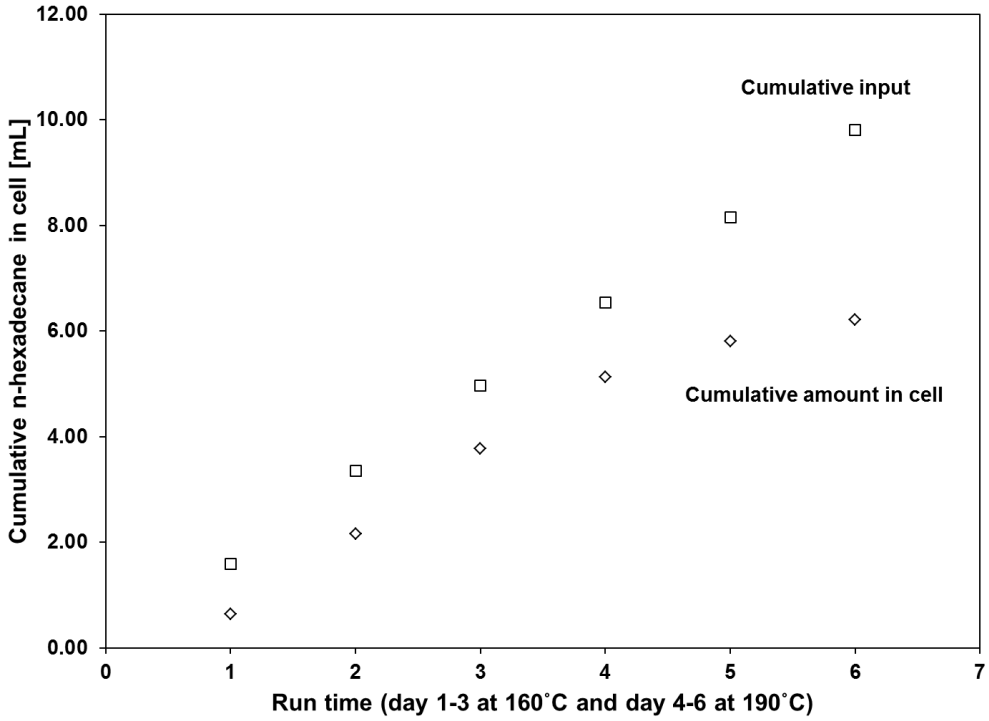


**Figure A.5 Cumulative n-hexadecane in cell [mL] versus run time.**

All the results discussed above were consistent with the conclusions we made. In another way, this part illustrated that more n-hexadecane reacted or deposited in our fuel cell at 190 ℃.

## A.5 References:

[1] Al-Othman, Amani. Composite Zirconium Phosphate/PTFE Polymer Membranes for Application in Direct Hydrocarbon Fuel Cells. Diss. University of Ottawa, 2012.

[2] Choudhury, Suman Roy. "Phosphoric acid fuel cell technology." Recent Trends in Fuel Cell Science and Technology. Springer New York, 2007. 188-216.

[3] Baker, Bernard S., and Hossein G. Ghezel-Ayagh. "Fuel cell system." U.S. Patent No. 4,532,192. 30 Jul. 1985.